GRAĐEVINSKI
MATERIJALI I KONSTRUKCIJE

Volume 66
December 2023
ISSN 2217-8139 (Print)
ISSN 2335-0229 (Online)
UDK: 06.055.2:62-03+620.1+624.001.5(497.1)=861

BUILDING
MATERIALS AND STRUCTURES

4

Society for Materials and Structures Testing of Serbia
University of Belgrade Faculty of Civil Engineering
Association of Structural Engineers of Serbia

(a) CF1 (b) CF2

(c) CF3 (d) CF4

(e) CF5 (f) CF6

GRAĐEVINSKI MATERIJALI I KONSTRUKCIJE

BUILDING MATERIALS AND STRUCTURES

ISSN 2217-8139 (PRINT)
ISSN 2335-0229 (Online)

VOLUME 66(4)
December 2023

CONTENTS

GRAĐEVINSKI MATERIJALI I KONSTRUKCIJE

BUILDING MATERIALS AND STRUCTURES

ISSN 2217-8139 (PRINT)
ISSN 2335-0229 (Online)

VOLUME 66(4)
December 2023

EDITORIAL BOARD

Aims and scope

Building Materials and Structures aims at providing an international forum for communication and dissemination of innovative research and application in the field of building materials and structures. Journal publishes papers on the characterization of building materials properties, their technologies and modeling. In the area of structural engineering Journal publishes papers dealing with new developments in application of structural mechanics principles and digital technologies for the analysis and design of structures, as well as on the application and skillful use of novel building materials and technologies.

The scope of Building Materials and Structures encompasses, but is not restricted to, the following areas: conventional and non-conventional building materials, recycled materials, smart materials such as nanomaterials and bio-inspired materials, infrastructure engineering, earthquake engineering, wind engineering, fire engineering, blast engineering, structural reliability and integrity, life cycle assessment, structural optimization, structural health monitoring, digital design methods, data-driven analysis methods, experimental methods, performance-based design, innovative construction technologies, and value engineering.

Publishers Society for Materials and Structures Testing of Serbia, Belgrade, Serbia, veb sajt: www.dimk.rs
University of Belgrade Faculty of Civil Engineering, Belgrade, Serbia, www.grf.bg.ac.rs
Association of Structural Engineers of Serbia, Belgrade, Serbia, dgks.grf.bg.ac.rs

Print Razvojno istraživački centar grafičkog inženjerstva, Belgrade, Serbia

Edition quarterly

Peer reviewed journal

Journal homepage www.dimk.rs

Cover Tested CFS built-up beams from *Behaviour of cold-formed steel built-up beams under flexural loading* by Sangeetha Palanivelu

Financial support Ministry of Education, Science and Technological Development of Republic of Serbia
University of Belgrade Faculty of Civil Engineering
Institute for testing of materials-IMS Institute, Belgrade
Faculty of Technical Sciences, University of Novi Sad, Department of Civil Engineering
Serbian Chamber of Engineers

CIP - Каталогизација у публикацији
Народна библиотека Србије, Београд

620.1

GRAĐEVINSKI materijali i konstrukcije = Building materials and structures / editor-in-chief Snežana Marinković
. - God. 54, br. 3 (2011)- . - Belgrade : Society for Materials and Structures Testing of Serbia : University of Belgrade, Faculty of Civil Engineering : Association of Structural Engineers of Serbia, 2011- (Belgrade : Razvojno istraživački centar grafičkog inženjerstva). - 30 cm

Tromesečno. - Je nastavak: Materijali i konstrukcije = ISSN 0543-0798. - Drugo izdanje na drugom medijumu: Građevinski materijali i konstrukcije (Online) = ISSN 2335-0229
ISSN 2217-8139 = Građevinski materijali i konstrukcije
COBISS.SR-ID 188695820

Građevinski materijali i konstrukcije
Building Materials and Structures
journal homepage: www.dimk.rs

https://doi.org/10.5937/GRMK2300010R UDK: 665.777.4:620.18

Original scientific paper

Negative impacts of petroleum coke as an energy source in the brick-making industry

Zagorka Radojević[1)], Milica Vidak Vasić[*1)]

[1)] *Laboratory for Building Ceramics, Institute for Testing of Materials IMS, Bulevar Vojvode Mišića 43, 11000 Belgrade, Serbia*

Article history
Received: 08 April 2023
Received in revised form: 25 May 2023
Accepted: 28 September 2023
Available online: 09 November 2023

Keywords
petroleum coke,
energy source,
ceramics industry,
refractory brick,
corrosion,
sulfate scum

ABSTRACT

The technical features of the issues caused by the brick industry's usage of petroleum coke as a fuel were identified in this study. The effects were evaluated in terms of the concentration of hazardous materials in petroleum coke, the CO2, SO2 and NOx emissions in the flue gases, the corrosion of refractory materials in the furnace, the corrosion of pipelines and metal structures in the dryer and furnace, the deposition of sulfate scum on dry products, and the fixation of white scum on finished products. To assess the microstructure and composition of the regions of the samples exposed to flue gases and that inside the material, refractory brick samples from the furnace walls were examined under a microscope. The compressive stress of the part of the sample affected by the flue gas from the kiln is lowered by 37.3 %, which is caused by the agglomeration of sulfate salts and the presence of a high quantity of vanadium. It was determined that, regardless of potential energy savings, the sulfur concentration in petroleum coke must be below 5% if utilized as an energy source in the brick sector since there are suitable conditions for accelerated corrosion processes.

1 Introduction

Petroleum coke (petcoke) is an important commercial product known since the 1930s that is obtained in several refining processes from all types of oil (light or heavy crude oil) during the refining process. This kind of coke has drawn more attention as a fuel substitute over the past 30 years as a result of the decline in high-quality energy sources. After the distillation of heavy fractions of oil, petroleum coke is produced by cracking and carbonizing the residue leftover. The chemical composition of this energy source depends on the characteristics of the raw material (including its geological background) and the production process, but it contains carbon as its main constituent. Petroleum coke exists in two forms: raw coke, which is used as fuel, and calcined coke, which is used as a raw material in the production of aluminum, steel, glass, paper, paints, coatings, fertilizers, etc. High-quality coke contains low amounts of sulfur and heavy metals and is used to produce electrodes in the aluminum and steel industries. About 80% of the world's petroleum coke production is of poorer quality (higher contents of sulfur and heavy metals) and is utilized as a fuel in electricity generation, cement kilns, and other industries. Calcined petroleum coke is used by brick and glass manufacturers because it has a significantly lower ash content compared to other fuels while minimizing the presence of residual hydrocarbons (volatile matter) [1-4]. The ash from the burnt petroleum coke, however, mostly consists of heavy metals [5].

The Environmental Protection Agency (EPA) classifies petroleum coke as a highly stable product that is non-reactive in environmental conditions and has a low potential for health hazards. Petroleum coke is chemically inert and non-toxic (it does not chemically react with water nor dissolve in water, and it is not bioavailable, i.e., organisms cannot absorb it and it does not accumulate in the organism) [6,7]. The majority of petcoke toxicity evaluations conclude that it poses no risk to human health or the aquatic or terrestrial environment and that there are no known carcinogenic, reproductive, or developmental effects. The facilities for the storage and handling of petcoke must include dust management and appropriate permits for the storage of flammable material [1]. Petroleum coke averagely contains 90-95 % carbon and 3-6% sulfur; the other ingredients are hydrogen, oxygen, and nitrogen. Also, metals and organic compounds are present in traces [8]. The heavy metal content present in petcoke makes it potentially dangerous, both due to air release during combustion and to the local environment during storage. Petroleum coke is most often stored in open dumps, although studies have shown that the risk to human respiratory systems is no different from regular coal [1]. Significant amounts of fugitive dust from coke storage and handling operations pose a health risk. A particular problem is created by particles with a diameter of ≥10 μm (PM10) because these can pass through the throat and nose and enter the lungs. When inhaled, these particles can affect the heart and lungs and cause serious health consequences. Petcoke is an extremely stable fuel, which

* Corresponding author:
E-mail address: milica.vasic@institutims.rs

means there is little risk of burning during transport. Due to its high carbon content, it releases up to 10% more CO_2 per unit of energy than ordinary coalwhen burned. This CO_2 footprint is higher than that of almost any other existing source of energy. Thus, increased pollution control during combustion is needed to remove the acid gas containing H_2S and CO_2, and/or sulfur recovery units [8].

Despite the environmental problems associated with the production and use of petroleum coke, it remains popular due to its cost-effectiveness. It is easily exported and is an attractive source of cheap fuel, especially for developing countries [1]. Notwithstanding the attention paid to the content of sulfur in liquid fuels, especially fuels for transoceanic ships [9], restrictions on manufactured solid fuels, including petroleum coke, have been introduced only in selected countries like Ireland [10] and Great Britain [11]. The sulfur level of coal products and manufactured solid fuels, including manufactured component biomass products, must be less than 2 wt.% on a dry ash-free basis, which is to be reduced to 1 wt.% by 2025 [10,11]. There are no regulations concerning the usage of petroleum coke in Serbia, as long as the flue gas composition is kept within the prescribed limits [12].

In this study, emphasis is given to the problems that petroleum coke causes in the brick industry, related to the wall of the kiln, metal pipes and installations, and the final appearance and quality of dry and fired products.

2 Methodology

In this research, an analysis of the possible negative impacts of using petroleum coke from Serbia with a higher sulfur content was performed.

The analysis included the determination of:

1. Content of harmful constituents in petroleum coke (*Chapter 3.1*),
2. Increases in SO_2 emission at the tunnel furnace emitter (*Chapter 3.2*),
3. Increased corrosion of refractory materials in the furnace at high temperatures (*Chapter 3.3*),
4. Increased corrosion of pipelines and metal structures in the dryer and furnace (*Chapter 3.4*),
5. Deposition of sulfate scum on the surface of dry products and fixation of white scum on fired products (*Chapter 3.5*).

The chemical composition of petroleum coke was determined by the method of energy dispersive X-ray fluorescence (XRF) using the Spectro Xepos device and adequate certified reference materials [13].

The emission of gases at the emitter of the tunnel furnace (without the use of an emission reduction system) was measured with the help of a flue gas analyzer (Environnement S.A., France, model MIR 9000 CLD). The detection limits of the device are for NO - 2000 ppm, NO_2- 200 ppm, NO_x- 2000 ppm, and SO_2 up to 2000 ppm.

Total organic carbon content was determined using Environnement S.A. of the Graphite 52M device, which contains a flame ionizing detector and measures range 0-10/100/1000/10000 ppm.

The quality of the refractory bricks from the wall of the ceiling of the tunnel furnace was tested by determining the resistance to the action of strong acids according to the standard SRPS B.D8.070:1981 [14]. The test was performed using sulfuric acid at boiling temperature for 6 hours. By measuring the mass of the sample before and after the test, the relative mass loss in percentage was determined.

The bulk density of the cut part of the samples is determined by measuring weight and dimensions. The compressive stress of refractory brick samples measuring 50x50x50 mm from the tunnel kiln ceiling is tested using a universal hydraulic machine by Alfred Amsler until the samples are completely crushed. Both results were gained from testing three samples.

Before microstructure analysis, samples were dried and evaporated using Au–Pd powder in a Fisons Instruments chamber. The surface micromorphology of the so-prepared samples was examined in a high vacuum using a JEOL JSM 5800 scanning microscope equipped with energy dispersive spectroscopy (SEM-EDS). The composition was determined using an Oxford Link Isis 300 with a SiLi X-ray detector calibrated using a Ni plate. The magnification employed was up to 500 μm.

3 Results and Discussion

3.1 Harmful constituents in petroleum coke

A thorough chemical investigation was carried out to demonstrate the potential impact of petroleum coke ingredients in addition to sulfur. The potential of employing petroleum coke of lesser quality—the composition of which is displayed in Table 1—was taken into consideration to reduce manufacturing costs. The lower and upper calorific values of the examined coke were 7387 and 8311 kcal/mol, which makes it somewhat below the usual petcoke used in cement production [2], but is found satisfactorily in the production of clay bricks. The high loss on ignition value shows the main constituent is carbon. The harmful elements in the examined petroleum coke were sulfur, iron, nickel,

Table 1. Chemical composition of the petroleum coke

Investigated parameters	Petroleum coke
Loss on ignition at 1000°C, %	97.73
Ash content, %	2.27
The moisture content at 105°C, %	0.25
Total S, %	8.80
Fe, mg/kg	338.8
Ni, mg/kg	480.0
Co, mg/kg	3.8
Cu, mg/kg	8.1
Zn, mg/kg	8.0
As, mg/kg	0.3
Sr, mg/kg	2.5
Mo, mg/kg	0.92
Cd, mg/kg	17.4
Sn, mg/kg	3.1
Sb, mg/kg	8.6
Ba, mg/kg	64
Hg, mg/kg	<0.2
Pb, mg/kg	1.4
Bi, mg/kg	0.3
V, mg/kg	100.9
W, mg/kg	1.3

cadmium, and vanadium. The total content of sulfur was higher than previously reported in the literature [2,5], so the sample is considered a high-sulfur petcoke [15]. Such petroleum coke can also be useful in syngas production [16]. The proportion of nickel and iron was higher than the average literature data [17]. The catalytic action of metals like Fe, Co, Mo, V, etc. present in a solid fuel can have a significant impact on the combustion process [2], while the concentration of vanadium is considered the most significant [18].

3.2 Flue gases from the tunnel furnace

During the firing of clay, the following combustion products may occur: dust, nitrogen oxides and other nitrogen compounds, carbon monoxide and carbon dioxide, leachable organic compounds, metals and their compounds, chlorine and its compounds, and fluorine and its compounds. The processing of clay, its mixing, drying, and firing result in the creation of dust. Nitrogen oxides and nitrogen compounds occur mainly as a product of fuel combustion, where nitrogen binds with oxygen from the air at high temperatures. Carbon monoxide and carbon dioxide are produced as products of the combustion of organic matter in clay, especially at low oxygen content. The combustion of fossil fuels produces CO_2, which further reacts with elemental carbon to produce CO. Volatile organic compounds that can appear in the waste gas originate not only from the raw material but also from possibly used additives. Depending on the firing temperature, various organic compounds may appear (benzene, styrene, phenol, formaldehyde, etc.). The content of heavy metals in most raw materials is very low. Metal oxides that appear from pigments used to color ceramic products have a hard crystal structure, so they are stable even at high temperatures. The content of chlorine and its compounds in most clays is low. Hydrogen chloride emissions can occur during the decomposition of mineral salts at temperatures over 850 °C and organic compounds containing chloride at temperatures between 450 and 550 °C, as well as from water used for soaking clay, if it is rich in chlorides. Fluorine and its compounds are present in all raw materials for ceramic products, which is why they are found in waste gas. The hydrogen fluoride found in waste gas is produced by the decomposition of fluorosilicate.

Table 2 shows the results of this investigation confronting Serbian [12] and EU regulations [19] about flue gas composition. Serbian legislation refers to the emission limit value for existing plants for firing clay-based ceramic products, while the EU´s directive is precise in the case of combustion facilities built before 2013 that use solid fuels. The allowances depend on the total rated thermal input that is divided into three groups (50-100, 100-300, and > 300 MW), while the maximum concentration of the waste gas allowed is lower in cases of higher energy input. According to Serbian regulations, the only limits that exceed them are found in the case of total organic carbon, which is expected due to the composition of petcoke. When compared to the EU Directive, the results of SO_2 and total organic contents are revealed as problematic. Other flue gas constituents` mass flow, like HF, HCl, and benzene, was below 0.09 kg/h.

The brick factory where the tests were conducted uses petroleum coke containing 4.5 % of sulfur. The results of the emission test from the tunnel furnace (Table 2) show the concentration of SO_2 is 291.93mg/Nm^3(mean value of three measurements). Applying a simple proportion, when using petroleum coke with 8.8% sulfur (considering that the calorific power of the fuel has not changed significantly), SO_2 emission at the tunnel furnace emitter of about 521.39mg/Nm^3 can be expected, which is above the limit [12], so there is a risk of exceeding the permitted emission if filters are not used. The excess air in the furnace must be reduced to produce as little SO_3 as possible, especially if temperatures above 1200 °C are reached, which is rarely achieved in the brick-making industry [20]. Sulfates are formed at firing temperatures below 1200, which then remain on the surface of the product as white fixed stains. [21] (see *Chapter 3.3*).

In the case of NO_x content (total nitrogen oxides expressed as NO_2), the plant meets the requirements of the current regulation, related to the emission limit values for new plants for the production of ceramic products by firing clay-based products in waste gas with a volume fraction of oxygen of 17 % [12]. The total volatile organic carbon content of the gas was unacceptably high. Additionally, the carbon in the exhaust gases does not only come from the fuel but also from the raw materials [12, 20]. The concentrations in the flue gas of a petroleum coke-heated tunnel kiln were lower than coal-fed kilns of different types reported in the literature [22]. However, the composition of the flue gases is also dependent on the mineralogical and chemical composition of clay, the chemical composition of the water used to produce the plastic mass, firing temperature, and possibly used additives to increase plasticity and porosity.

3.3 Corrosion of refractory bricks in the furnace ceiling

The quality of the refractory bricks from the wall of the ceiling of the tunnel furnace in Serbia was tested by determining the resistance to the action of strong acids according to the standard [14]. The mass loss of refractory bricks after the action of sulfuric acid according to the prescribed procedure is 3.55%, while the maximum permissible mass loss is 4%. It was concluded that refractory bricks met the demand for special-purpose products.

The petroleum coke constituents that have the greatest influence on corrosion processes (corrosion agents) are sulfur, nitrogen, vanadium, nickel, chlorine, potassium, and sodium. Sulfur and its compounds accelerate the corrosion processes of construction materials. Sulfur from petroleum

Table 2. Composition of the flue gases

Investigated parameters	Results	Maximum allowed in Serbia [12]	Maximum allowed in the EU [19]
Flue gas temperature	62.6 °C	/	/
Water vapor content	4.0 %	/	/
Dust	14.8 mg/Nm^3	20 mg/Nm^3	20-30 mg/Nm^3
Concentration of SO_2	291.93mg/Nm^3	500 mg/Nm^3	200-400 mg/Nm^3
Concentration of NO_x	31.99mg/Nm^3	500 mg/Nm^3	200-300 mg/Nm^3
Total organic carbon content	22.43mg/Nm^3	50 mg/Nm^3	10 mg/Nm^3

coke turns into hydrogen sulfide during combustion in reducing local conditions, oxidizes into sulfur dioxide, or, in the presence of catalysts (vanadium pentaoxide and iron oxide), turns into sulfur trioxide or sulfuric acid. Sulfur trioxide reacts with sodium and potassium compounds to form highly corrosive sulfates, low-melting pyrosulfates, and/or sulfuric acid. Sulfur compounds increase the corrosion rate of deposits containing vanadium and sodium [17, 23, 24].

The concentration of vanadium in the fuel is approximately 100.9 mg/kg, however, the deposit can contain over 80% of that amount (on the refractory walls of the furnace walls and ceiling and the walls of the wagon). It creates compounds with a low melting point when combined with other deposit components. Melted vanadium compounds create conditions for accelerated corrosion and swelling processes. At high temperatures, V_2O_4 and V_2O_5 combine with metal oxides to form solid solutions [17]. Bricks made of refractory material are destroyed by vanadium oxides at high temperatures. Molten V_2O_5 reacts with the refractory wall surface's oxide components at temperatures above 690 °C. It also causes slag to penetrate the material's pores, which lowers the melt's surface tension and viscosity. To reduce this effect (the formation of V_2O_5), it is recommended that the process be conducted without excess air. This will result in the production of far more refractory V_2O_3 and V_2O_4, which will lessen the corrosion of refractory materials brought on by the presence of vanadium [17, 21]. The literature also describes one such issue that occurred when the ceiling in the tunnel furnace suffered severe damage (dropping off the wall at a length of 80 m) [25].

Images of refractory bricks removed from the ceiling of the tunnel kiln are displayed in Figure 1. The sample from the ceiling of the kiln is pale red in color. The lower part of the brick, which was directly exposed to smoke gases and water vapor, is greyish-yellow in height, ranging from 25 to 30 mm.

To determine the nature of brick corrosion in the lower part, the brick is divided into two positions:

- - Pale red part (without corrosion) - Position I (P I)
- - Greyish yellow part (with corrosion) – Position II (P II).

The average compressive stress on the 50x50x50 mm samples (Figures 1c and 1d, Table 3) determined on parts of the samples that were not directly influenced by the flue gas is 36.2, while the affected part showed 22.7 MPa (37.3% decrease). Bulk density decreased by 3.40%.

SEM-EDS analysis of deposits on a sample of refractory bricks removed from the furnace ceiling (Figure 2, Table 4) showed that sulfur, iron, and vanadium are deposited on the exposed surfaces of refractory materials but also penetrate the interior of the bricks. The proportion of sulfur in certain parts of the examined material was up to a maximum of 6.59% (Position I), while the vanadium content was detected up to 11.65% (Position II) in the spots not presented in Figure 2. Such high amounts of vanadium in bricks from the walls significantly lower the refractoriness of the Al2O3-SiO2 system [21, 26]. Furthermore, the density of the deteriorated sample is detected to be lower than the initial one (Figure 2), which is consistent with the results gained through bulk density tests.

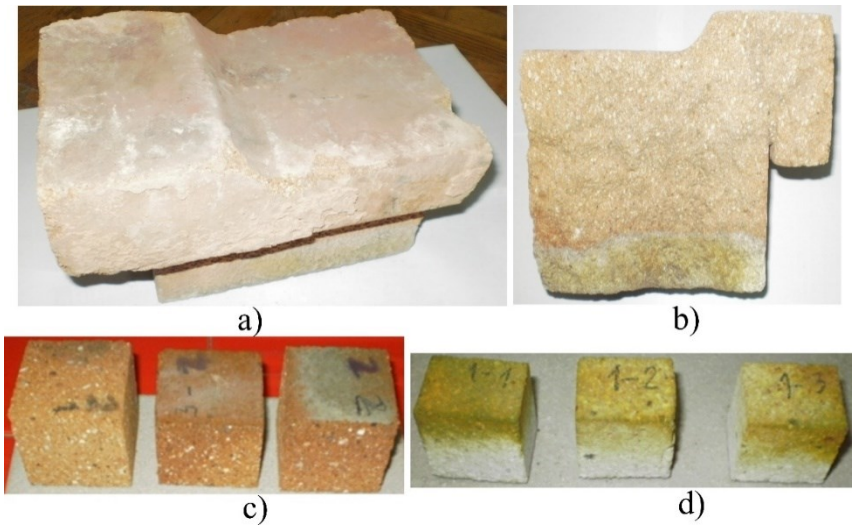

Figure 1. The visual appearance of the sample from the furnace wall: a) sample, b) section of the sample with the appearance of positions I and II, c) Position I, and d) Position II.

Table 3. Compressive stress of different parts of samples

	Compressive stress(MPa)		Bulk density (g/cm^3)	
	Position I	Position II	Position I	Position II
Test sample 1.	33.2	25.7	1.76	1.72
Test sample 2.	36.8	18.3	1.78	1.69
Test sample 3.	38.7	24.2	1.81	1.70
Average	36.2	22.7	1.76	1.70

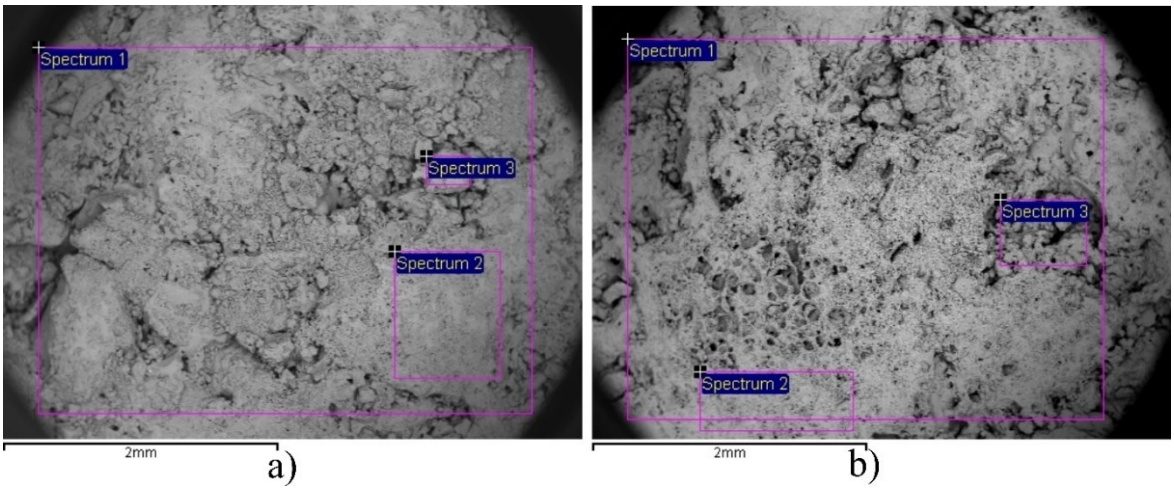

Figure 2. Microscopic appearance of the sample from the furnace wall: a) Position I, b) Position II.

According to the composition of the material itself, the presence of sodium and potassium is also evident (Table 4). All of the above confirms that there are conditions for accelerated corrosion processes. In addition, based on the difference in micromorphologies, it is observed that the discolored part of the sample (Position II) also contains widened cracks and more pores as a result of the service life of the material. At increased magnification of that part of the material (Figure 3), micron-sized acicular crystals of primary mullite containing feldspars, quartz, and vanadium (Figure 3a) [26] and secondary mullite formed at temperatures above 1400 °C (Figure 3b) [27, 28] can be observed.

Table 4. Composition of refractory bricks from the walls of the tunnel kiln

Composition (%)	P I Spectrum 1	P I Spectrum 2	P I Spectrum 3	P II Spectrum 1	P II Spectrum 2	P II Spectrum 3
Na	0.66	0.37	0.51	0.70	0.60	1.45
Mg	0.32	0.33	0.45	0.80	0.52	0.54
Al	14.67	12.56	12.92	13.40	14.38	13.22
Si	26.78	25.68	20.36	25.26	25.12	27.54
P	0.00	0.00	0.00	0.00	0.00	0.00
S	1.59	3.66	6.59	0.65	0.46	0.30
Cl	0.00	0.19	0.00	0.00	0.00	0.00
K	2.04	1.92	1.81	2.65	1.34	3.63
Ca	2.38	3.69	6.28	1.07	0.67	1.29
Ti	0.31	0.68	0.25	0.56	0.41	0.45
V	0.00	0.00	0.00	4.93	6.00	1.92
Mn	0.00	0.00	0.00	0.00	0.00	0.00
Fe	2.58	1.83	2.14	1.81	1.83	1.69
Ni	0.00	0.00	0.00	0.00	0.00	0.00
O	48.68	49.09	48.69	48.17	48.69	47.99

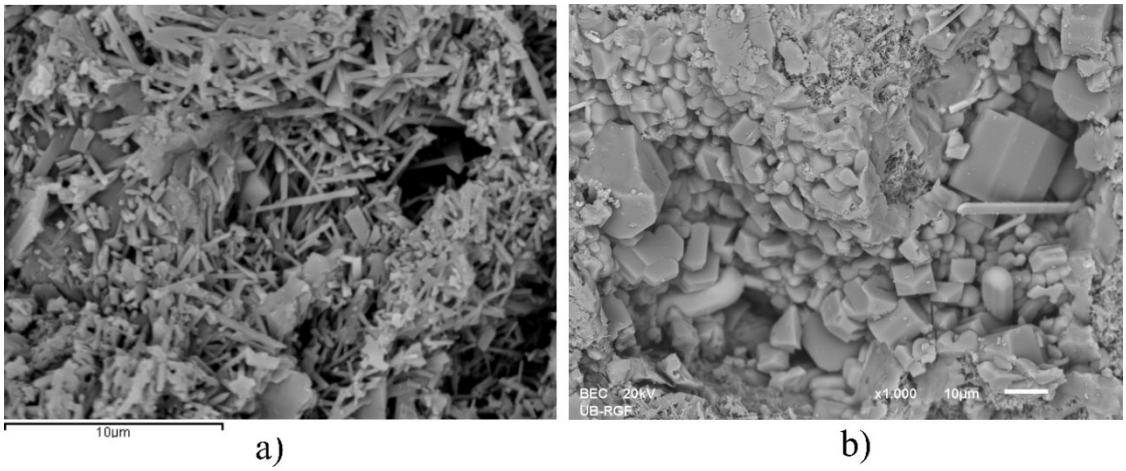

Figure 3. Microscopic appearance of the sample *from the furnace wall (Position II): a) Crystals of primary mullite containing vanadium, b) Crystals of secondary mullite.*

3.4 Corrosion of pipelines and metal structures in the dryer and furnace

Increased corrosion of pipelines and metal structures on the furnace and dryer is caused by the presence of sulfur oxides. In contact with water vapor, these compounds condense at lower temperatures and form acids (sulfuric and sulfurous), which affect the intense corrosion of metal structures. Any increase in sulfur concentration causes corrosion to grow noticeably, and there is a risk of rapid deterioration of metal pipelines and structures. Vanadium can also act as a catalyst to combine with sulfur from petroleum coke and generate a corrosive sulfate, which can seriously harm alloys at high temperatures [17, 29].Moreover, the presence of CaO in petroleum coke causes the agglomeration of $CaSO_4$ under high-temperature circumstances, severely damaging the metal components [30].

3.5 Deposition of sulfate scum on the products

The dryer scum is formed if products enter the kiln with residual moisture that is suddenly released in the heating zone. For this to happen, the necessary conditions are that there is a certain amount of sulfur in the flue gases (usually waste heat from the kiln) and a low temperature of the flue gases. This way, sulfurous and sulfuric acids form salt scum with water on the external (free) surfaces of the products. Moreover, soluble salts present in raw materials can be driven off to the surface with water while drying, and thus again, sulfate scums are formed and bound (fixed) to the surface of products. The negative effects caused by these salts can be prevented by adding $BaCO_3$ to the raw materials, and the products must be sufficiently dried before reaching the heating zone in the kiln.

These drying-related salts typically become apparent only after firing. Kiln scum develops by a similar mechanism during the firing process and is mainly caused by the sulfurous gas in the kiln [31, 32].

Thus, when using petroleum coke as an energy source in the brick kiln, the increased content of sulfur significantly risks the appearance of sulfate scum and, thus, a poor appearance of the finished product (Figure 4). Depositing is possible in the dryer and the heating zone of the kiln. The strength of the scum spots varies, and the "coloring" is more intense as a result of the products being stacked at the wagons and having differently exposed surfaces to the atmosphere in the kiln (flue gases).

Sulfate scum on the produced blocks is mainly the aesthetic problem that affects their poor placement on the market. Besides, since those sulfates are water-soluble, they may react with mortar during the construction phase and deplete their binding properties [33].

4 Conclusions

The impact of petroleum coke with a higher sulfur content was investigated concerning SO_2 emission from the furnace, corrosion of the furnace walls, metal pipes, and structures in the dryer and tunnel furnace. Moreover, the appearance of dried and fired products caused by sulfate scum was discussed. This investigation was the first of its kind available in the literature.

Due to numerous adverse effects, it is not advised to use petroleum coke with a high sulfur content (over 5%) as a fuel in tunnel kilns for the manufacture of ceramic bricks. The increased content of sulfur negatively affects the dryer, kiln, and final products and requires the use of flue gas filters. In the study, only the technical aspects of the negative impacts of the high sulfur content in petroleum coke were analyzed, while the health aspects were not considered.

Acknowledgments

The authors of the study are thankful for the funds achieved by the Ministry of Science, Technological Development and Innovation of the Republic of Serbia, Contract No. 451-03-47/2023-02/200012. This article is based on work from COST Action CA20133, supported by European Cooperation in Science and Technology.

Figure 4. Macroscopic appearance of the samplescontaining sulfate scum

References

[1] What is Petcoke? And What is it Used For? https://www.petro-online.com/news/fuel-for-thought/13/breaking-news/what-is-petcoke-and-what-is-it-used-for/33235(accessed 27 March 2023)

[2] J.-M. Commandre, S. Salvador, Lack of correlation between the properties of a petroleum coke and its behaviour during combustion, Fuel Process. Technol. 86(7) (2005) 795-808. 10.1016/j.uproc.2004.08.001, https://hal.science/hal-01845780

[3] G. Fuyan, L. Jianzhong, W. Chuancheng, Z. Junhu, C. Kefa, Effects of the physical and chemical propertiesof petroleum coke on its slurryability, Pet.Sci.9(2012)251-256. https://doi.org/10.1007/s12182-012-0206-9

[4] S.Stanković, B. Tanaskovski, B. Zlatić, M. Arsenović, L. Pezo, Analysis of trace elements in surfacesediments, mussels, seagrass and seawateralong the southeastern Adriatic coast – achemometric approach, Pure Appl. Chem. 86(7) (2014) 1111–1127. https://doi.org/10.1515/pac-2014-0201

[5] A. Andrews, R.K. Lattanzio, Petroleum Coke: Industry and EnvironmentalIssues, Congressional Research Service Report, 2013.

[6] Health Effects of Petroleum Coke, United States Environmental Protection Agency. https://archive.epa.gov/epa/petroleum-coke-chicago/health-effects-petroleum-coke.html(accessed 27 March 2023)

[7] J.A. Caruso, K. Zhang, N.J. Schroeck, B. McCoy, S.P. McElmurry, Petroleum Coke in the Urban Environment: A Review ofPotential Health Effects, Int. J. Environ. Res. Public Health 12 (2015) 6218-6231.https://doi.org/10.3390/ijerph120606218

[8] Feasibility Studyon the Utilization of High Sulfur Pet. Coke as a By-ProductatSINOPEC Fujian Petrochemical Company Limited, March 2001, Chiyoda Corporation, China

[9] Directive (EU) 2016/802 ofthe European Parliament and of the Council of 11 May 2016relating to a reduction in the sulphur content of certain liquid fuels, Official Journal of the European Union (2016). https://eur-lex.europa.eu/legal-content/EN/TXT/PDF/?uri=CELEX:32016L0802&rid=1 (accessed 18 May 2023)

[10] Government agrees new regulations on solid fuels, Government of Ireland (2022). https://www.gov.ie/en/press-release/26f90-government-agrees-new-regulations-on-solid-fuels/ (accessed 18 May 2023)

[11] The Air Quality (Domestic Solid Fuels Standards) (England) Regulations 2020. (draft legislation) https://www.legislation.gov.uk/ukdsi/2020/9780348210194(accessed 18 May 2023)

[12] Uredba o graničnim vrednostima emisija zagađujućih materija u vazduhu iz stacionarnih izvora zagađivanja, osim postrojenja za sagorevanje, "Sl. glasnik RS", br. 111/2015 & 83/2021 (Regulation on limit values of pollutant emissions in the air from stationary sources of pollution, except for combustion plants, "Official Gazette of Republic of Serbia", no. 111/2015 and 83/2021)

[13] N. Mijatović, M. Vasić, Lj. Miličić, M. Radomirović, Z. Radojević, Fired pressed pellet as a sample preparation technique of choice for an energy dispersive X-ray fluorescence analysis of raw clays, Talanta 252 (2023) 123844. https://doi.org/10.1016/j.talanta.2022.123844

[14] SRPS B.D8.070:1981. Keramičke pločice – Određivanje otpornosti na kiseline za pločice specijalne namene – Metoda sa zrnastim materijalima (Ceramic tiles - Determination of acid resistance for special purpose tiles - Method with granular materials), in Serbian.

[15] M.A.Abdelzaher, Experiential investigation on the effect of heavy fuel oil substitution by high sulfurpetcoke on thephysico-mechanical features and microstructure ofwhite cement composites, Eng. Res. Express 3 (2021) 015028. https://doi.org/10.1088/2631-8695/abe9fa

[16] Z. Li, H. Xu, W. Yang, S. Wu, Numerical study on the effective utilization of high sulfur petroleumcoke for syngas production via chemical looping gasification, Energy 235 (2021) 121395. https://doi.org/10.1016/j.energy.2021.121395

[17] X. Fan X,The fates of vanadium and sulfur introduced with petcoke to lime kilns, Master thesis, University of Toronto, 2010.

[18] S. Salvador, J.M. Commandré, B.R. Stanmore, R. Gadiou, The catalytic effect of vanadium on the reactivityof petroleum cokes with NO, Energy and Fuels 18 (2004) 296. https://doi.org/10.1021/ef0300489

[19] Directive 2010/75/EU ofthe European Parliament and of the Council of 24 November 2010on industrial emissions (integrated pollution prevention and control)(Recast). https://eur-lex.europa.eu/legal-content/EN/TXT/?uri=celex%3A32010L0075(accessed 24 May 2023)

[20] M.V. Vasić, G. Goel, M. Vasić, Z. Radojević, Recycling of waste coal dust for the energy-efficientfabrication of bricks: A laboratory to industrial-scale study, Environm. Technol.Inno. 21 (2021) 101350.https://doi.org/10.1016/j.eti.2020.101350

[21] G.C. Wei, V.J. Tennery, Impact of Alternate Fuels on Industrial Refractories and Refractory Insulation Applications - An Assessment, Oak Ridge national laboratory, 1976.

[22] M.I. Haque, K. Nahar, M.H. Kabir, A. Salam, Particulate black carbon and gaseous emission from brick kilnsin Greater Dhaka region, Bangladesh, Air Qual. Atmos.Health 11 (2018)925–935.https://doi.org/10.1007/s11869-018-0596-y

[23] B. Ošljanac,Somecorrosionproblems on flame – fume side of boiler, Structural integrity and life 7(2) (2007) 96–100.

[24] A.D. Manasrah, Conversion of Petroleum Coke into Valuable Products using Catalytic and Non-Catalytic Oxy-Cracking Reaction, Ph.D. thesis, University of Calgary, 2018.

[25] F. Mödinger, Advances in the utilization of waste materials and alternative sources of energy in clay brick making - A South Tyrolean case study investigating environmental and financial impacts, Ph.D. thesis, Staffordshire University, 2010.

[26] M.V. Vasić, L. Radovanović, L. Pezo, Z. Radojević, Raw kaolinitic–illitic clays as high-mechanical-performancehydraulically pressed refractories, J. Therm. Anal. Calorim. 148 (2023) 1783–1803. https://doi.org/10.1007/s10973-022-11848-w

[27] M.V. Vasić, N. Mijatović, Z. Radojević, Aplitic GraniteWaste as Raw Material for the Production of Outdoor Ceramic Floor Tiles, Materials 15 (2022) 3145.https://doi.org/10.3390/ma15093145

[28] Y.-F.Chen, M.-C.Wang, M.-H.Hon,Secondary mullite formation in kaolin-Al_2O_3 ceramics, J. Mater. Res. 19(03), 806-814.https://doi.org/10.1557/jmr.2004.19.3.806

[29] J. Chen, X.Lu, Progress of petroleum coke combusting in circulating fluidized bed boilers—A review and future perspectives, Resour.Conserv. Recycl. 49(3)(2007) 203-216. https://doi.org/10.1016/j.resconrec.2006.03.012

[30] J.V. Iribarne, E.J. Anthony, A. Iribarne, A scanning electron microscope study on agglomeration in petroleum coke-fired FBC boilers, Fuel Process. Technol. 82 (2003) 27 – 50. doi:10.1016/S0378-3820(03)00024-9

[31] L.A. Palmer, Cause and prevention of kiln and dry-house scum and of efflorescence on face-brick walls, Technologic papers of the Bureau of Standards 22(370) (1928), Department of Commerce, United States of America.

[32] A. Andrés, M.C. Díaz, A. Coz, M.J. Abellán, J.R. Viguri, Physico-chemical characterisation of bricks all through the manufacture process in relation to efflorescence salts, J. Eur. Ceram. Soc. 29(10)(2009) 1869-1877. https://doi.org/10.1016/j.jeurceramsoc.2008.11.015

[33] EN 772-5: 2016, Methods of test for masonry units – Part 5: Determination of the active soluble salts content of clay masonry units

Građevinski materijali i konstrukcije
Building Materials and Structures
journal homepage: www.dimk.rs

https://doi.org/10.5937/GRMK2300011P UDK: 691.714:620.17
624.014.2

Preliminary report

Behaviour of cold-formed steel built-up beams under flexural loading

Sangeetha Palanivelu*[1)]

[1)] *Associate Professor, Department of Civil Engineering, Sri Sivasubramaniya Nadar College of Engineering, Kalavakkam, Chennai, Tamilnadu, India*

Article history
Received: 28 June 2023
Received in revised form:
06 October 2023
Accepted: 23 October 2023
Available online: 09 November 2023

Keywords
CFS built-up beam,
flange plate,
channel section,
bolted connections,
ANSYS

ABSTRACT
Cold-Formed Steel (CFS) built-up beams are most commonly used as structural elements such as columns, beams, and trusses. They are also used to avoid buckling and increase member flexibility by providing flanges and side plates/batten plates. This study describes the flexure behaviour of the CFS built-up beam. Six CFS built-up beams were tested to failure with a Universal Testing Machine (UTM). CFS built-up beams of thickness 2 mm were developed using channel sections put back to back and close to close, as well as a lip and flange plate. The overall deflection and strain against the incremental load were discussed and compared with the control beam without a lip and flange plate. A back-to-back CFS built-up beam with lip a section could withstand 32% greater load under flexure than a back-to-back built-up beam without a lip. The Finite Element Analysis (FEA) was performed using the software ANSYS, and there was a high correlation between the experimental and analytical results.

1 Introduction

CFS built-up sections are extensively used in industrial buildings due to their high strength-to-weight ratio. The failure of structural elements is mainly due to buckling, which can be overcome by providing a flange plate or side plate. The presence of these plates increases the moment of inertia of the section and thus improves the flexibility of the member. The bolted built-up CFS beam with extended stiffener shows good flexural strength based on the location and spacing of the bolts[1]. The spacing of connectors has a less significant effect on the ultimate capacity of the CFS built-up beam made of three or four channel sections [2]. A design equation was proposed by the direct strength method specification for the CFS built-up hat section and also reported that, except thickness, all other dimensions of the built-up section significantly affect the strength and behaviour of beams [3]. The addition of intermediate web stifeners and edge stifeners improves the behaviour and strength of the CFS built-up channel section with a lip [4]. An extensive parametric study on the CFS built-up beam was carried out to examine the bending moment carrying capacity [5]. The effects of distortional buckling on a hollow flange channel beam are investigated, and the results of a finite element model are compared to the codal provisions for cold-formed steel constructions [6]. The flexural behaviour of CFS hollow beams with perforation was studied and reported that the rectangular hollow beams withstand 41 % more load than that square hollow beams [7]. The CFS channel column with circular, diamond, and elliptical holes along with and without lip was investigated to study the strength and buckling behaviour [8].

From the literature study, it was observed that more investigation on the strength and behaviour of the CFS built-up beams are found. However, the effect of the flange plate, web hat, and lip section on the CFS built-up beams was limited. Thus, this study was carried out for the innovative CFS built-up beams to examine the ultimate load-carrying capacity, moment-carrying capacity, and its behaviour under flexural loading.

2 Materials and Methods

Cold-formed steel of grade St 34-1079 (S355MC as per EN – 10027-1)was used to produce the CFS built-up beams in compliance with IS 811-1975[9] requirements. Cold-formed steel plate with a thickness of 2 mm was used to create channel sections with or without a 15 mm lip. Six different built-up beams were fabricated with various arrangements such as beam with or without flange plate (CF1, CF2, CF3, CF4, CF5 & CF6), beam with or without lip (CF3 & CF4), and beam with web hat (CF5) and box section (CF6). The flange plates are bolted to the built-up beam (CF1 to CF5) to behave as a single unit. The hexagonal bolt of size 12 mm diameter was used to connect the channels back-to-back. The mild steel bolt of 4 nos was utilised to connect the channel back to back to obtain the CFS built-up beam. The spacing between the bolt of 320 mm was maintained. The bolt hole of diameter 14 mm was drilled along the web of the channel for bolting. In specimens CF2, CF4 &CF6 the flange

* Corresponding author:
E-mail address: sangeethap@ssn.edu.in

plate has been welded using a semi-automatic arc welding process at four places to the length of 15 mm. The spacing between the weld maintained was 300 mm. The box section was obtained by welding the lip of the channel section (CF6) as mentioned in Table 1. The built-up beam measured 1000 mm in length was tested with the ends as simply supported condition. The coupon test [10] was used to investigate material parameters such as yield stress, ultimate stress, modulus of elasticity, and specimen elongation after fracture, which were determined to be 260 N/mm^2, 470 N/mm^2, and 2.02 x 10^5 N/mm^2 and 50 mm respectively and stress-strain behaviour was shown in Fig.1. The specimen details and its dimensions are shown in Table.1.

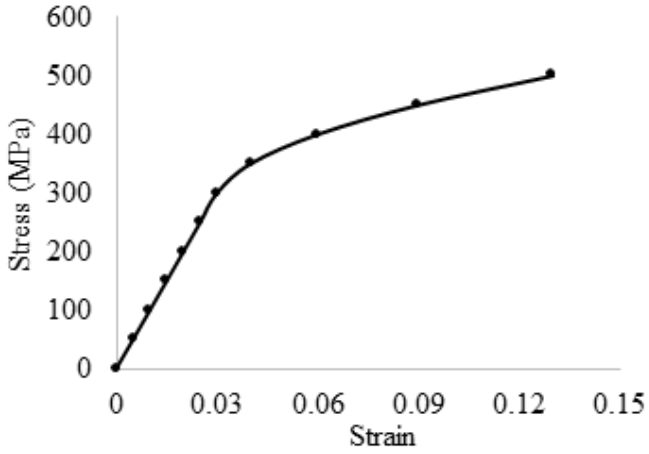

Figure 1. Stress - strain behaviour of the CFS material

Table 1. Description of the CFS built-up beams

Specimen ID	Specimen Description	Channel Dimension (mm)	Lip (mm)	Thickness of flange plate (mm)	Sectional view of the CFS beam
CF1	Channel section Back-to-back arrangemnet without flange plate	100 x 50 x 2	-	2	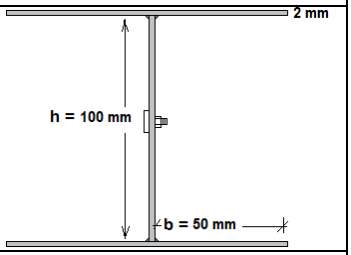
CF2	Channel section Back-to-back arrangemnet with flange plate	100 x 50 x 2	-	2	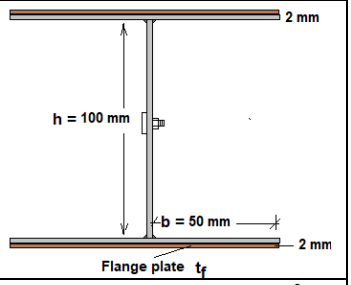
CF3	Channel section Back-to-back arrangemnet without flange plate	100 x 50 x 2	15	2	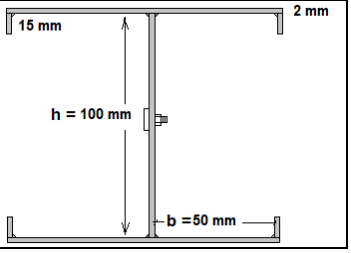

CF4	Channel section Back-to-back arrangemnet with flange plate	100 x 50 x 2	15	2	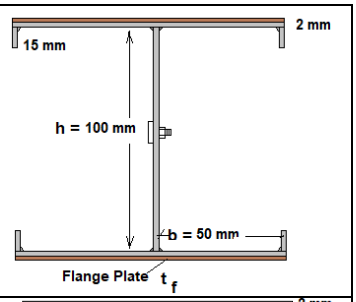
CF5	Channel section with hat arrangement in the web	100 x 50 x 2	-	2	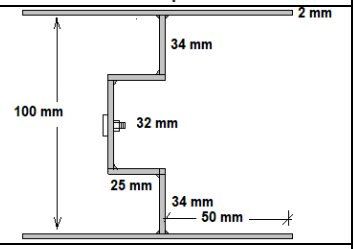
CF6	Closed channel section with flange plate	100 x 50 x 2	15	2	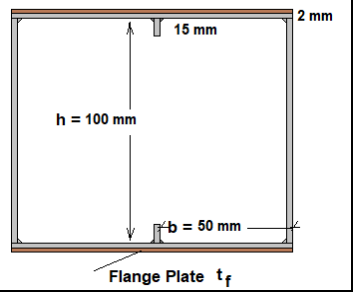

2.1 Experimental study

The built-up beams are supported at the ends and tested for failure under flexure. The loads are applied using a 600 kN capacity Universal Testing Machine, all CFS built-up beams were tested until they failed under flexure. Hydraulic stroke control was used to apply the static stress at a rate of 0.5 mm/min [11]. Using a dial gauge with a count of 0.01 mm, the central vertical deflections were measured. Figure 2 illustrates where the dial gauge is located to measure the centre deflection. Using a 20 mm strain gauge pasted horizontally along the length of the beam to measure the strain in x- direction of the CFS built-up beam. The 5-channel strain indicator was used to measure the strain levels as shown in Figure 2. All of the built-up beams were tested until the maximum load was reached, and the deflection and strain were measured for a 2 kN load interval. Figure 2 shows the schematic test setup and experimental test setup. The tested specimens are shown in Figure 3. From Figure 3, it is observed that all the beam specimens show the local flange failure and overall torsional buckling of the CFS beam. The specimen with a flange plate was able to resist deformation, thus local bucking of the flange can be minimised (CF2).

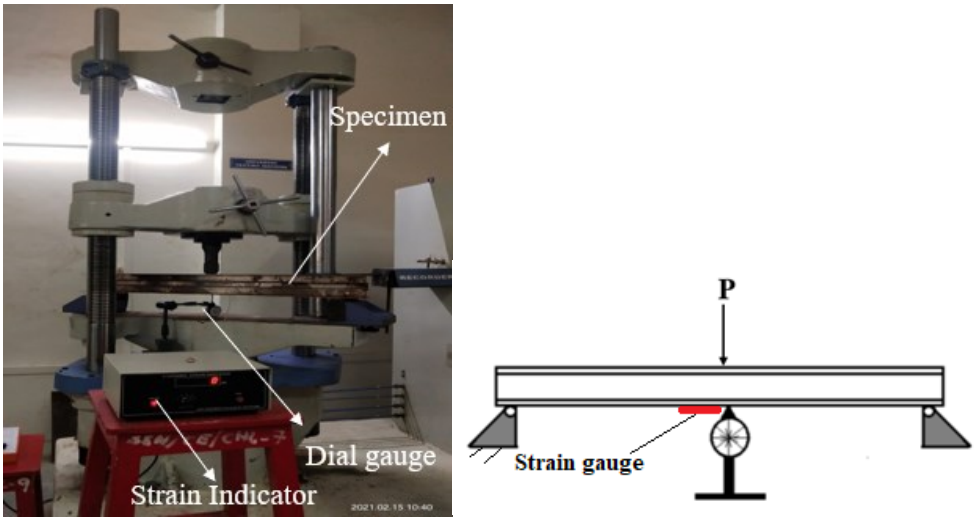

Figure 2. Expermental set-up

Figure 3. Tested CFS built-up beams

2.2 Numerical Study

All CFS built-up beams are modelled in AutoCADD and imported into the ANSYS programme. The CFS built-up beam was meshed using element SOLID 185 from the element collection of ANSYS. The simple support conditions in terms of displacement and rotation are simulated in the FEA at the ends of the beam. The translations along x, y and z were also constrained at the ends. The load was applied in increments as sub-steps using the Newton-Raphson method from the ANSYS library. The overall imperfection was taken as 1/1000 of the overall length of the column, including both the initial bending of the member and the initial eccentricity of the loading. For each incremental step of end-shortening, the total reaction at the end is obtained. Using, the 'UPGEOM' command in ANSYS, buckling mode was obtained. To validate the results, the material properties acquired from the experimental study were allocated to the built-up-beam models. At the mid-span of the CFS built-up beam, an axial load was applied. The mesh model of the CFS built-up beams is shown in Figure 4.

The deformed shape of the CFS built-up beams is shown in Figure 5. The local buckling of flange was observed for the beam CF1 and CF3 and it was compared based on the intensity of red colour patches. The CFS built-up beam CF2 and CF4 shows that the overall deflection of the beam is less for the CFS built-up beam. The local inward and outward buckling of the box built-up beam (CF6) and similar failure were noted in the tested specimen.

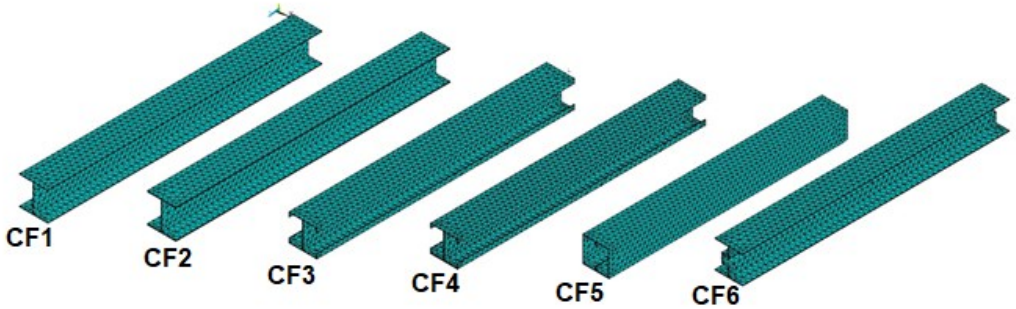

Figure 4. Mesh models of CFS built-up beams

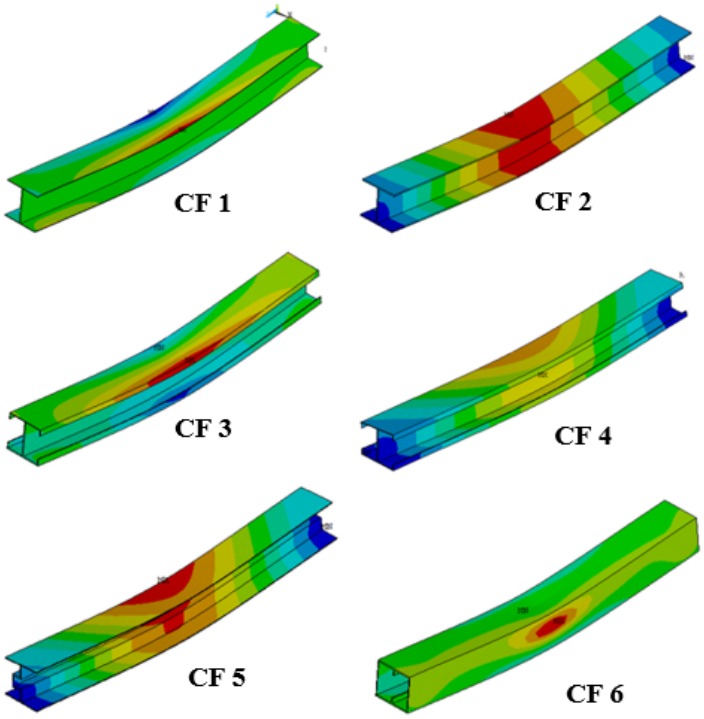

Figure 5. Deformed shape of the CFS built-up beams

3 Results and discussions

3.1 Effect of lip on the load-carrying capacity of the built-up beam

The Cold-formed steel built-up beams were tested for failure under one-point loading. The specimens were grouped as built-up beams without lip (CF 1, CF 2 & CF 5) and built-up beams with lip section (CF 3, CF 4 & CF 6). The behaviour between load carrying capacity and the central deflection is shown in Figures 6(a) & 6(b). From Figure 6(a), it was clear that the behaviour of the build-up beam without lip section(CF 1, CF 2 & CF 5) was uniform with the average load carrying capacity of 21 kN. The built-up beam CF 5 was able to resist the deflection up to 5.2 mm which was 33 % more than the CF 1 & CF 2(3.5 mm). The beam with that arrangement in the web avoids web torsional buckling and hence resisted more deflection under single point loading.

From Figure 6(b), it was seen that the load-carrying capacity was more for the built-up beam with a lip section of 15 mm. In that, the beam CF 4 was found to be stiffer due to the presence of a flange plate of thickness 2 mm and also observed that the failure of the beam CF 4 was due to web torsional buckling. The built-up beam CF 6 was made by connecting two-lipped channel sections close-to-close, from Figure 6(b) it was observed that CF 6 was able to resist the deflection up to 6.15 mm (Max. central deflection = 1.85 mm as per theoretical calculation). The % decrease in the load-carrying capacity from CF 4 to CF 3 and from CF 4 to CF 6 is 45% and 48% respectively.

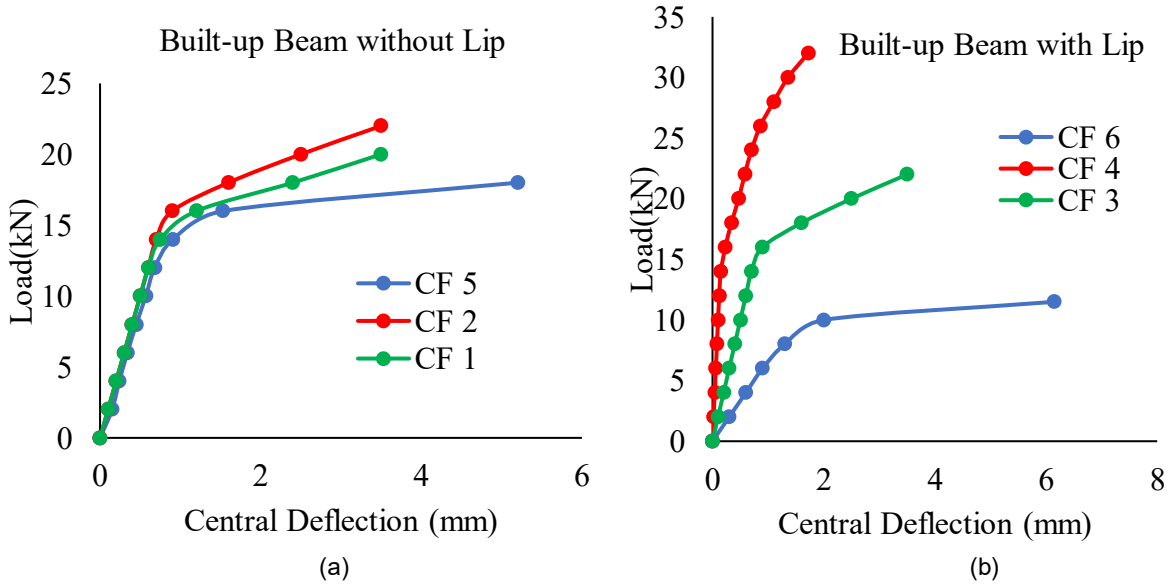

Figure 6. Load-central curve for the built-up beam without a lip and with a lip section

3.2 Effect of flange plate on the load-carrying capacity of the built-up beam

The built-up beams CF 1 and CF 2 are made with the channel section arranged back-to-back without a flange plate and with a flange plate (top and bottom) respectively. The behaviour of CF 1 and CF 2 without a lip section is shown in Figure 7(a). It was observed that from Figure 7(a), the load-deflection behaviour was linear until the load of 14.5 kN which is 18.5 % of the average load-carrying capacity of 22.25 kN (CF 1 & CF 2). Figure 7(b) shows that the load-deflection behaviour of the lipped built-up beam CF 3 and CF 4 with and without a flange plate respectively. The mode of failure of the CF 3 involves a rotation of the lip/flange components upon loading. The same was overcome by providing a flange plate of thickness 2 mm both at the top and bottom flange (CF 4) which increases the moment of inertia. The built-up beam CF 3 and CF 4 shows the linear behaviour up to the load of 16 kN.The strength of CF 4 was 1.5 times more than that of CF 3. Thus the use of a flange plate improves the strength and stiffness of the built- up beam.

Figure 8 shows the deflections observed from the experimental and numerical study. From the bar chart, it was observed that the numerical model is stiffer than the experimental one due to rigid body connections between the flange plates and channel sections.

3.3 Load-strain behaviour

The strain corresponding to the gradually applied load was recorded using a strain indicator and a graph was plotted between them. Figure 9. shows the load-strain plot of the built-up beams. CF 2 and CF 4 were able to resist the maximum strain in the range of 600-700 microstrain, this may be due to the presence of flange plates. Thus energy absorption capacity of CF 2 and CF 4 was also improved significantly. Whereas, the specimens CF 1, CF 3, CF 6 and CF 5 were able to resist microstrain values of 200, 50, 220 and 450 respectively.

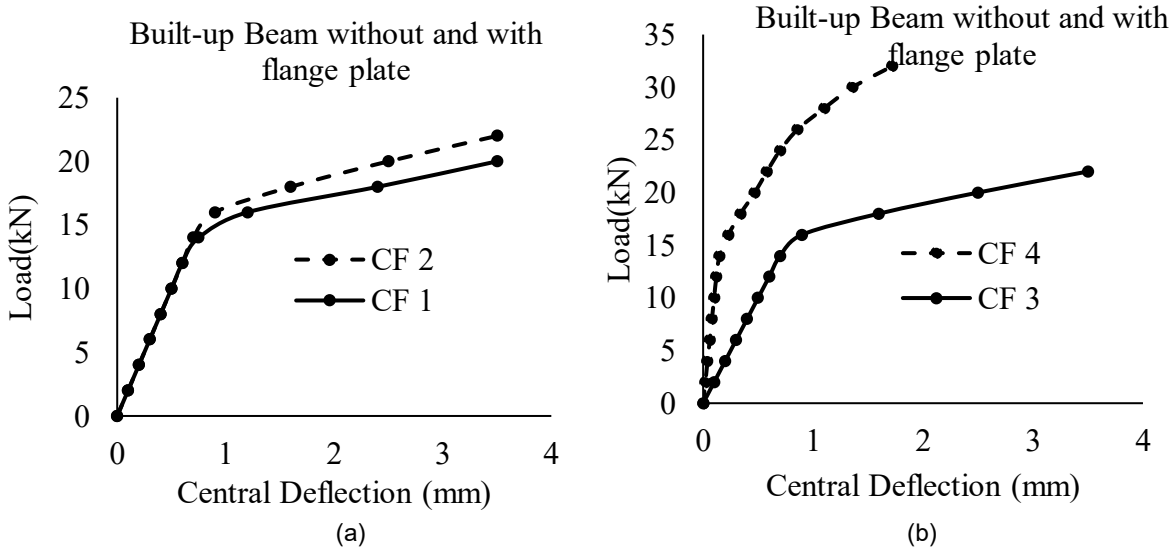

Figure 7. Load-deflection behaviour of the built-up beam with a flange plate

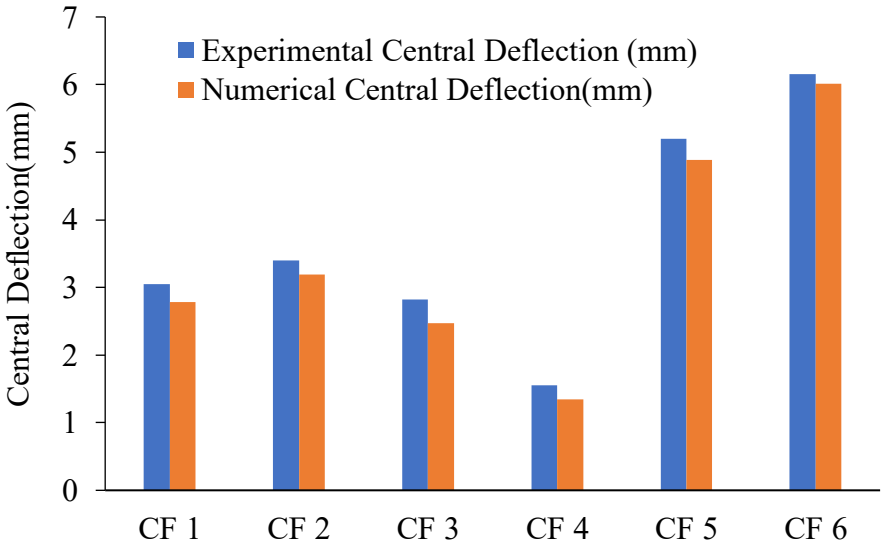

Figure 8. Bar chart comparison of the maximum central deflection

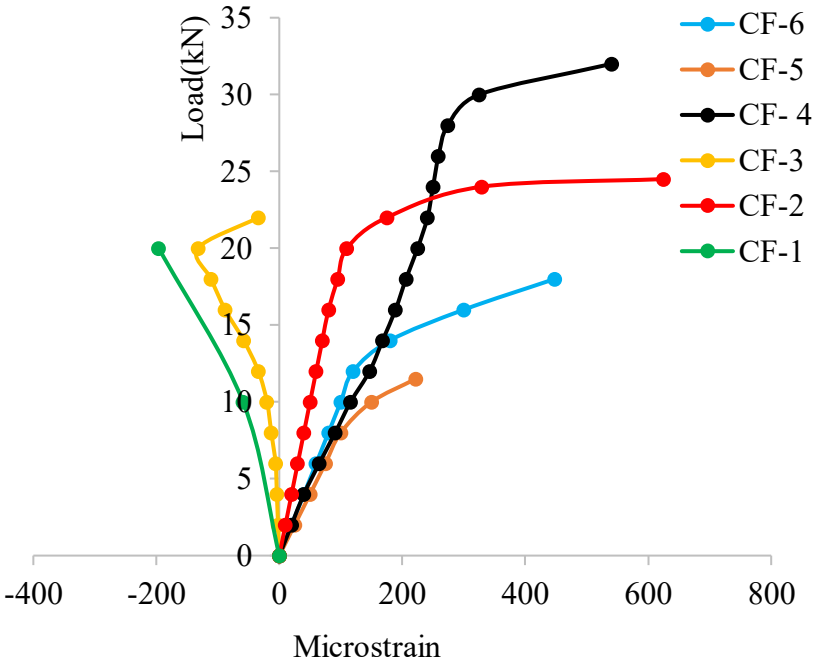

Figure 9. Load- strain behaviour of CFS built-up beams

3.4 Theoretical Investigation

The nominal flexural strength (M_{DSM}) for CFS structures, according to the DSM [12], is the minimum of lateral-torsional buckling (M_{ne}), local buckling (M_{nl}), and distortional buckling (M_{nd}), as shown below.

The lateral-torsional buckling strength (M_{ne}) is

For $M_{cre} < 0.56\ M_y$; $M_{ne} = M_{cre}$

For $2.78\ M_y > M_{cre} > 0.056 M_y$; $M_{ne} = \frac{10}{9} My\left(1 - \frac{10My}{36\ Mcre}\right)$

Where , M_{cre} - Critical Moment Capacity
M_y - Yield moment capacity
M_{nl} - Lateral-Torsional Buckling coefficients

Table 2. compares the results of the FEA model to the theoretical outcome. According to Table 2, the Direct Stiffness Method is conservative in calculating the flexural strength of CFS beams. The calculated mean and standard deviation for the ratio of M_{FEA} and M_{DSM} are 0.91 and 0.03 respectively. The percentage difference between the flexural strength of M_{FEA} and M_{DSM} is less than 10 %. The linear regression analysis is made between M_{DSM} and M_{FEA} of the CFS built-up beams and it is shown in Figure 10. M_{DSM} and M_{FEA} have a relationship of M_{FEA} = 0.901 M_{DSM} with a regression coefficient of 0.901. Thus, the flexural strength of CFS built-up beams could be determined using FEA models, and a satisfactory correlation between numerical and theoretical studies was attained.

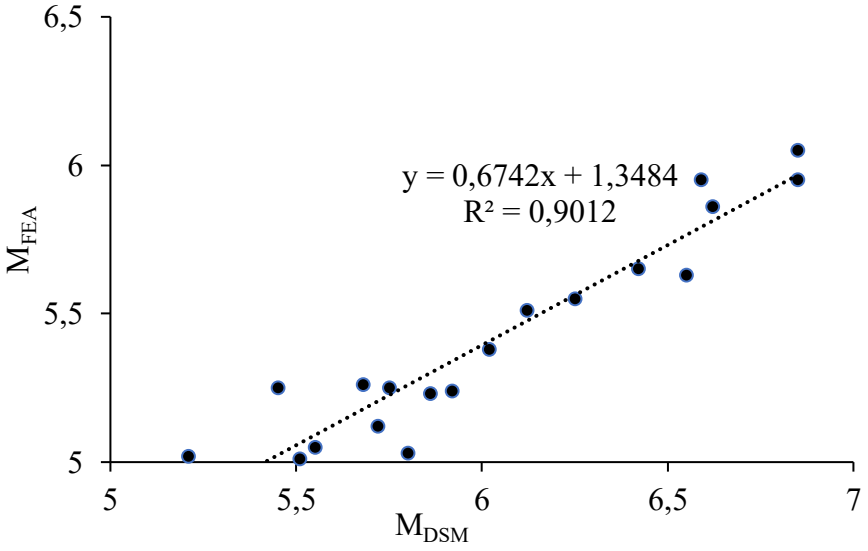

Figure 10. Variations of M_{DSM} and M_{FEA}

Table 2. Comparison between the results of FEA model and theoretical outcome

Specimen	Section dimension (mm)						M_{FEA} (kN.m)	M_{DSM} (kN.m)	M_{FEA}/M_{DSM}	Failure Mode
	h	b	D/S	t	t_f	L				
CF1 -L800 -H100	100	50	6.85	2	0	800	5.95	6.25	0.87	L
CF1 -L1000 -H100	100	50	6.62	2	0	1000	5.86	6.12	0.89	L + LT
CF1 -L1200 -H100	100	50	6.42	2	0	1200	5.65	6.01	0.88	L + LT
CF1 -L1400 H100	100	50	6.12	2	0	1400	5.51	5.99	0.90	L + LT
CF2 -L800 - H100	100	50	6.02	2	2	800	5.38	5.89	0.89	LT
CF2 -L1000 -H100	100	50	5.92	2	2	1000	5.24	5.72	0.89	F + LT
CF2 -L1200 -H100	100	50	5.72	2	2	1200	5.12	5.53	0.90	F + LT
CF2 -L1400 -H100	100	50	5.51	2	2	1400	5.01	5.24	0.91	F + LT
CF3 -L800 -H100	100	50	6.85	2	0	800	6.05	6.42	0.88	L
CF3 -L1000 -H100	100	50	6.59	2	0	1000	5.95	6.21	0.90	L + LT
CF3 -L1200 -H100	100	50	5.86	2	0	1200	5.23	5.54	0.89	L + LT
CF3 -L1400 -H100	100	50	5.13	2	0	1400	4.96	5.01	0.97	F + LT
CF4 -L800 -H100	100	50	6.55	2	2	800	5.63	6.31	0.86	LT
CF4 -L1000 -H100	100	50	6.25	2	2	1000	5.55	6.10	0.89	F + LT
CF4 -L1200 -H100	100	50	5.80	2	2	1200	5.03	5.62	0.87	F + LT
CF4 -L1400 -H100	100	50	5.01	2	2	1400	4.55	4.95	0.91	F + LT
CF5 -L800 -H100	100	50	5.75	2	0	800	5.25	5.42	0.91	F + LT
CF5 -L1000 -H100	100	50	5.55	2	0	1000	5.05	5.35	0.91	F + LT
CF5 -L1200 -H100	100	50	5.25	2	0	1200	4.95	5.02	0.94	F + LT
CF5 -L1400 -H100	100	50	5.01	2	0	1400	4.45	4.89	0.89	F + LT
CF6 -L800 -H100	100	50	5.45	2	2	800	5.25	5.35	0.96	L + F
CF6 -L1000 -H100	100	50	5.68	2	2	1000	5.26	5.46	0.93	L + F
CF6 -L1200 -H100	100	50	5.21	2	2	1200	5.02	5.12	0.96	L + F
CF6 -L1400 -H100	100	50	5.02	2	2	1400	4.95	5.00	0.99	L + F
								Mean	**0.91**	
							Standard Deviation		**0.03**	

4 Conclusions

Six distinct specimens were tested for the flexural behaviour of cold-formed steel built-up beams. Single-point loading was applied to all specimens at the centre of the CFS built-up beam. The flexural test was performed under UTM of capacity 600kN. The maximum central deflection at the centre of the beam was recorded and load-strain behaviour was studied and compared for all the test specimens. All of the specimens were further evaluated using the ANSYS Finite Element Analysis programme. The following results were drawn from the experimental, numerical, and theoretical research.

- Flange plates are used in cold-formed steel built-up beams to increase their flexural capacity. By adding stiffeners to the top and bottom flanges of the beam, the section's resistance to bending moments is enhanced.
- Flange plates also contribute to the overall stability of the cold-formed steel beam. They reduce the potential for lateral-torsional buckling and help maintain the beam's integrity when subjected to bending loads.
- The back-to-back cold-formed steel channel section with a lip section was able to resist 32 % more load under flexure as compared to a back-to-back built-up beam without a lip.
- The cold-formed steel beam with that section inside was found to resist less load due to a weaker axis along the hat portion of the back-to-back beam section.
- The load-strain behaviour of CF-5 (Cold-formed channel closed section) was found to resist more load and strain.
- From the analytical results, the percentage difference between the experimental and analytical central deflection is within 10 %. This shows good correlation between the experimental and analytical models was obtained.
- The built-up beam CF 2 and CF 4 were able to resist the maximum strain in the range of 600 – 700 microstrain, this may be due to the presence of flange plates. Thus energy absorption capacity of CF 2 and CF 4 was also improved significantly.
- The DSM is conservative in predicting the flexural strength of CFS built-up beams. The calculated mean and standard deviation for the ratio of M_{FEA} and M_{DSM} is 0.91 and 0.03 respectively. The percentage difference between the flexural strength of M_{FEA} and M_{DSM} is less than 10 %. Thus, the flexural strength of CFS built-up beams could be determined using FEA models, and a satisfactory correlation between numerical and theoretical studies was attained.

List of symbols

Mcre	Critical Moment Capacity
My	Yield moment capacity
Mnl	Lateral-Torsional Buckling coefficients
$M_{c,Rd}$	Cross-section design bending moment of resistance
M_{FEA}	Finite element moment resistance
M_{DSM}	Direct Design Method moment resistance

Abbreviations

CFS	Cold-Formed Steel
UTM	Universal Testing Machine
ANSYS	Finite element software
DSM	Direct Design Method

References

[1] Fadhluhartini Muftah, Mohd Syahrul Hisyam Mohd Sani, Mohd Mawardi Mohd Kamal(2019) ,Flexural Strength Behavior of Bolted Built Up Cold Formed Steel Beam with Outstand and Extended Stiffener, International Journal of Steel Structures 19(3):719–732

[2] Meza, F.J., Becque, J. and Hajirasouliha, I. (2020), Experimental study of cold-formed steel built-up beams, Journal of Structural Engineering, 146 (7). 04020126.

[3] Manikandan.P, Ezhilan.A, (2019), Investigation on cold formed steel built up new innovative hat shaped closed section under bending, International Journal of Advanced Structural Engineering 11:1–8.

[4] Manikandan.P, Thulasi.M, (2019) ,Investigation on cold formed steel lipped channel built up I beam with intermediate web stiffener, International Journal of Advanced Structural Engineering 11:97–107.

[5] Mohamed Ghannam (2019), Bending Moment Capacity of Cold Formed Steel Built Up Beams, International Journal of Steel Structures 19(2):660–671

[6] R. Senthilkumar, T. S. Sunil, P. Jayabalan,(2019) ,Buckling Behaviour of Hollow Flange Channel Beam Sections in Bending, International Journal of Steel Structures 19(5):1454–1464.

[7] Sangeetha P, Revathi S.M, Sudhakar V, Swarnavarshini D & Sweatha S(2021), Behaviour of cold-formed steel hollow beam with perforation under flexural loading, Materials Today: Proceedings, 38: 3103-3109.

[8] Sangeetha P, Dhinagaran M, Gobinaath A S, Saravana Kumar A S & Jeevan Raj A D(2022),Performance Assessment of the Perforated CFS Unlipped and Lipped Channel Section Under Compression, Lecture Notes in Civil Engineering 179:265 – 277.

[9] IS 801: 1975, Code of Practice for Use of Cold Formed Light Gauge Steel Structural Members In General Building Construction

[10] IS 1608: 2005, Indian standard code of practice for Metallic Materials: Tensile testing at ambient temperature.

[11] Davison, B., & Owens, G. W. (Eds.). (2011) Steel designers' manual. New York: Wiley.

[12] AISI S100: 2007, Specification for the design of cold-formed steel structural members: American Iron and Steel Institute.

Građevinski materijali i konstrukcije
Building Materials and Structures
journal homepage: www.dimk.rs

https://doi.org/10.5937/GRMK2300013B UDK: 691.32:620.17

Original scientific paper

Effect of aggregate origin on freeze/thaw resistance of self-compacting concrete with and without a de-icing agent

Gordana Broćeta[1)], Mirjana Malešev[2)], Vlastimir Radonjanin[2)], Slobodan Šupić[*2)], Aleksandar Savić[3)], Ivan Lukić[2)], Anđelko Cumbo[1)], Marina Latinović Krndija[1)]

[1)] *University of Banja Luka, Faculty of Architecture, Civil Engineering and Geodesy, Bulevar vojvode Petra Bojovića bb, 78000 Banjaluka, Bosnia and Herzegovina*
[2)] *University of Novi Sad, Faculty of Technical Sciences, Department ofCivil Engineering, Trg Dositeja Obradovića 6, 21000 Novi Sad, Serbia*
[3)] *University of Belgrade, Faculty of Civil Engineering, Bulevar kralja Aleksandra 73, 11000 Belgrade, Serbia*

Article history
Received: 08 November 2023
Received in revised form:
06 December 2023
Accepted: 11 December 2023
Available online: 20 December 2023

Keywords
self-compacting concrete,
natural aggregate,
recycled concrete aggregate,
water absorption,
freeze/thaw resistance,
freeze-thaw resistance with de-icing agent

ABSTRACT

Freezing and thawing cycles, with or without de-icing agents, are the principal causes of concrete structure degradation during the winter. This paper explores the effects of aggregate type on the level of degradation of self-compacting concrete (SCC) due to freeze-thaw (f/t) action. Natural river (NRA) and/or natural crushed (NCA) aggregate, as well as the recycled aggregate of known (RCA-N) and unknown provenance (RCA-A), were employed to produce six different SCC mixtures. The temperature, density, air content, and consistency were determined for fresh concrete, while compressive strength, water absorption by gradual immersion and vacuuming, and frost resistance with and without de-icing salts were tested for hardened concrete. Even though all tested concretes have met the criteria for frost resistance with and without the de-icing salts, it was found that the type of aggregate has a noticeable influence on it. The type of natural aggregate has little effect on SCC frost resistance, but it does influence its behavior when frost and salt are present at the same time. In f/t conditions, RCA-N can be used the same way as natural aggregate, while RCA-A causes the biggest frost resistance reduction. However, both RCAs are not recommended for application in conditions of simultaneous frost and salt impacts.

1 Introduction

The durability of concrete is a very current issue, given that it is regarded as the core material of modern buildings and that the problem of its degradation owing to the aggressive effects of numerous environmental conditions is obvious. One of the most prominent deteriorating mechanisms in regions with cold winter conditions is the action of frost [1], [2]. The destructive force of this impact is amplified in the presence of salt, which is commonly used in the winter regime to accelerate the process of thawing snow and ice [2], [3], and [4]. As a result, it is crucial to conduct any research that can help reduce the level of degradation this mechanism causes. In this regard, it is especially vital to define criteria for the selection of component materials for self-compacting concrete (SCC). Given the issue of overuse of natural resources, it is critical to use the potential of waste materials as a way to produce valuable but greener components for new environmentally friendly concrete [3].

The selection of the appropriate type of aggregate is one of the possibilities for modeling the durability properties of concrete in terms of resistance to frost effects with and without the presence of salt. Several studies revealed that increasing the presence of RCA increases the value of water absorption in concrete [5], [6], [7], [8], [9], [10], [11], [12], and [13]. Some examples are Modani et al. [6], who found that adding 20, 40, 60, 80, or 100% RCA to coarse natural aggregate in SCC increases absorption by 21, 28, 31, 36, and 41%, respectively (absorptions of fine and coarse NA and coarse RCA were 0.84, 1.31, and 5.64%, respectively).

M. Gesoglu et al. [9] investigated the durability performance of concrete produced by varying two types of aggregate blended with silica fume. The concrete with the lowest permeability (measured by gas permeability, water impermeability, and capillary absorption) was made with NRA as the coarse aggregate. The concrete with the highest permeability was made with RCA. The combination of coarse RCA and fine NRA proved to be even more advantageous than the combination of coarse NRA and fine RCA.

Oliveira et al. [14] varied the participation of the coarse RCA in SCC, manufactured with limestone filler, in proportions of 20, 40, and 100%. It was discovered that using

* Corresponding author:
E-mail address: ssupic@uns.ac.rs

RCA has no effect on the gas permeability, water permeability, or water impermeability of SCC. When evaluating the water permeability results, it was discovered that permeability coefficients of insignificant value were achieved for all types of SCC, compared to the usual level of such values for conventional concrete. The coefficient of capillary absorption also goes down as the amount of RCA goes up, by about 5 to 13 percent, when coarse NA is completely replaced by RCA. This is due to the beneficial influence of limestone filler, but it is also considered that RCA disrupts the concrete structure, favorably affecting the creation of barriers or voids that interrupt the capillary pore system.

Despotović [15] conducted research on the effect of RCA application on the level of absorption of SCC as assessed by the gradual immersion method. Higher absorptions of concrete with NRA were recorded by substituting the coarse aggregate fraction (8/16mm) in amounts of 0, 50, and 100% with RCA. Tuyan et al.'s research [16] also indicates the usefulness of using RCA with regard to capillary absorption of SCC. The amount of water to powder (w/p) was changed from 0.43 to 0.48 to 0.53, and the coarse part of the crushed aggregate (NCA) was switched out for RCA in increments of 0, 20, 40, and 60%. The amounts of fine and coarse NCA and RCA that were absorbed were 0.67, 0.21, and 4.80%, respectively. It was discovered that the participation of RCA impairs chloride absorption and penetration. At the same time, the higher w/p had an even stronger influence on the growth in the values of the aforesaid tests' results. Nonetheless, RCA participation improves the capillary pore system, particularly in concrete with higher w/p (0.48 and 0.53). Concretes with 20% RCA have the lowest coefficients of capillary absorption, but as the proportion of RCA increases, the sorption power of the concrete rises as well (it should be noted that, regardless of the stated increase in sorption, the coefficients of capillary absorption of concrete with RCA are lower than the same coefficients of concrete with NA). Finally, a considerable number of studies have established that permeability, as seen primarily through water permeability, is dependent on the capillary porosity of the cement stone of new concrete and the capillary porosity of the cement stone of recycled concrete. If RCA was obtained by crushing low-porosity concrete, the level of water permeability of the new concrete will be primarily determined by the granulometric composition and the achieved structure of the new cement stone. Hence, RCA can be successfully used to produce concrete with a high level of water impermeability.

According to research conducted by M. S. Hameed et al. [17], replacing the fine fraction of river aggregate in SCC with waste material – marble powder (more than 60% of grains smaller than 0.125 mm) and finely crushed rubble (D_{max}=4.75mm for both materials), lowers concrete permeability, as measured by absorption, waterimpermeability, and chloride diffusion tests, while having no influence on compressive strength. Similarly to the preceding, substituting the fine fraction of river aggregate with waste material – granite powder enhances compressive and flexural strength by up to 40% and reduces the absorption of SCC by up to 60%, according to the research by Jain et al. [18].

Although permeability is one of the good indirect indicators of resistance to the effect of frost and the simultaneous effect of frost and salt, the direct measurements of concrete resistance according to the mentioned durability aspects are also extremely important due to the cold climatic conditions of the winter period in the Balkans. Tuyan et al. [16] found that increasing w/p and the amount of coarse RCA in SCC makes it less resistant to frost after 300 cycles (tested according to ASTM C666). However, it turned out that w/p had a greater influence on the property in question. In addition, this research showed that there is a strong link between mass loss after full f/t cycles and absorption using the gradual immersion method. Using the same standard, Öznur et al. [19] investigated the impact of pumice stone application in coarse aggregate fractions by varying its involvement in quantities of 10, 20, 25, and 30%. It was demonstrated that the use of pumice reduces compressive strength, but that the lowest strength drop after 300 cycles is obtained for concretes containing 10, 15, and 20% pumice, respectively. According to the authors, this is a result of the porous nature of the pumice and its propensity to absorb water, which migrates from the cement stone's capillary system into the pumice 's pore space during the freezing process. However, the use of pumice in the proportion of 30% coarse aggregate provides additional "space," which reduces frost resistance. The mass loss measurement findings revealed that increasing the number of cycles caused the samples' mass loss to increase. In this regard, tests of concrete containing 10% pumice yielded the best results, whereas those containing 30% pumice yielded the worst. Finally, the subject research concluded that SCC with a 10% pumice involvement has the best resistance to the effect of frost after 300 cycles of freezing and thawing, both in non-destructive and destructive ways. This lightweight aggregate can be used up to 20% of the volume of the coarse aggregate. However, as its percentage increases, SCC resistance decreases according to this breakdown process.

Huda et al. [20] demonstrated that all designed concrete mixtures, blended with fly ash, met the frost resistance criterion after 300 f/t cycles when the coarse NA aggregate was substituted by RCA in amounts of 0, 30, 40, and 50% in SCC (in accordance with ASTM C666). Regardless of the foregoing, it was shown that RCA participation reduces frost resistance, with 40% RCA participation offering the least resistance. The resistance to 200 frost cycles of SCC was evaluated in line with GB/T50082 in the study of Hao Yan et al. [21], in which the involvement of aeolian sand in the amounts of 0, 20, 40, and 60% and the coarse RCA in the amounts of 0, 25, and 50% were varied. It was discovered that increasing the proportion of aeolian sand increases the loss in frost resistance, but increasing the proportion of RCA inhibits this tendency. In this regard, the most effective shares of sand and RCA were determined to be 20 to 40% and 25 to 50%, respectively.

Resistance to the simultaneous action of frost and salt as a function of aggregate application is a less explored topic for newer forms of concrete composites, such as SCC. I.F. Bosque et al. [22] investigated the influence of RCA in the amounts of 0, 25, and 50% on frost resistance of SCC, with and without the addition of deicing agents, in line with the provisions of CEN/TS 12390-9 and ASTM C666.

All RCA concretes met the resistance criteria for exposure classes XF1 and XF3, with a durability factor of over 90% and scaled materials weighing under 0.1 kg/m^2 after 56 cycles. However, the same concrete mixtures are not resistant to freeze–thaw (f/t) in the presence of de-icing salts – exposure classes XF2 and XF4, generating scaled material weighing over 1.00 kg/m^2 and grade 5 visual deterioration.

Although the use of SCC in Bosnia and Herzegovina is extremely limited, a portion of the professional public has recognized the benefit of using this concrete technology to

produce prefabricated buffers on roads, which are among the most vulnerable to the aggressive simultaneous effects of frost and salt.

Figure 1 illustrates the progressive deterioration of traditional concrete safety barriers, raising concerns about safety and necessitating expensive replacement costs. The first series of barriers built by SCC were constructed in Banjaluka in the city parking area and on sections of the Banjaluka-Gradiška highway (Figure 2). It turns out that the first-placed blocks made using the SCC-NCA recipe (given in the experimental section of this study) have not been affected by any degradation mechanisms after 12 years of use.

Figure 1. Safety barrier built of traditional concrete with NRA

Figure 2. Safety barrier built of SCC-NCA, highway Banja Luka –Gradiška, after 12 years of exploitation

This research investigated the effects of various natural aggregates (NA) and their combinations, as well as recycled aggregates (RCA) generated by crushing waste concrete, on the resistance of SCC to frost effects with and without the presence of de-icing agents. Water absorption tests via gradual immersion and vacuuming were chosen as an indirect method.

2 Experimental study

As part of the experiment, six different types of concrete mixes were tested to see how the type of aggregate affected the resistance of SCC to frost, with and without de-icing salt. Natural aggregates (river – NRA and/or crushed – NCA) and recycled aggregates (known – RCA-N and unknown origin – RCA-A) were utilized. All aggregate mixes are designed with three fractions, with a nominal grain size of 16 mm.

The concrete mixtures labels and aggregate types utilized are listed below:

- SCC-NRA–self-compacting concrete produced with natural river aggregate,
- SCC-NCA–self-compacting concrete produced with natural crushed aggregate,
- SCC-NMA-I–self-compacting concrete produced with a mixture of natural river and natural crushed aggregate (water to cement ratio = 0.40),
- SCC-NMA-II–self-compacting concrete produced with a mixture of natural river and natural crushed aggregate (water to cement ratio = 0.43),
- SCC-RCA-N–self-compacting concrete is produced with a mixture of fine river aggregate and coarse recycled concrete aggregate of known origin and
- SCC-RCA-A–self-compacting concrete is produced with a mixture of fine river aggregate and coarse recycled concrete aggregate of unknown origin.

The following properties were tested on fresh concrete:

- temperature, according to EN 12350-1 [23] and SRPS U.M1.032 [24],
- density, according to EN 12350-6 [25],
- entrapped air content, according to EN 12350-7 [26] and
- consistency, according to EN 12350-8 [27].

The following properties were tested on hardened concrete:

- compressive strength at the age of 28 days, according to EN 12390-3 [28],
- water absorption by the test of gradual immersion at atmospheric pressure, according to EN 13755 [29],
- water absorption by vacuuming, according to EN 1936 [30],
- freeze/thaw resistance, according to SRPS U.M1.016 [31] and
- freeze/thaw resistance with a de-icing agent, according to SRPS U.M1.055 [32].

2.1 Component materials

The following materials were utilized for concrete production:

- Cement CEM II/B-M (S-LL) 42,5 N, "Dalmatia-cement", "St. Juraj" Split, (Kaštel Sućurac), specific gravity of 3140 kg/m^3,
- Addition type I –limestone filler, "Japra" Ltd. Novi Grad, specific gravity of 2780 kg/m^3,
- Aggregates:
  - NRA – river aggregate "Petroševci", "Road Structures" Laktaši, Bosnia and Herzegovina, were washed and separated into fractions of 0/4, 4/8, and 8/16 mm (the results of the tested properties are listed in Table 1);
  - NCA – crushed aggregate "Dobrnja", "Binis", Banja Luka, Bosnia and Herzegovina, separated into fractions of 0/4, 4/8, and 8/16 mm (the results of the tested properties are listed in Table 2);

- RCA-N – recycled aggregate of known origin, obtained by crushing waste concrete classes C25/30 and C35/45, fractions of 4/8 and 8/16 mm (the results of the tested properties are listed in Table 3);
- RCA-A – recycled aggregateof unknown origin, obtained by crushing waste concrete taken from the construction debris landfill, fractions of 4/8 and 8/16 mm (the results of the tested properties are listed in Table 4);
- Admixture–superplasticizer "Cementol®Zeta Super S", "TKK", Srpenica, Slovenia, and
- Tap water.

Table 1. Physical, mechanical and chemical properties of NRA

Property	Standard	Units of measurement and category, according to EN 12620		Fraction		
				0/4 mm	4/8 mm	8/16 mm
Loose bulk density	EN 1097-3 [33]	[kg/m^3]		1606	1554	1582
Particle density	EN 1097-6[34]	[kg/m^3]		2740	2696	2683
Water absorption	EN 1097-6	[%]		0.6	0.8	0.4
Resistance to weathering	EN 1367-2 [35]	[%]	MS_{18}	0.6	0.6	1.3
Total sulphur content (SO_3)	EN 1744-1 [36]	[%]	S_1	0	0	0
Water-soluble chloride ion content (Cl^-)	EN 1744-1	[%]	-	0.007	0.007	0.007
Resistance to fragmentation (LA)	EN 1097-2 [37]	[%]	LA_{30}		27.4	

Table 2. Physical, mechanical and chemical properties of NCA

Property	Standard	Units of measurement and category, according to EN 12620		Fraction		
				0/4 mm	4/8 mm	8/16 mm
Loose bulk density	EN 1097-3	[kg/m^3]		1546	1354	1318
Particle density	EN 1097-6	[kg/m^3]		2709	2746	2718
Water absorption	EN 1097-6	[%]		1.64	1.22	0.71
Resistance to weathering	EN 1367-2	[%]	MS_{18}	0.2	0.2	0.1
Total sulphur content (SO_3)	EN 1744-1	[%]	S_1	0	0	0
Water-soluble chloride ion content (Cl^-)	EN 1744-1	[%]	-	0.014	0.014	0.014
Resistance to fragmentation (LA)	EN 1097-2	[%]	LA_{30}		28.6	

Table 3. Physical, mechanical and chemical properties of RCA-N

Property	Standard	Units of measurement and category, according to EN 12620		Fraction	
				4/8 mm	8/16 mm
Loose bulk density	EN 1097-3	[kg/m^3]		1278	1231
Particle density	EN 1097-6	[kg/m^3]		2350	2350
Water absorption*	EN 1097-6	[%]		2.4	2.2
Resistance to weathering	EN 1367-2	[%]	MS_{18}	1.0	0.5
Total sulphur content (SO_3)	EN 1744-1	[%]	S_1	0.04	0.04
Water-soluble chloride ion content (Cl^-)	EN 1744-1	[%]	-	0.007	0.007
Resistance to fragmentation (LA)	EN 1097-2	[%]	LA_{25}	23.1	

*Note: after 30 min in accordance with [5], [38].

Table 4. Physical, mechanical and chemical properties of RCA-A

Property	Standard	Units of measurement and category, according to EN 12620		Fraction	
				4/8 mm	8/16 mm
Loose bulk density	EN 1097-3	[kg/m^3]		1267	1221
Particle density	EN 1097-6	[kg/m^3]		2330	2330
Water absorption*	EN 1097-6	[%]		3.6	3.1
Resistance to weathering	EN 1367-2	[%]	MS_{18}	1.0	0.5
Total sulphur content (SO_3)	EN 1744-1	[%]	S_1	0.04	0.04
Water-soluble chloride ion content (Cl^-)	EN 1744-1	[%]	-	0.007	0.007
Resistance to fragmentation (LA)	EN 1097-2	[%]	LA_{25}	21.8	

*Note: after 30 min in accordance with[5], [38].

2.2 Mix proportion

The mixtures were designed to meet the SF2 consistency class criteria (according to The European Guidelines for Self-Compacting Concrete, Specification, Production, and Use, 2005), i.e., to provide the requisite slump-flow range of 660 to 750 mm.

Table 5 displays the component material quantities in 1 m^3 of the designed concrete mixtures, as well as the water-to-cement ratio and computed densities of concrete in the fresh state.

2.3 Experimental program

Mixing was performed in a laboratory mixer manufactured by "CONTROLS", model "TTM 140V". The temperature of the fresh concrete was measured using digital thermometers manufactured by "CONTROLS", model "82-D1226/A" and manufactured by "HANNA", according to EN 12350-1. The consistency assessment was conducted by using the slump-flow test, according to EN 12350-8, at the normal position of the cone during the test. Tests were performed using an Abrams cone, manufactured by "CONTROLS", model "C150/A" and a baseplate, manufactured by the same manufacturer, model "54 C0149/20". The entrapped air content was measured by the pressure gauge method, according to EN 12350-7. As all the utilized aggregates belong to the group of normal-weight aggregates, the value of G is negligible and was consequently set to zero in accordance with the standard. According to EN 12350-6, the density of fresh concrete was derived as a mean value measured on three cube-shaped samples with a 15cm edge.

The compressive strength was obtained as a mean value measured on three cube-shaped samples, with an edge of 15 cm, at the age of 28 days, according to EN 12390-3.

Table 5. Mixture compositions, water-to-cement ratio and density of designed SCC

Mix identity				SCC-NRA	SCC-NCA	SCC-NMA-I	SCC-NMA-II	SCC-RCA-N	SCC-RCA-A
Cement			[kg/m^3]	453	448	460	442	450	450
Limestone filler			[kg/m^3]	181	153	169	162	196	193
Aggregate	NRA	0/4 mm	[kg/m^3]	909	–	337	332	832	860
		4/8 mm	[kg/m^3]	185	–	–	–	–	–
		8/16 mm	[kg/m^3]	460	–	–	–	–	–
	NCA	0/4 mm	[kg/m^3]	–	827	481	474	–	–
		4/8 mm	[kg/m^3]	–	239	237	233	–	–
		8/16 mm	[kg/m^3]	–	539	534	526	–	–
	RCA	4/8 mm	[kg/m^3]	–	–	–	–	234	262
		8/16 mm	[kg/m^3]	–	–	–	–	394	335
Admixture – HRWRA			[kg/m^3]	6.74	6.73	6.61	6.58	6.75	6.75
Effective water			[kg/m^3]	202.4	188.7	183.6	190.4	189.0	189.0
Additional water*			[kg/m^3]	–	–	–	–	14.3	19.9
Water-cement ratio			[–]	0.45	0.42	0.40	0.43	0.42	0.42
Density			[kg/m^3]	2397	2401	2408	2366	2316	2316

*Note: Aiming to reach the required consistency, an additional amount of water, which the recycled aggregate absorbs in 30 minutes, was added (in accordance with the guidelines [39], [40]).

In the absence of a suitable standard for testing SCC water absorption, stone material water absorption regulations were used, including the progressive immersion at air pressure method – EN 13755 [29] and the vacuum method – EN 1936 [30]. The collected data were used to calculate the saturation coefficient, determined as the ratio of water absorption obtained by the gradual immersion method to absorption obtained by vacuuming. Based on practical experience, this value may be utilized as an indirect measure of frost resistance in concrete [41]. The number of specimens required for testing one concrete mixture is nine for the gradual immersion method (Figure 3), and three for testing by vacuuming (Figure 4).

The destructive approach was used to test the frost resistance of concrete in accordance with the national standard SRPS U.M1.016 [31]. Each concrete mixture contains fifteen specimens, separated into the following groups:

- E_0 - reference specimens, whose compressive strength is determined on the day the test starts,
- E_I - reference specimens that were not exposed to freezing, whose compressive strength is determined on the day of equivalent age, compared to specimens that were exposed to 150 f/t cycles,
- E_{II} - reference specimens that were not exposed to freezing, whose compressive strength is determined on the day of equivalent age, compared to specimens that were exposed to 200 f/t cycles,
- M_{150} - specimens exposed to 150 f/t cycles and
- M_{200} - specimens exposed to 200f/t cycles.

The concrete surface's resistance to frost and de-icing salt was tested in accordance with SRPS U.M1.055 [32], which included 25 f/t cycles. Four prism specimens with dimensions of 15x7.5x7.5 cm were tested for the SCC-NRA, SCC-NCA, SCC-NMA-I, and SCC-NMA-II concretes, while three cube specimens with edge lengths of 15 cm were tested for the SCC-RCA-N and SCC-RCA-A concretes.

The freezing-thawing procedure was carried out for both test methods in the cooling chamber of the manufacturer "CONTROLS", model – 65-D1409, with a capacity of 50 kg and the ability to maintain a constant air temperature from -20^{0}C to +65^{0}C with an accuracy of 0,1^{0}C and automatic air temperature registration.

3 The results

Table 6 shows the findings of testing concrete in its fresh form – temperature (T), density (D), entrapped air content (Ac), and the slump-flow (SF)

Figure 3. Water absorption by the test of gradual immersion at atmospheric pressure

Figure 4. Water absorption by vacuuming

Table 6. Test results of fresh concrete properties

Mix identity	T [^{o}C]	D [kg/m^3]	A_c [%]	SF [mm]
SCC-NRA	26	2396	1.1	760
SCC-NCA	25	2400	1.8	700
SCC-NMA-I	27	2408	2.0	650
SCC-NMA-II	27	2366	3.0	630
SCC-RCA-N	29	2316	4.2	660
SCC-RCA-A	29	2317	4.2	710

Table 7 illustrates the results of the compressive strength at the 28 days of age ($f_{c,cube,28}$), absorption by the gradual immersion method (A_b), absorption by vacuuming (A_p), and the calculated saturation coefficient (k_p).

Table 8 displays the mean compressive strengths of the reference specimens, tested on the first day of f/t cycles, fc, cyl(E0), specimens subjected to 150 and 200 f/t cycles, fc,cyl (M150) and fc,cyl (M200), and reference specimens of equivalent age, fc,cyl (EI) and fc,cyl (EII).

Table 9 displays the results of testing f/t resistance with de-icing salt as the least favorable values of the cumulative results of mass loss (L) and depth of damage (H_{FTR-S}) measurements, visual assessment, and damage degree. Figures 5-14 also illustrate the photographed surfaces of the specimens before and after the first and 25th test cycles, as well as after the NaCl solution was removed from the samples.

Table 7. Test results of compressive strength, water absorption and concrete saturation indicators

Mix identity	$f_{c,cube,28}$ [MPa]	A_b [%]	A_p [%]	k_p [-]
SCC-NRA	59.1	3.332	5.164	0.645
SCC-NCA	63.1	3.219	3.845	0.814
SCC-NMA-I	54.1	3.229	3.982	0.811
SCC-NMA-II	47.1	3.398	4.753	0.715
SCC-RCA-N	65.1	3.612	6.414	0.563
SCC-RCA-A	60.9	3.822	6.507	0.587

Table 8. Test results of freeze/thaw resistance

Mix identity	$f_{c,cyl}(E_0)$	$f_{c,cyl}(E_I)$*	$f_{c,cyl}(M_{150})$ [MPa]	$f_{c,cyl}(E_{II})$*	$f_{c,cyl}(M_{200})$
SCC-NRA	56.3	62.7	61.8	66.1	57.4
SCC-NCA	63.0	70.7	64.8	74.4	65.0
SCC-NMA-I	55.3	69.8	69.0	72.6	65.1
SCC-NMA-II	57.3	64.4	63.5	65.6	62.9
SCC-RCA-N	65.9	66.0	65.8	66.1	60.7
SCC-RCA-A	60.1	60.3	59.3	60.3	47.5

*Note: The equivalent age is lower than the calendar age and is determined according to the standard due to the slow increase in compressive strength during the freezing period.

Table 9. Test results of freeze/thaw resistance with de-icing salt

Sample mark	Number of f/t cycles	L [mg/mm^2]	H_{FTR-S} [mm]	Visual assessment	Damage degree*
SCC-NRA	5	0.01	0.00	without surface changes	0 – without scaling
	10	0.02	0.00	without surface changes	0 – without scaling
	15	0.04	0.03	without surface changes	0 – without scaling
	20	0.07	0.05	local damage of cement mortar	0 – without scaling
	25	0.10	0.08	damage of cement mortar	1 – a little scaling
SCC-NCA	5	0.00	0.00	without surface changes	0 – without scaling
	10	0.00	0.00	without surface changes	0 – without scaling
	15	0.00	0.00	without surface changes	0 – without scaling
	20	0.01	0.00	without surface changes	0 – without scaling
	25	0.02	0.01	without surface changes	0 – without scaling
SCC-NMA-I	5	0.00	0.00	without surface changes	0 – without scaling
	10	0.00	0.00	without surface changes	0 – without scaling
	15	0.00	0.00	without surface changes	0 – without scaling
	20	0.01	0.01	without surface changes	0 – without scaling
	25	0.03	0.02	without surface changes	0 – without scaling

Sample mark	Number of f/t cycles	L [mg/mm^2]	H_{FTR-S} [mm]	Visual assessment	Damage degree*
SCC-NMA-II	5	0.00	0.00	without surface changes	0 – without scaling
	10	0.00	0.00	without surface changes	0 – without scaling
	15	0.00	0.00	without surface changes	0 – without scaling
	20	0.01	0.01	without surface changes	0 – without scaling
	25	0.03	0.02	without surface changes	0 – without scaling
SCC-RCA-N	5	0.00	0.00	without surface changes	0 – without scaling
	10	0.03	0.04	without surface changes	0 – without scaling
	15	0.08	0.10	local damage of cement mortar	0 – without scaling
	20	0.10	0.15	damage of cement mortar	1 – a little scaling
	25	0.12	0.20	damage of cement mortar	1 – a little scaling
SCC-RCA-A	5	0.01	0.00	without surface changes	0 – without scaling
	10	0.05	0.06	without surface changes	0 – without scaling
	15	0.06	0.12	local damage of cement mortar	0 – without scaling
	20	0.09	0.18	damage of cement mortar	1 – a little scaling
	25	0.12	0.25	damage of cement mortar	1 – a little scaling

*Note:0 – without scaling (L≈0mg/mm^2, H_{FTR-S}≈0 mm),1 – a little scaling (L≈0.2 mg/mm^2, H_{FTR-S}≈1.0 mm), 2 – medium scaling (L≈0.5 mg/mm^2, H_{FTR-S}≈4.0 mm),3 – severe scaling (L≈1.0 mg/mm^2, H_{FTR-S}≈10.0 mm).

Figure 5. SCC-NRA surface appearance before testing

Figure 6. SCC-NRA surfaceappearance after 25 f/t cycles with de-icing salt

Figure 7. SCC-NCA surface appearance before testing

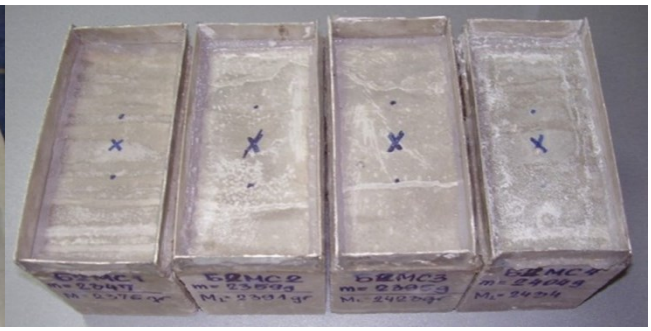

Figure 8. SCC-NCA surface appearance after 25 f/t cycles with de-icing salt

Figure 9. SCC-NMA-I surface appearance before testing

Figure 10. SCC-NMA-I surface appearance after 25 f/t cycles with de-icing salt

Figure 11. SCC-NMA-II surface appearance before testing

Figure 12. SCC-NMA-II surface appearance after 25 f/t cycles with de-icing salt

Figure 13. SCC-RCA-N and SCC-RCA-Asurfaces appearance before testing

Figure 14. SCC-RCA-N and SCC-RCA-Asurfaces appearanceafter 25 f/t cycles with de-icing salt

4 The results analysis and discussion

4.1 Freeze-thaw resistance

The frost resistance coefficient, calculated as the ratio of the mean value of the compressive strength of the specimens subjected to f/t cycles and the mean value of the compressive strength of the reference samples tested at the equivalent age, was used to assess freeze-thaw resistance. The results of testing the frost resistance revealed that for all of the concretes tested, the frost resistance coefficient is not below 75% (150 and 200 cycles) (Figure 15). According to the criterion [31], all tested types of concrete meet the quality requirements after 150 and 200 f/t cycles.

A more comprehensive analysis of the acquired results revealed that the type of aggregate used, the achieved compressive strength, and porosity all have an effect on the resistance of concrete to frost effects.

Frost resistance is the lowest in SCC-RCA-A. This concrete has great resistance up to 150 cycles, and after only 50 additional cycles, the indicator of its resistance has dropped by 24.1% (which is much higher than the 8.3% average decline of all other concrete types). Furthermore, after 200 cycles of frost exposure, the SCC-RCA-A specimens were physically destroyed, evaluated visually, and documented by mass loss (5%), implying that this concrete would not exceed the more severe frost resistance requirements. Results of water absorption support these findings. Regardless of the exceptionally beneficial value of

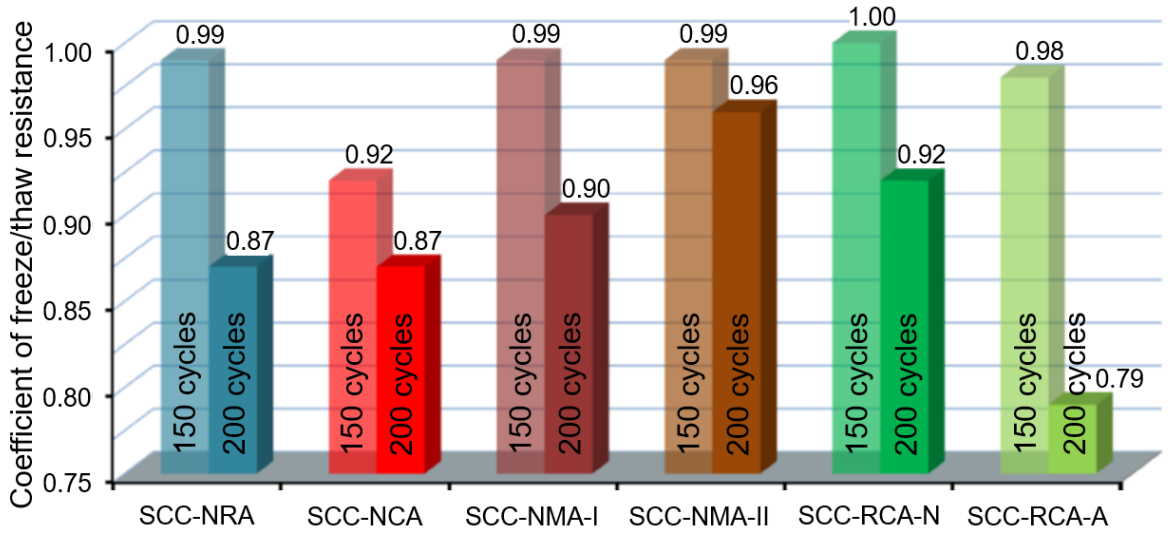

Figure15. The frost resistance coefficient (r_{FTR})

k_p, the largest values of water absorption (by both methods used) also contribute to the least desirable frost result after 200 cycles.

SCC-RCA-N exhibits a completely different behavior due to the effects of frost. This concrete has a high degree of resistance for both series of f/t cycles (150 and 200), with a decline in frost resistance coefficient (r_{FTR}) of about 8.3% between the 200 and 150 cycles. Except for SCC-RCA-A, this is close to the average abovementioned value. When compared to the SCC-NRA concrete, the SCC-RCA-N concrete is found to be more frost-resistant. SCC-NRA and SCC-RCA-N concretes were chosen for comparison as the original RCA-N grains employed are of river origin (the aggregates differ in the presence of old cement stone). This implies that, based on the investigated attributes, the presence of old cement stone in RCA is not a disadvantage of this aggregate. Furthermore, the pores of the old cement stone in RCA enabled the migration of water from the new transition zone and, therefore, the expansion of ice during freezing. Similarly, Öznur et al. [19] reported that the strength reductions after 300 f/t cycles for the application of 10, 20, and 30% pumice in the coarse aggregate are lower compared to reference concrete (due to the porous structure of pumice, a comparison with RCA can be made to some extent). In the case of SCC-RCA-N concrete, a higher porosity of the cement stone was obtained, implying a greater pore space (large pores and capillaries) for ice expansion and water migration during freezing (a lower k_p value). As a result, porosity also has an impact on concrete's resistance to frost. When comparing the concrete SCC-NCA, SCC-NMA-I, and SCC-NMA-II, the same rule applies.

In addition to the frost resistance coefficient of concrete after 200 cycles (r_{FTR}), the values of the 28-day compressive strength of concrete ($f_{c,cube,28}$), entrapped air content (A_c), and saturation coefficient (k_p) are illustrated in Figure 16 for easier comparison and calculation of mutual dependency. A following correlation for concretes produced with crushed aggregate and dominantly crushed aggregate (SCC-NCA, SCC-NMA-I and SCC-NMA-II) may be detected: greater frost

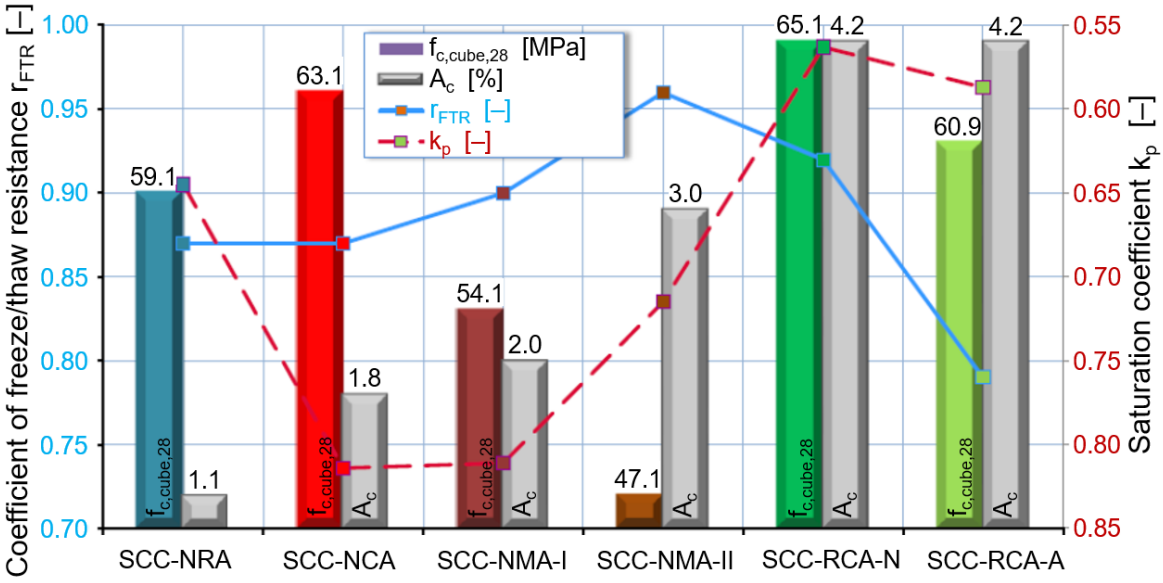

Figure16. Frost resistance coefficient as a function of influencing parameters

resistance – lower compressive strength – higher air content– lower saturation coefficient. Based on these observations, the effect of replacing a portion of the fine fraction of crushed aggregate with river aggregate in the tested concretes can be ignored.

When comparing concrete with river and crushed aggregate, it is clear that there is no substantial difference in frost resistance.

According to the preceding, due to the distinctive behavior of RCA during frost action,natural aggregates are the only ones that have a reliable one-parameter functional dependence on one of the influential properties of concrete. With the inclusion of RCA, such a strong correlation in functional dependence could not be achieved, as when only NA is addressed. The obtained compressive strength, in particular, has less of an impact on the frost resistance of RCA concrete than it does on NA concrete. Figure 17 displays the relationship between the frost resistance coefficient and the compressive strength of concrete made with natural aggregates, which can be explained by the following formula:

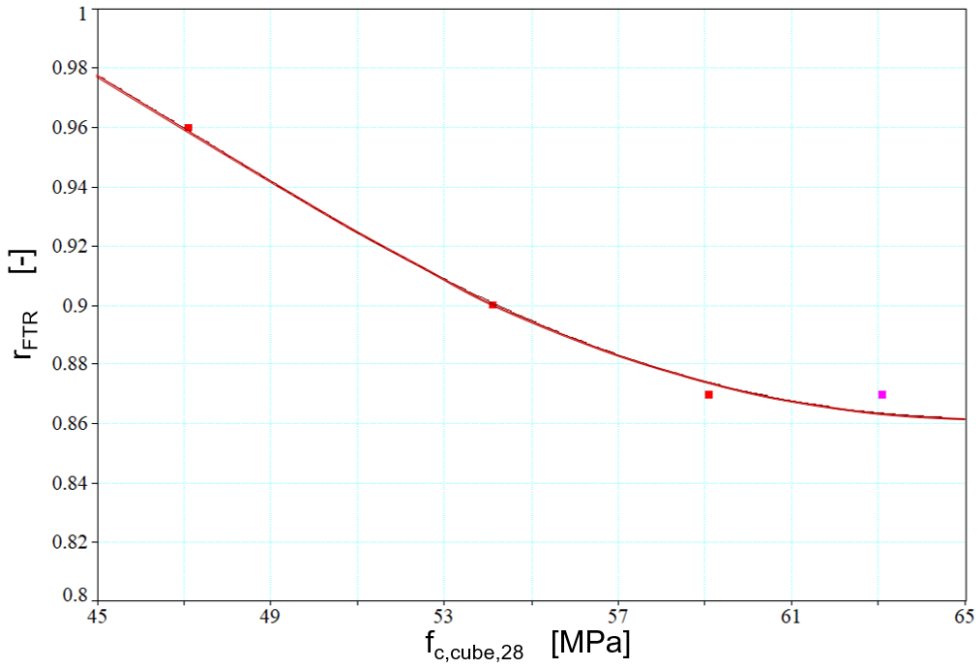

Figure 17. Frost resistance coefficient of concrete produced with NA as a function of compressive strength

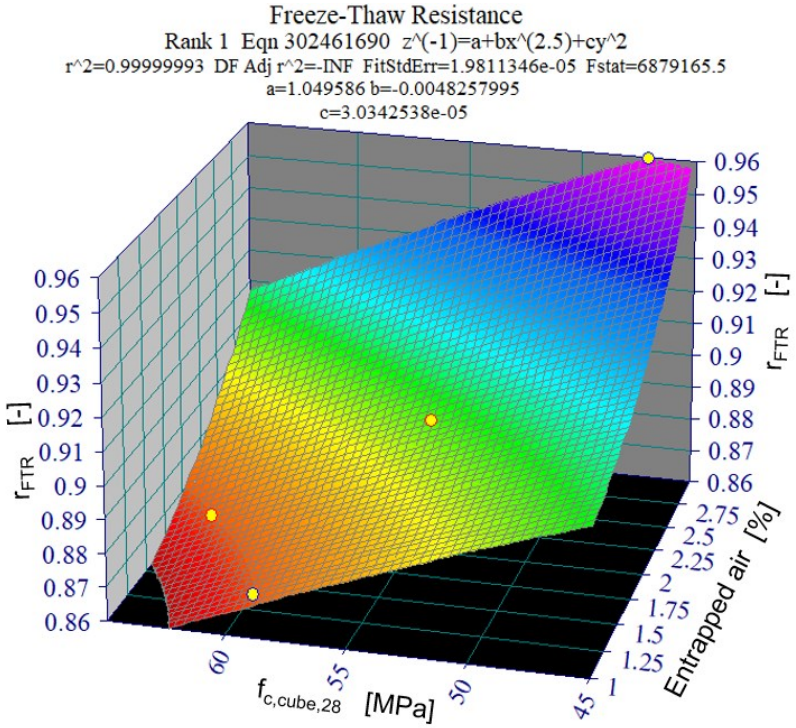

Figure18. Frost resistance coefficient of concrete produced with NA as a function of compressive strength and entrapped air content

$$r_{FTR} = -1.5827 \cdot 10^{-6} - 1.6796 \cdot 10^{-2} \cdot f_{c,cube,28} + 6.5056 \cdot 10^{-3} \cdot f_{c,cube,28}^{2} - 2.7345 \cdot 10^{-4} \cdot f_{c,cube,28}^{3} + 4.\dot{7} \cdot 10^{-6} \cdot f_{c,cube,28}^{4} - 3.8404 \cdot 10^{-8} \cdot f_{c,cube,28}^{5} + 1.1719 \cdot 10^{-10} \cdot f_{c,cube,28}^{6} \quad [–] \quad (1)$$

R^2 = 0,9949326674

where:

r_{FTR} – frost resistance coefficient after 200 f/t cycles,
$f_{c,cube,28}$ – compressive strength at the age of 28 days, MPa and
R – correlation coefficient.

Using the TableCurve 3D v4.0 software, which allows for the establishment of a two-parameter dependence of the analyzed property, a correlation between frost resistance, compressive strength, and percentage of entrapped air in fresh concrete produced with natural aggregates was obtained. Figure 18 depicts the aforementioned function, denoted by the expression:

$$r_{FTR} = \frac{1}{1.049586 - 0.004826 \cdot A_c^{2.5} + 3.03425 \cdot 10^{-5} \cdot f_{c,cube,28}^{2}} \quad [–] \quad (2)$$

R^2 = 0,9999999273

where:

r_{FTR} – frost resistance coefficient after 200 f/t cycles,
A_c – entrapped air content, %,
$f_{c,cube,28}$ – compressive strength at the age of 28 days, MPa and
R – correlation coefficient.

4.2 Resistance to the simultaneous action of frost and de-icing salt

All of the tested concretes met the requirements for the grade "frost resistant" after 25 f/t cycles in the presence of a 3% salt solution, according to SRPS U.M1.055.

A deeper review of the test findings revealed that the aggregate type influences the mass of scaled material and the depth of concrete surface damage caused by the simultaneous action of frost and de-icing salts. Crushed aggregate (concrete SCC-NCA) application yields the best test results – the so-called zero degree of damage, with no sign of surface alterations during visual inspection. A zero degree of damage was also noted by replacing part of the fine fraction of the crushed aggregate with river aggregate (concretes SCC-NMA-I and SCC-NMA-I), with no clear indications of changes in the surface during the visual evaluation. Only sporadic changes in shade and the "smoothness" of the concrete surface are observed under a microscope.

Furthermore, according to the analyzed effect, still good resistance is obtained by employing river aggregate (SCC-NRA), rated with the degree of damage "1" –localized damage to the cement stone is detected. Finally, although meeting the criteria for the grade "resistant" with the degree of damage "1", the SCC-RCA-N and SCC-RCA-A concretes have evident surface damages to the cement stone.

Given that these damages are distributed across the entire exposed surface of the concrete, SCC-RCA-N and SCC-RCA-A are unlikely to achieve the higher requirements for resistance to the simultaneous actions of frost and salt. At the same time, the type of RCA based on their origin is irrelevant, RCA-A delivered negligibly less favorable results. The aforementioned result is supported by the work of Bosque et al. [22], who employed a blend of RCA-N and RCA-A as RCA. Those concretes, like in the subject experiment, demonstrated greater resistance to the action of frost in the absence of de-icing salt than in the presence of salt.

Bosque et al. [22] employed a greater number of f/t cycles with de-icing agents (56 cycles) in their study. The concretes were found to be non-resistant for exposure classes XF2 and XF4.

5 Conclusion and recommendation

This paper aimed to explore the effects of aggregate type on the level of degradation of self-compacting concrete due to freeze-thaw action. The key conclusions that arise from the study are given below:

- The frost resistance of concrete is determined by the type of aggregate used. This mostly concerns the decision between recycled concrete aggregate of unknown origin and other, more often used types of aggregate (river, crushed, blend of river and crushed, and recycled concrete aggregate of known origin). The use of recycled concrete aggregate of unknown origin reduces frost resistance compared to the resistance of concrete to some of the other aggregate types. The frost resistance reduction occurs only after 200 f/t cycles, which was undoubtedly aided by the fact that this concrete is characterized by: 1) a greater amount of cement stone; 2) the greatest amount of absorbed water; and 3) the highest possibility that ingredients that reduce the quality of the aggregate remain to a lesser extent (it should be noted that the raw material used to produce this aggregate was recycled concrete). As a result, it cannot be envisaged that the use of recycled aggregate of unknown origin will meet the more demanding requirements for frost resistance. However, using all of the listed materials and the technology for producing self-compacting powder-type concrete, it was discovered that it was possible to produce concrete resistant to 200 f/t cycles.

- The choice of river and/or crushed or recycled material of known origin has no major effect on frost resistance. It has been demonstrated that the lower the compressive strength of the concrete, the higher the air content, and the lower the saturation coefficient, the better the resistance to frost impacts. It should be emphasized that these findings are specific to SCC and may not entirely apply to other types of concrete, such as typical normal-weight concrete.
- Very reliable functional correlations between frost resistance coefficient and compressive strength, as well as two-parameter functions between frost resistance coefficient, compressive strength, and entrapped air percentage, were established for concrete produced with natural aggregates.
- In terms of resistance to the simultaneous impacts of frost and deicing salt, all tested types of SCC meet the standard's requirements. However, the quality of the concrete surfaces differs once the test cycles are completed. It was discovered that the type of aggregate has the greatest impact. In comparison to the other concrete parameters studied in the experiment, it was established that the type of aggregate used had the largest influence on the degree of damage to the concrete surface.
- The following aggregate grades may be established in terms of favorability to frost resistance with and without de-icing salt: crushed natural aggregate, mixture of natural crushed and river aggregate, natural river aggregate, recycled concrete aggregate of known origin, and recycled concrete aggregate of unknown origin.
- Although it meets the prescribed requirements for frost resistance with and without de-icing salt, recycled concrete aggregate should be used sparingly. It is especially not recommended for the production of concrete used for structural repair, bridge structures, concrete pavements, elements that will be exposed to a direct sprinkling of deicing salt solutions during exploitation, hydrotechnical concrete in highly aggressive environments, and generally hydrotechnical concrete that is exposed to changing water levels in climates with cold climatic conditions in the winter period.

Acknowledgement

The paper presents the part of research realized within the project "Development of new binders based on agricultural and industrial waste from the area of Vojvodina for the production of eco-friendly mortars" financed by the Provincial Secretariat for Higher Education and Scientific Research in Vojvodina.

The authors gratefully acknowledge the resources and expertise provided within the experimental program by "The Institute for testing, assessment, and repair of structures doo" in Novi Sad, Serbia.

References

[1] K. Ma, K. Feng, Z. Wang, G. Long, Y. Xie, W. Li, Mechanical properties and crack evolution of SCC with macro-crack under freeze-thaw cycles, Journal of Building Engineering 69 (2023) 106323. https://doi.org/10.1016/j.jobe.2023.106323

[2]J. Nilimaa, V. Zhaka, An Overview of Smart Materials and Technologies for Concrete Construction in Cold Weather,Eng 4 (2023) 1550–1580. https://doi.org/10.3390/eng4020089

[3] H. Luan, J. Wu, F. Geng, X. Zhao, Z. Li,Freezing Characteristics of Deicing Salt Solution and Influence on Concrete Salt Frost Deterioration,Journal of Advanced Concrete Technology 21 (2023) 643-654. doi:10.3151/jact.21.643 https://www.jstage.jst.go.jp/article/jact/21/8/21_643/_pdf

[4] P. Misák, D. Kocáb, P. Bayer, T. Vymazal, P. Rovnaníková, Effect of De-Icing Chemicals on Concrete Scaling: The Role of Storage Water, Materials 16 (2023) 4928. https://doi.org/10.3390/ma16144928

[5] M. Malešev, V. Radonjanin, S. Marinković, Recycled Concrete as Aggregate for Structural Concrete Production, Sustainability, 2, no. 5 (2010) 1204-1225. https://doi.org/10.3390/su2051204

[6] P. O. Modani, V. M. Mohitkar, Self-compacting concrete with recycled aggregate: A solution for sustainable development, International Journal of Civil and Structural Engineering 4-1 (2014) 430-440. https://www.ijert.org/research/recycled-aggregate-self-compacting-concrete-a-sustainable-concrete-for-structural-use-IJERTV4IS010200.pdf

[7] M. G. Beltrán, F. Agrela, A. Barbudo, J. Ayuso A. Ramírez, Mechanical and durability properties of concretes manufactured with biomass bottom ash and recycled coarse aggregates, Construction and Building Materials 72 (2014) 231-238. https://doi.org/10.1016/j.conbuildmat.2014.09.019

[8] M. Malešev, V. Radonjanin, G. Broćeta, Properties of recycled aggregate concrete, Contemporary Materials 5-2 (2014) 240-249. https://doi.org/10.7251/COMEN1402239M

[9] M. Gesoglu, E. Güneyisi, H. ÖznurÖz, M. Taner Yasemin, I. Taha, Durability and Shrinkage Characteristics of Self-Compacting Concretes Containing Recycled Coarse and/or Fine Aggregates, Advances in Materials Science and Engineering 2015 (2015) 278296.1-18. https://doi.org/10.1155/2015/278296

[10] V. Bulatović, M. Malešev, M. Radeka, V. Radonjanin, I. Lukić, Evaluation of sulfate resistance of concrete with recycled and natural aggregates, Construction and Building Materials 152 (2017) 614-631. https://doi.org/10.1016/j.conbuildmat.2017.06.161

[11] A. Singh, Z. Duan, J. Xiao, Q. Liu, Incorporating recycled aggregates in self-compacting concrete: a review, Journal of Sustainable Cement-Based Materials 9-3 (2020) 165-189. https://doi.org/10.1080/21650373.2019.1706205

[12] D. V. P. Tran, A. Allawi, A. Albayati, T. N. Cao, A. El-Zohairy, Y. T. H. Nguyen, Recycled Concrete Aggregate for Medium-Quality Structural Concrete, Materials 14 (2021) 4612.1-16. https://doi.org/10.3390/ma14164612

[13] T. Ayub, W. Mahmood, A.R. Khan, Durability Performance of SCC and SCGC Containing Recycled Concrete Aggregates: A Comparative Study, Sustainability 13-15 (2021) 8621.1-21. https://doi.org/10.3390/su13158621

[14] L. Pereira-de-Oliveira, M. Nepomuceno, J. Castro-Gomes, M. Vila, Permeability properties of self-compacting concrete with coarse recycled aggregates, Construction and Building Materials 51 (2014) 113-120. https://doi.org/10.1016/j.conbuildmat.2013.10.061

[15] I. Despotović, Properties of self-compacting concrete made of recycled aggregates and various mineral

additives, Građevinskimaterijaliikonstrukcije, vol. 58, no. 4 (2015) 3-20. https://doi.org/10.5937/grmk1504003D.
[16] M. Tuyan, A. Mardani-Aghabaglou, K. Ramyar, Freeze–thaw resistance, mechanical and transport properties of self-consolidating concrete incorporating coarse recycled concrete aggregate, Materials & Design 53 (2014) 983-991. https://doi.org/10.1016/j.matdes.2013.07.100
[17] M. Shahul Hameed, A. S.S. Sekar, S. Velu, Strength and Permeability Characteristics Study of Self-Compacting Concrete Using Crusher Rock Dust and Marble Sludge Powder, Arabian Journal for Science and Engineering 37 (2012) 561-574. https://doi.org/10.1007/s13369-012-0201-x
[18] A. Jain, R. Gupta, S. Chaudhary, Sustainable development of self-compacting concrete by using granite waste and fly ash, Construction and Building Materials 262 (2020) 120516. https://doi.org/10.1016/j.conbuildmat.2020.120516
[19] H. ÖznurÖz, H. Erhan Yücel, M. Güneş, Freeze-Thaw Resistance of Self Compacting Concrete Incorporating Basic Pumice, Theoretical and Applied Mechanics 1 (2016) 285-291. https://www.iaras.org/iaras/filedownloads/ijtam/2016/009-0043.pdf
[20] S.B. Huda, M.S.Alam,Mechanical and Freeze-Thaw Durability Properties of Recycled Aggregate Concrete Made with Recycled Coarse Aggregate, Journal of Materials in Civil Engineering 27-10 (2015) 04015003. https://doi.org/10.1061/(ASCE)MT.1943-5533.0001237
[21] H. Yan, Qi. Liu, F. Han, S. Liu, T. Han, B. He,Frost Durability of Self-Compacting Concrete Prepared with Aeolian Sand and Recycled Coarse Aggregate, Materials 16-19 (2023) 6393. https://doi.org/10.3390/ma16196393
[22] I.F. Sáez del Bosque, P. Van den Heede, N. De Belie, M.I. Sánchez de Rojas, C. Medina, Freeze-thaw resistance of concrete containing mixed aggregate and construction and demolition waste-additioned cement in water and de-icing salts, Construction and Building Materials 259 (2020) 119772. https://doi.org/10.1016/j.conbuildmat.2020.119772
[23] EN 12350-1:2019Testing fresh concrete – Part 1: Sampling and common apparatus.
[24] SRPS U.M1.032:1981 Concrete – Measuring temperature of concrete.
[25] EN 12350-6:2019Testing fresh concrete – Part 6: Density.
[26] EN 12350-7:2019Testing fresh concrete – Part 7: Air content – Pressure methods.
[27] EN 12350-8:2019Testing fresh concrete – Part 8: Self-compacting concrete – Slump-flow test.
[28] EN 12390-3:2019Testing hardened concrete – Part 3: Compressive strength of test specimens.
[29] EN 13755:2008 Natural stone test methods – Determination of water absorption at atmospheric pressure.
[30] EN 1936:2006 Natural stone test methods – Determination of real density and apparent density, and of total and open porosity.
[31] SRPS U.M1.016:1992Beton – Ispitivanje otpornosti betona prema dejstvu mraza(Concrete – Method of test for resistance of concrete against freezing and thawing).
[32] SRPS U.M1.055:1984Beton – Ispitivanje otpornosti površine betona na dejstvo mraza i soli za odmrzavanje (Concrete – Method of test for resistance of concrete against freezingand thawing with de-icing agent).
[33] EN 1097-3:1998Tests for mechanical and physical properties of aggregates – Part 3: Determination of loose bulk density and voids.
[34] EN 1097-6:2022Tests for mechanical and physical properties of aggregates – Part 6: Determination of particle density and water absorption.
[35] EN 1367-2:2009 Tests for thermal and weathering properties of aggregates – Part 2: Magnesium sulfate test.
[36] EN 1744-1:2009+A1:2012Tests for chemical properties of aggregates – Part 1: Chemical analysis.
[37] EN 1097-2:2020Tests for mechanical and physical properties of aggregates – Part 2: Methods for the determination of resistance to fragmentation.
[38] V. Radonjanin, M. Malešev, I. Lukić, V. Milovanović, Polimer-betonski kompoziti na bazi recikliranog agregata, Materijali i konstrukcije, 52, no. 1 (2009) 91-107. https://scindeks.ceon.rs/article.aspx?artid=0543-07980901091R
[39] S. Marinković, I. Ignjatović, V. Radonjanin, M. Malešev, Recycled Aggregate Concrete for Structural Use –An Overview of Technologies, Properties and Applications, Innovative Materials and Techniques in Concrete Construction (2011). https://doi.org/10.1007/978-94-007-1997-2_7
[40] V. Radonjanin, M. Malešev, S. Marinković, A. E. Sead Al Malty, Green recycled aggregate concrete, Construction and Building Materials, 47 (2013) 1503-1511. https://doi.org/10.1016/j.conbuildmat.2013.06.076
[41] G. Broćeta, M. Malešev, V. Radonjanin, Trajnostsamougrađujućegbetona u funkcijiprimijenjenevrsteagregata, Naučnamonografijaizuzetnogznačaja, Univerzitet u Banjaluci, Arhitektonsko-građevinsko-geodetskifakultet, Banjaluka (2021). ISBN 978-99976-978-0-6

Građevinski materijali i konstrukcije
Building Materials and Structures
journal homepage: www.dimk.rs

https://doi.org/10.5937/GRMK2300012Y UDK: 624.21.046
624.21:339.13

Technical paper

The supply and demand of infrastructure robustness, resilience and sustainability – Part II

Bojidar Yanev*[1)]

[1)] *Dept. of Civil Engineering & Engineering Mechanics, Columbia University, New York, NY 10027, USA*

Article history
Received: 03 October 2023
Received in revised form:
29 October 2023
Accepted: 02 November 2023
Available online: 09 November 2023

Keywords
bridge,
crisis,
management,
supply,
demand,
robustness,
resilience,
stability,
sustainability

ABSTRACT

Engineering and economics seek equilibria in the disparate dimensions of money and energy. In Part I of the present development [1] the mechanical instability of conservative systems in the domain of energy was compared to the five typical stages of events considered crises in any field, including those dimensioned in money. In that view, the economic, and engineered stability of the built infrastructure can be qualified, and to an extent quantified in terms of robustness, resilience, and sustainability. It is expanded herein with details and examples.

1 Introduction

Simply stated, *a structure* (or any system) *is stable if a small change in the initial conditions* (input) *leads to a small change in the solution* (output, response). The foregoing definition of stability, due to Lyapunov (1892), is generally used in all fields – not only structural mechanics, but also biology, economics, etc. [2].

In 1637, René Descartes [3] concluded that "the diversity of our opinions does not arise from some being endowed with a larger share of reason than others, but solely from the fact, that we conduct our thoughts in different ways and do not fix our attention on the same objects". The Cartesian *Méthode* sought to streamline the thought process. More modestly, the present objective is to identify the fundamental differences between the engineering constraints and economic restraints governing infrastructure, and in particular, bridge management. Energy is viewed as the rigid constraint of engineered products, whereas money is regarded as a negotiable restraint of economic processes. Hence, infrastructure management must reconcile the supply of and demand for structural performance under rigid physical constraints, dimensioned in energy, and negotiable, largely monetized economic restraints, subject to political priorities. As a result, the balancing of supply (R) and demand (Q) in economics and engineering can diverge. Fig. 1 is one way of illustrating the contrast between the respective governing priorities.

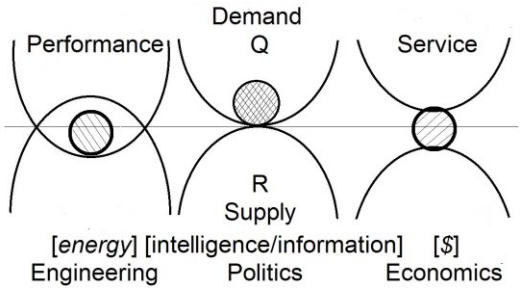

Figure 1. The supply(R) and demand (Q) in engineering, economics and politics

At least since Sir Isaac Newton professed induction, the deductive / inductive methods, more recently referred to as top-down / ground-up, have constrained engineering in the domain of energy. In [4], they are described as follows: "It must be realized that deductive justification is based on quantities and concepts determined inductively." Engineered products must supply performance R (in terms of energy) exceeding the demands Q of service and extreme events by codified load, resistance, and serviceability factors. In [4, 5] the latter are denoted by γ, φ, and η, respectively, according to Eq. 1.

$$\varphi R \geq \eta_{1,2,3} \sum \gamma_i Q_i \quad (1)$$

* Corresponding author:
E-mail address: bojidaryanev1@gmail.com

In contrast, competing and even conflicting interests and schools of thought negotiate on the public, academic, and executive levels of economic processes in terms of money over strategically and tactically diverse time horizons. Except in the extreme high- and low- income areas, where social programs and philanthropy may reverse the general pattern, service demands exceed the supply by an indeterminate degree, thus motivating social progress. The diverging engineering constraints and economic restraints are reduced to Eqs. 2 – a and – b [1], as follows:

Engineering products: $R > Q$ [*Energy*] (2–a)

Economic processes: $R < Q$ [$] (2–b)

Thus, since the Industrial Revolution, engineering has improved the production of assets, whereas economics and politics are perfecting the process of transacting them. Social development depends on a reconciliation between the disparate political-economic restraints on public funds and engineering constraints on physical energy. Herein is extended the argument proposed in [1] that this reconciliation requires new terminology, coherent in the domains of engineering, economics, and politics in the 3-D space of energy, time, and money. The long-governing standards of engineering design, including structural strength, stability, and durability do not reach far enough into the economic aspects of bridge management. If defined to the satisfaction of all concerned, robustness, resilience, and sustainability can serve those management criteria, as they more or less implicitly have been serving engineering design.

2 Bridge conditions

In the interest of completeness, the evolution of the bridge condition database in the US is briefly reiterated from [1] herein. Following the collapse of the Silver Bridge at Point Pleasant in 1967, the Federal-Aid Highway Act of 1968 [6] mandated biennial inspections of highway bridges, thus initiating their nation-wide and, by extension, worldwide management. The National Bridge Inventory (NBI), established by the Federal Highway Administration (FHWA), rapidly built a database of 230,000 highway bridges, eventually expanding it to nearly 650,000. A vehicular tunnel database was launched in 2015. Incorporating more than 220,000 railroad bridges is pending. Milestones in that process were the introduction of the LRFD Bridge Design Specifications by the American Association of State Highway Transportation Officials [5] and the AASHTO Bridge Element Condition States [7].

The biennial inspections update the NBI with descriptive and prescriptive assessments. The original 10 – level condition ratings [6] were essentially descriptive. The four element-level condition states [7] supersede them by combining the descriptive opinions of qualified engineers with quantitative measurements and, at the lowest level 4, by prescribing corrective actions. Also prescriptive are the 'flag' reports of potential hazards according to the New York State Department of Transportation (NYS DOT), defined in [8, 9]. Based on its bridge inventory, NYS DOT also recognizes a number of vulnerabilities, such as steel details, concrete details, seismic, hydraulic, collision, overload, and acts of destruction. The vulnerability to overload was withdrawn. Advanced technologies are offering a rapidly expanding variety of non-destructive testing and evaluation (NDT & E) techniques [20], allowing for the quantification of previously purely qualitative assessments.

The prescriptive, quantified assessments can help with budgeting for future needs, while the descriptive, qualitative assessments can help with long-term predictions of, if not actual conditions, then at least the ratings of conditions for each bridge and network. As the data accumulated, both deterministic and stochastic methods were used, yielding generally coherent results. Theoretical models tended to assume convex *condition* deterioration paths, whereas inspection records indicated concave *condition rating* histories. S – shapes (inverted either way) have been suggested as both more adaptable and realistic. Yanev [11] argued that in large networks where both bridge age and conditions are normally distributed, a linear model can be sufficiently accurate for rough estimates. Typical forecasts based on the condition ratings obtained by the biennial inspections conducted according to [6, 8] are illustrated in Fig. 2. They could not be generated directly based on the element condition states of [7, 9].

Stable bridge networks ought to demand a relatively constant level of annual preservation activities, consisting of reconstruction, component rehabilitation, and maintenance. Thus, over a large network, the pattern in Fig. 2(b) should converge to a near-constant level of annual expenditures, adjusted for inflation. (New construction is viewed herein as network expansion, to be planned on a comprehensive socio-economic level with all its long-term implications.)

Let T_o and T_n be the estimated life-cycle durations with and without preservation interventions. Let R be the bridge condition rating assessed by one or more methods of Table 1 and *Rsust* be the sustainable level maintained by periodic preservation actions at times t_i up to a declining t_n, when full rehabilitations and replacements become more cost-effective. The durations of preservation actions are denoted by Δt_i. They are associated with costs C_i (direct and indirect) and, contrary to Δt_i, tend to grow longer and costlier. Yanev [11, 12] argues that money expenditures cannot measure structural and social benefits with sufficient rigor. Moreover, the costs and benefits of capital reconstruction are more readily monetized than those of 'preservation' and its constituent 'routine maintenance'.

Engineering plans discrete condition upgrades at times t_i to prevent demands from becoming critical. Economics funds them as corrective actions responding to such demands. Economic processes are not only dynamic but also subject to divergent assessments. Thus, engineering and economic views of risk and stability are contrasted. Economic expansion is expected. Engineers study product failures in controlled tests. The 'market adjustments' favored by economists imply localized process failures. In a market democracy, economic restraint governs infrastructure management. Hence, process instabilities can eventually affect product performance. The proliferation of potential hazards [8] in New York City (NYC), discussed in [1, 12], is an instructive example. In a bridge network managed according to the models in Fig. 2, potential hazards ought to be the exception. However, between 1988 and 1992, their number in NYC increased from 180 to 3071.

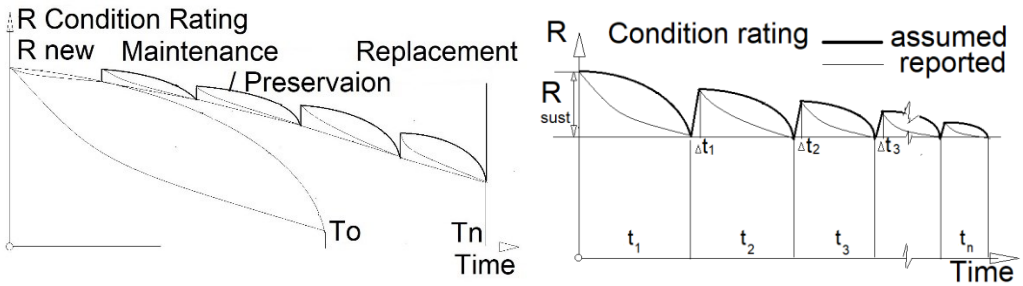

Figure 2. Hypothetical effect of periodic preservation interventions on extending the useful life of a bridge and a network

Figure 3 [1] pertains to approximately 690 vehicular (including the 4 landmark East River and 25 movable) and 100 pedestrian bridges in NYC. The following five periods are discernible:

A – B : 1982 –1 987 Apparent equilibrium following initial adjustments;

B – C : 1987 – 1992 Increase reaching an annual factor of 2;

C – D : 1992 – 1996 Peaking approximately 24 times above the initial level;

D – E : 1996 – 1999 Annual decrease by a factor of approximately 1.24;

E – : 1999 – 2006 Apparent equilibrium at approximately 10 times the initial level (sustained into the 2020s).

Similar 5-stage patterns are common to crisis histories, such as the developments of the Covid-19 epidemic and the financial crisis of 2008. The stages of grief comprise a comparable sequence of denial, anger, bargaining, depression, and acceptance. The ultimately constructive 'Future Tech Hype Cycle' includes analogous innovation, exaggerated expectations, a trough of disillusionment, enlightenment, and a plateau of productivity. Common to the described processes are the occurring instabilities. The inverted outline of Fig. 3 and similar histories of crises parallel energy behavior during mechanical instability, in particular those of the 2-bar von Mises truss, strain-softening materials, and bodies retained by friction [2].

3 The stability analogy

Bažant and Cedolin [2] illustrate the snap-though and snap-down instability modes of the von Mises truss, as shown in Fig. 4. The typical stages A-E of Fig. 3 and similar crises loosely fit as shown into the path of P on Fig. 4-b.

Reiterating [1] for completeness, Bažant and Cedolin [2] state: "The question of stability may be most effectively answered on the basis of the energy criterion of stability, which follows from the dynamic definition if the system is conservative." The authors present catastrophe theory as a "strictly qualitative viewpoint," analyzing the stability of conservative systems by energy methods as follows: "[Catastrophe theory] seeks to identify properties that are common to various catastrophes known in the fields of structural mechanics, astrophysics, atomic lattice theory, hydrodynamics, phase transitions, biological reactions, psychology of aggression, spacecraft control, population dynamics, prey-predator ecology, neural activity of the brain, economics, etc. Simply, the theory deals with the basic mathematical aspects common to all these problems." Parrochia [13] takes a similar view. Both [2, 13] refer to René Thom's [14] demonstration that in a conservative system with one control parameter, only one type of catastrophe is possible (the limit point or snap-through), with two independent control parameters, the fold and the cusp types

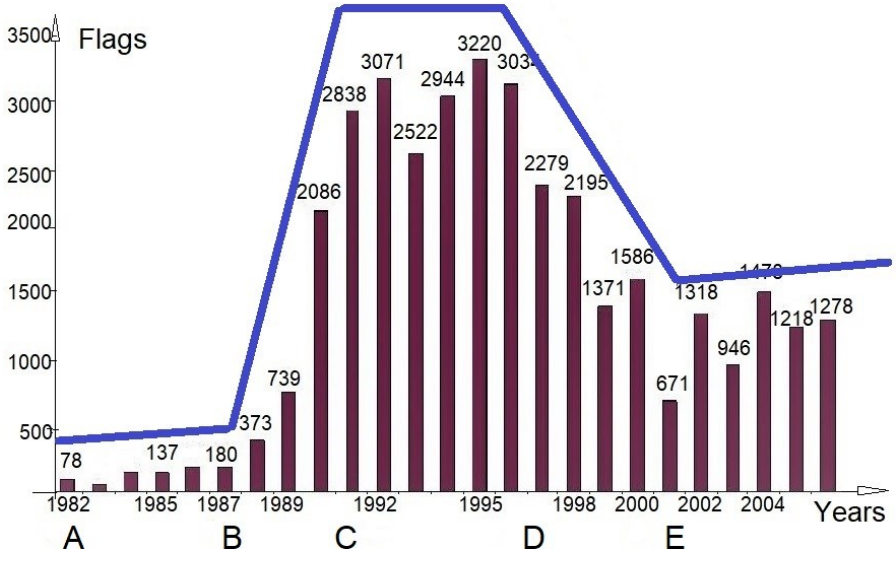

Figure 3. Bridge – related potential hazards in NYC, 1982 – 2006

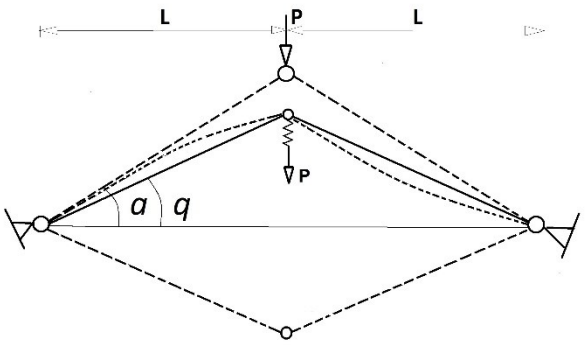

Figure 4 – a. The Von Mises truss

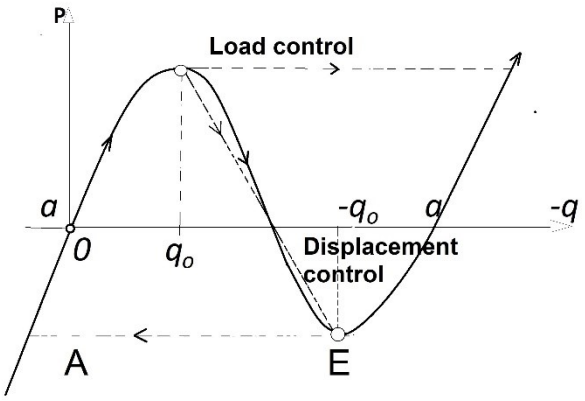

– b. Snap-through and snap-down equilibrium paths

of catastrophes are possible (asymmetric and symmetric bifurcation). For systems with three control parameters, five types of catastrophes become possible; and systems with up to four control parameters allow at most seven types of catastrophes. The seven types of catastrophes are called 'elementary'.

Under load control [2, Section 4.4], the bars with area A and length L do not buckle locally. A global snap-through instability occurs when the potential energy $\Pi(q)$ of the elastically deformed system reaches a critical value. The equilibrium condition for the potential energy $\partial\Pi / \partial q = 0$ obtains Eq. 3, where α and q are the initial and deformed angles of the inclined bars. The truss is unstable for $-\alpha/\sqrt{3} \leq q \leq \alpha/\sqrt{3}$.

$$P = EAq(\alpha^2 - q^2) \quad (3)$$

Under displacement control [2, section 4.8], the bars of the von Mises truss can buckle locally in a snap-down mode. A snapback is possible under certain constraints. Critical loads and displacements can coincide. Interacting buckling modes and the inevitable 'passive' system imperfections strongly influence near-instability behavior, adding further indeterminacy. The authors stress that "there are buckling problems that are inherently nonlinear and cannot be linearized, even if the deflections are very small". Despite its non-redundancy, the von Mises truss can fail in a number of ways. Either bar can fail in compression or tension. The system snaps 'through' globally and snaps 'down' locally. More than one mode can coincide.

Damage-related material instabilities, including strain-softening and friction, discussed in [2, Ch. 13], provide another applicable analogy. Particularly relevant are the possibility of material rehardening (after strain-softening) and the drop of the static friction force F_s to a smaller dynamic one F_d as initial friction is overcome. Both phenomena correspond to the behavior of structures and networks gradually losing their original resistance, as shown in the inset of Fig. 5.

Infrastructure networks, with their broadly estimated multi-parameter dynamic equilibria of vaguely quantified and qualified supply and demand, do not qualify for rigorous stability analysis. Nevertheless, the patterns of Figs. 3 and 4-b, as well as those of other crises, share important features. To those already enumerated in [1] can be added the following:

– An equilibrium of supply and demand, dimensioned in energy, is essential to both conservative mechanical systems and infrastructure networks.

– Adding the non-conservative parameter of money recalls that it is the social equivalent of energy. Treating the money supply as potentially unstable allows for identifying the potential crises precipitated by budget shortages.

The energy constraint governs Peter Drucker's (1909-2005) view that "everything degenerates into work.". The economic restraint drove Napoleon (1769-1821) to conclude that "all politics is money." If energy and money were viewed as the two active parameters controlling the bridge network, each could cause its own type of instability, expanding the near-unstable domain. For four control parameters, for example, if intelligence and information were regarded as additional parameters (e.g., the inevitable political restraints), the possible types of catastrophes would increase to seven [2, Table 4.7.1., p. 300].

4 Robustness, resilience, and sustainability of products and processes

The definition of a new category requires the introduction of at least one new term. Henri Léon Lebesgue (1875-1941)

The position herein is that abrupt discontinuities in engineered and economic products and processes are preceded by a gradual buildup (or depletion) of effects in overlooked dimensions. Therein lies the relevance of mechanical stability, where force equilibrium alone overlooks the relationship between energy accumulation and structural form in space. Quantifying in terms of forces (energy), the product's resistance (supply), and the service demand according to Eq. 1 similarly overlooks stability. That is addressed separately, along with ductility, redundancy, and importance under the general umbrella of serviceability. The traditional scope of designing and managing engineering products and processes in energy and space-time is illustrated in the inset of Fig. 5 herein. Inverting the contour obtains a crisis pattern similar to that of Fig. 3 with comparable stages A-E. Yanev [12] correlated bridge-related potential hazards with element condition ratings, enabling anticipating their proliferation into 'extreme events'. Network performance instabilities, however, cannot be fully anticipated absent the money dimension. The potentially catastrophic structural conditions, illustrated in Fig. 3, were preceded by political and economic instabilities. (In the late 1970s, New York City narrowly avoided bankruptcy.) The argument advanced herein is that engineering, economics, and politics can manage a sustainable (i.e., stable) infrastructure network only jointly in an integrated 3-D space defined by energy, money, and time, as illustrated in Fig. 5.

The inset of Fig. 5 [1] represents a possible lifecycle of the engineered asset(s) in the plane of *energy and time* under 'normal' demands and an extreme event. It illustrates the following sequence:

The bridge strength, stability, ductility, redundancy, and importance prescribed by current specifications deteriorate over time at variable rates, depending on many external and intrinsic factors. Eventually, the accumulated decline disrupts sustainability. To represent sustainability, robustness and resilience must reflect the condition of the network in the domains of energy and money over time. At both project and network levels, they imply redistributing a constrained supply of resistance in response to an expanded demand, as do structural redundancy and ductility. Inverting that history obtains the crisis pattern already familiar from Figs. 3 and 4, with discernible, although differently spaced, points A, B, C, D, and E.

In order to capture all parameters controlling the product and process depicted in the *Energy / Time* plane, Fig. 5 combines Figs. 5 and 6 of [1]. The *$* axis expands the plane into a 3-D space. The lines drawn in the plane of *Energy / Time* expand to surfaces in *$ / Energy / Time*. Second, the axes of *Robustness*, *Resilience*, *Sustainability* are introduced in the 3 planes of *Energy / Time*, *Energy / $*, and *$ / Time*, respectively. In keeping with the engineering practice of reducing problems to actionable tasks, the 3-D model can be examined in three constitutive planes. Those planes, however, can be defined by *$ / Energy / Time*, as well as by *Robustness / Resilience / Sustainability*. The advantage of the latter is to demand, respectively, the collaboration and cooperation of economics and engineering [*$, energy*], politics and engineering [*time, energy*], and economics and politics [*$, time*]. Restraining economics to the dimension of money [*$*] makes it (arguably) the only one of the three disciplines whose models can be formulated entirely within (although they should not be necessarily limited to) a social construct. Contradictory top-down economic models are notoriously resilient over extended time periods by ignoring the ground-up constraints of robustness and sustainability. By integrating energy, time-space and money, the new 'control parameters' of social and physical performance restrain engineering, economics and politics into collaborating. The implicit 'control parameters' of intelligence / information account for the occasional contradictions between engineering, economics and politics.

Consistently with Lebesgue, sustainability is treated as a 'new category' requiring (at least) the new terms of robustness and resilience. FHWA [15] has advanced bridge management towards the standardizing and codifying of their assessments. Thus far, robustness is defined as the ability of a possibly impaired structure or network to retain functionality under the demands of 'extreme events' in constrained time. In the explicit forms of redundancy and ductility, robustness redistributes and sustains the load demands in the defined space of the asset and time of the event. According to [16], resilience describes lifecycle network performance under typical and extreme conditions as "the ability to prepare and plan for, absorb, recover from, and more successfully adapt to adverse events". Deterioration reaching a point of system instability (e.g., state of emergency) is qualified herein as an extreme event. Resilience pertains to the process of network response, not only in terms of energy but also in terms of money and extra-monetary considerations over extended but nonetheless foreseeable time periods. Simplifying, robustness quantifies essentially the product, and resilience qualifies and quantifies the process.

Politics, economics, environmental protection, and so on discuss the noun 'sustainability' in purely qualitative terms, ultimately reducing their interpretations of qualitatively 'sustainable' policies to quantifiable affordable budgets. To narrow down the scope, [1] proposed the *sustainability factor* (*SF*) of Eq. 4. It should estimate the affordability of an infrastructure network under the governing social restraints and physical constraints of money, energy, and time as follows:

$$SF = \Sigma\ benefits\ /\ \Sigma\ costs \tag{4}$$

Constraining sustainability in time, Eq. (4) must be amended to Eq. 4 – a.

$$SF = \Sigma\ (benefits\ /\ costs)\ /\ time \tag{4–a}$$

Recognizing the qualitative and quantitative differences between the three major contributors to Eq. 4 – a, it can be further expanded to Eq. 4 – b.

$$SF = d\ \Sigma\ (benefits\ /\ costs)\ /\ time_{direct} + u\ \Sigma\ (benefits\ /\ costs)\ /\ time_{user} + e\ \Sigma\ (benefits\ /\ costs)\ /\ time_{environ.} \tag{4 – b}$$

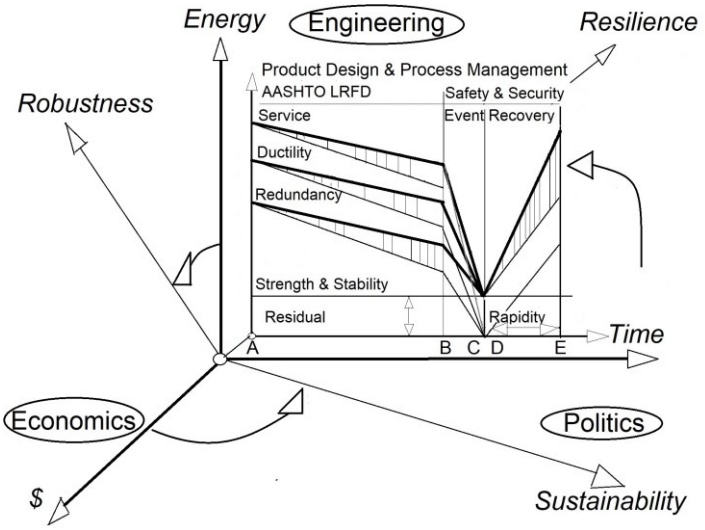

Figure 5. Robustness, resilience and sustainability in engineering, economics, and politics

where: $time_{direct}$; $time_{user}$; $time_{environ}$ are the timespans for assessing direct, user, and environmental costs and benefits, and

d, *u*, and *e* are weights designating the relative importance of each term, respectively.

The *direct*, *user*, and *environmental benefits / costs* and *times* differ as (partially) follows:

- *Direct*

- *costs*: They are relatively straightforward, particularly as the majority of infrastructure assets are publicly owned and, hence, subject to stricter accountability. However, reconstruction and maintenance can be funded by national and local budgets, respectively, restrained by different priorities. In the US, such differences partly contributed to local preferences for capital construction over maintenance from the 1960s to the 1980s. Government policies aside, the costs of maintenance activities are much harder to trace, particularly if some preservation activities are privatized whereas others are performed in-house. Yanev [11] argued that the notoriously delinquent bridge painting can be managed effectively only as capital reconstruction. That policy is currently standard.

- *benefits*: They can be estimated only tentatively over long periods, thus reflecting intractable user and environmental influences. The value of a bridge network is monetized in terms of its replacement cost, which is subject to inflation and other fluctuations. The cost evolution of major capital projects in the US suggests that construction costs have been rising for the past century at an annual rate of approximately 5%. For example, the George Washington Bridge in New York City was completed in 1931 for $US 50 m, and its lower deck was added in 1951 for $US 4 billion. At present, a comparable bridge could realistically cost $US 4 billion. Yanev's [12] correlation of maintenance costs and their benefits in terms of bridge conditions stressed both the value and the limitations of that model.

- $time_{direct}$: Since the 1990s, the time for assessing infrastructure asset performance has been its useful life. If a network deteriorates, its depreciation can be monetized in terms of the increased demand for reconstruction and preservation (e.g., maintenance). These demands, in turn, can be expressed as losses of robustness, resilience, and sustainability. Yanev [12] argued that, for a relatively large network in a 'steady state', the average overall condition ought to be near constant. Hence, time horizons for such networks can be based on 'perpetuity'. In contrast, management budgets are annual. Capital construction plans have 5, 10, and 20-year horizons, with the shorter ones typically slipping into the longer ones. Thus, short- and long-term sustainability estimates are appropriate.

- *User*

- *benefits / costs*: They are only tentatively estimated based on the time users spend in the transportation network. The quantitative and qualitative differences between private users and industries are considerable, since the former are passive consumers, whereas the latter (or some of them) are active contributors. Monetizing the costs incurred by large populations due to declining service obtains quantities incomparably superior to the direct ones. The benefits supplied by existing services are linked to taxes only tentatively through the political domain. The relatively constant 'gas tax' in the US is debated perpetually, with structural robustness and resilience informing the arguments only in unquantifiable terms (e.g., the American Association of Structural Engineers rates the condition of the transportation infrastructure as "D" or "C+").

- $time_{user}$: It can be correlated with the corresponding $time_{direct}$, for short- and long-term sustainability estimates.

- *Environmental*

- (*benefits / costs*) / $time_{environ}$: Sustainability is directly addressed, as robustness and resilience apply better to built infrastructure than to the natural environment. Hence, the debates are conducted under disparate standards and currencies. Some consensus is attainable on long-term global considerations, however short-term local ones inevitably reduce to economy and politics. Engineering is well qualified to lead by creating a more sustainable infrastructure, however, political decisions govern the largest projects. Quantifying an environmental sustainability factor is even harder than the user one, at even larger magnitudes. Its presence in Eq. 4-b is qualitative but essential. Milton Friedman (1912-2006) [17] argued that "neighborhood effects" are *circumstances* where "the actions of individuals have effects on other individuals for which it is not feasible to charge or recompense them". The sustainability of infrastructure management strategies should be qualified and, to the extent possible, quantified based on such effects, e.g., those affecting environmental resilience.

As the times over which direct, user and environmental benefits and costs are accrued and sustained differ, *SF* of alternative strategies must be compared over similar short- and long-time windows. Certain options could be disqualified for failing to address one or the other. This would render the Present Worth (PW) method and its somewhat arguable discounting moot.

Robustness, *Resilience*, and *Sustainability* can be modeled as functions $f(\$, energy, t)$, $\psi(\$, energy, t)$, and $\theta(\$, energy, t)$ in various ways (e.g., continuous, piece-wise continuous, convergent, divergent, and so on) for forecasting purposes. They can have positive projections on the original axes of *$*, *Energy*, and *Time*, as illustrated in Fig. 6-a, or they can coincide with reduced consumption of *Energy* and *$*, as in Fig. 6-b. In more realistic representations, the axes need not be rectilinear, orthogonal or similarly oriented.

In Fig.7, the different possible scenarios are reduced to the planes of expenditures and sustainability with respect to time. If the ratios in Eq. 4-b were continuous functions with respect to time, hypothetical cycles might evolve as shown in Fig. 7. Physical and social randomness render actual processes discontinuous. The period shifts and first derivative sign reversals of $time_{direct}$ and $time_{user}$ can be tentatively assumed or deduced from statistical data. The cycles of $time_{environ}$ would have much longer periods at higher costs. Given the enumerated differences between the three contributors, a compound 'sustainability' would be fraught with speculation. If, however, such a 'sustainability' were assumed, several elementary possibilities might arise. In Figs. 8-a, -b, and -c they are illustrated as follows:

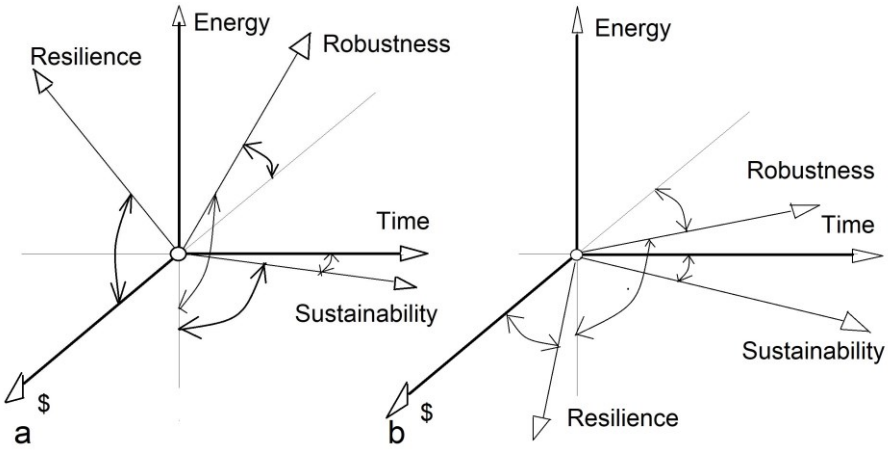

Figure 6. Possible 3-D rotations of Robustness, Resilience and Sustainability with respect to Money, Energy and Time

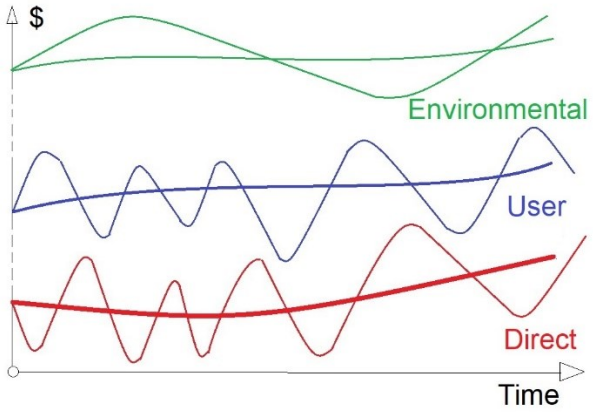

Figure 7. Hypothetical cycles of direct, user and environmental costs

a) Initial costs are low, sustainability is perceived as high. Over time, costs increase, sustainability declines, and cycle periods and amplitudes stretch. This is typical of infrastructure networks built at a low initial cost and, hence, an apparently favorable short-term sustainability, as well as of low-maintenance long-term practices. The A-E stages of Fig. 3 are discernible. Increasing demands for network maintenance and inflation are considered correlated, but the causality is bilateral. Both provoke the customary lament for the 'good old days' when current conditions and circumstances would have been 'unacceptable'.

b) Initial costs are high and sustainability is low. Over time, costs decrease, sustainability increases, cycle periods and amplitudes drop. This can reflect more cost-effective asset design and management and reduced user and environmental costs. Networks serving more energy-efficient modes of transportation (including pedestrians and bicycles) are expanding. Given the expanding populations and demands for services, this is not a very likely scenario.

c) Costs and sustainability can increase or decrease concurrently, with decreasing or increasing cycle periods and amplitudes, respectively, representing improving or declining infrastructure performance. Examples of benefits increasing with added costs include the elimination of environmentally harmful materials such as lead from bridge construction and preservation and deicing salts from roadways. Considerations of economic sustainability motivate the policies favoring local suppliers.

Figures 7 and 8 remind that, whereas cost cycles are considered routine, the energy cycles of robustness and resilience implied in sustainability alternate between stable and unstable paths. Combinations of the various idealized scenarios are more likely.

5 Examples

In [18], Albert Einstein stated: "So far as the laws of mathematics refer to reality, they are not certain, and so far as they are certain, they do not refer to reality". Several familiar examples are reviewed in terms of their robustness, resilience, and sustainability in order to test the realism of these terms.

- Brooklyn Bridge (1883) East River, New York City, John (1806-1869), Washington (1837-1926), and Emily (1843-1903) Roebling (Fig. 9).

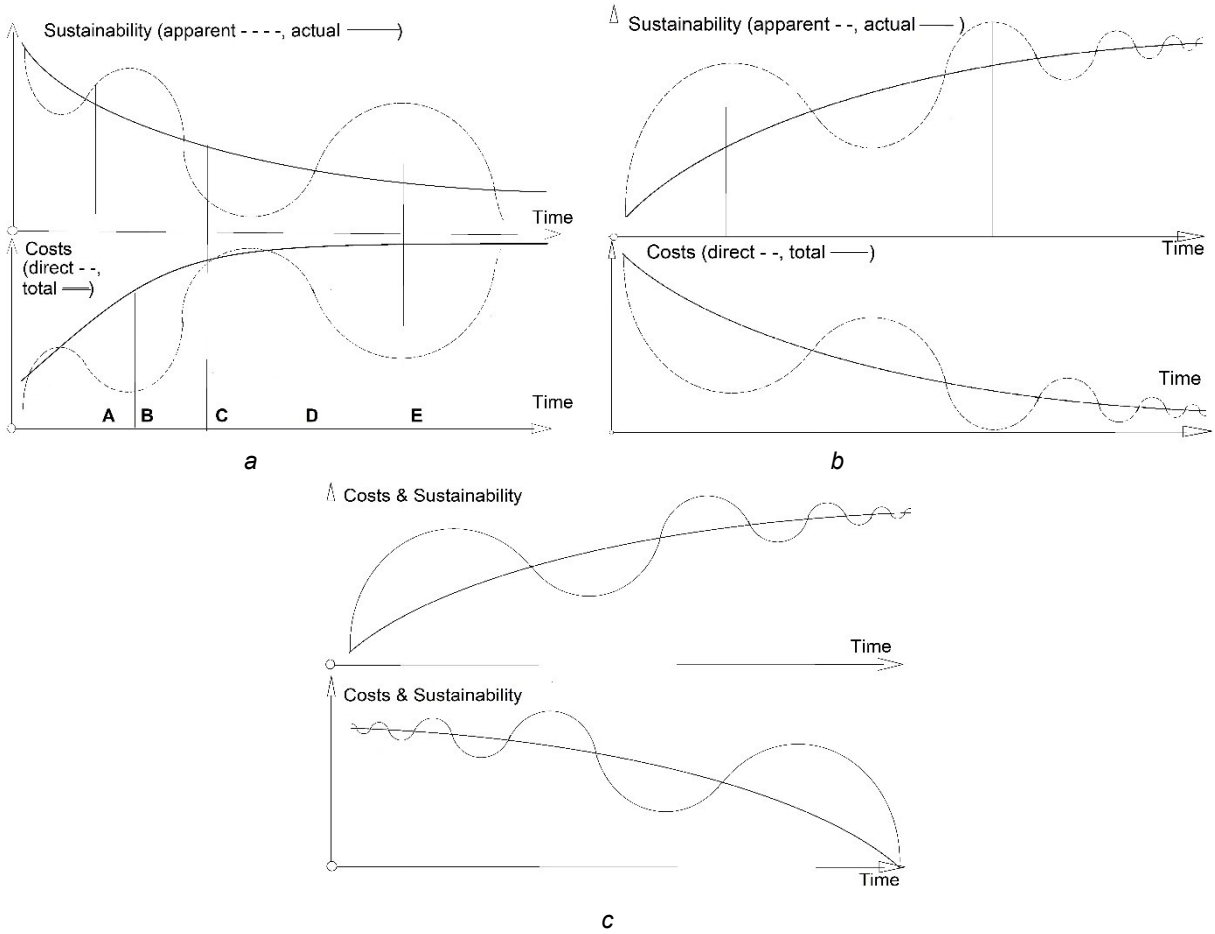

Figure 8. Possible costs / sustainability cycles

Figure 9. Brooklyn, Manhattan and Williamsburg Bridges across East River, New York City

With a main span of 486 m, the bridge was the longest in the world. The structure is a hybrid, combining a suspension system with four main cables, multiple diagonal stays, and four stiffening trusses (Fig. 9). John Roebling famously stated that if one of the three systems malfunctions “the bridge may sag but shall not fail”. This integration of robustness and resilience was occasionally criticized as “belt and suspenders”. It allowed the bridge to survive a deterioration of the stays and the suspenders, culminating in a suspender rupturing in 1981. The ensuing replacement of all stays and suspenders was conducted without traffic interruption. The bridge, which once served carriages and tramways, today carries four automobile lanes, a bicycle, and a pedestrian path. The bridge demands relatively high maintenance, however, its indispensable service and landmark status make it eminently sustainable. Deicing salts were eliminated from all East River bridges.

- Williamsburg Bridge (1903), East River, New York City, Leffert Lefferts Buck (1837-1909) (Fig. 9)

The bridge carries four traffic lanes and two subway tracks. The 488-m main span was the longest suspended structure at its completion. The side spans were not suspended. In 1998, two strands in one of the four main cables, each consisting of 208 high-strength wires, were found to have ruptured due to corrosion. As the inspection progressed, many more wires were found to be broken or

severely damaged. The bridge was closed to traffic pending evaluation, impacting city traffic severely. The subsequent investigations ultimately concluded that the structure could be rehabilitated. The prohibitive traffic interruptions rendered a replacement unsustainable. The original 'factor of safety' in the four main cables had been approximately 4, and the estimated corrosion damage had reduced it to approximately 3. The robust 'overdesign' saved the bridge. In contrast, cable resilience was poor because the high-strength wires had not been galvanized. The reasoning (primarily motivated by the desire to eliminate the weight of the zinc coating) had been that the cables should be kept dry and, hence, did not need galvanization. As it turned out, cable wrapping failed, water penetrated, and the wires corroded. The double protection 'belt and suspenders' policy would have been more resilient and sustainable. The rehabilitation with partial traffic closures took more than 10 years at a cost exceeding $US 1b. The Williamsburg Bridge crisis demonstrated conclusively that investing in bridge robustness and resilience benefits long-term sustainability. The events inspired Japanese engineers of the Honshu-Shikoku Bridge Authority to develop a dehumidification system for their many record-length suspension cables, as at the Akashi-Kaikyo and Kurushima bridges. The system has been adopted by other long-span bridge owners. The improved resilience and, hence, sustainability offset the added maintenance cost. That, however, also supplies an argument for reducing cable robustness, e.g., to factors of safety approaching 2, as at the record-holding Çanakkale Bridge across the Dardanelles.

- George Washington Bridge (1931, 1956) (Fig. 10), Hudson River, Othmar Ammann (1879 – 1965)

At its opening, the main suspended span of 1067 m was the longest in the world. Its 8 traffic lanes were the heaviest. Originally, the bridge had no stiffening trusses (reducing the construction costs), but its weight rendered it sufficiently robust and resilient. The design anticipated a lower level carrying either trains or vehicles, depending on the demand. In 1956, the lower deck with six traffic lanes was added, improving robustness, resilience, and sustainability. The bridge links the states of New York and New Jersey and currently earns more than $US 3 million in tolls daily. Suspenders and roadways have been replaced.

- Tacoma Narrows Bridge (1940), Washington State, Leon Moisseiff (1872-1943)

With a length of 835.4 m, the main span of this vehicular bridge was the third longest in the world (after George Washington and the Golden Gate). The traditional stiffening trusses were replaced by innovative girders on the reasoning that the reduced stiffness would attract reduced stresses. The structural lightening presumably improved initial sustainability. Robustness was consciously reduced. Resilience proved immediately inadequate under normal traffic. On November 7, 1940, moderate wind caused a torsional failure ultimately attributed to flutter. The dynamic vulnerability of the bridge was repeatedly analyzed, advancing subsequent designs, however, in the simplest terms, the structure lacked the robustness and resilience consciously built into the earlier examples. The costs, including those of the following replacements, would render short-term sustainability very low. The transportation link was clearly necessary, and the long-term sustainability of the two replacement bridges should prove superior.

Sliver Bridge (1928), Point Pleasant, West Virginia

The suspension vehicular bridge at Point Pleasant had a main span of 213 m and two equal sidespans of 116 m. It was designed as a two-cable suspension bridge, but the bid was changed to a two parallel eye-bar suspension system, with two eyebars per panel point. On December 15, 1967, it collapsed due to a corrosion fatigue-induced brittle fracture of one eyebar. The subsequent investigation found a flaw in the metal, however, the structure's non-redundancy doomed it. The event kicked off mandatory bridge inspections in the US, even though no visual inspection could have spotted the fatal defect. In addition to the global non-redundancy, replacing the cables with pairs of eyebars further eliminated the structural internal robustness and resilience. In recognition, a similar bridge was deemed unsustainable and demolished promptly. Structural redundancy, alternate load paths, load redistribution, and ductility became performance-based design criteria, amounting to robustness and resilience.

Mianus River Bridge (1958), Interstate I-95, Greenwich, Connecticut

On June 28, 1983, a 30-meter- long span of the east-bound steel girder bridge over the Mianus collapsed. A pin and hanger linkage supporting the span had failed due to the accumulation of debris and corrosion. As with the Silver Bridge eyebars, such linkages are non-redundant and next to impossible to inspect. The standard design at the time lacked both robustness and resilience, and hence, long-term sustainability. Details of this type were designated as fracture-critical, requiring 100% hands-on inspection, and scheduled for retrofit and replacement. The NBI enabled the rapid identification of similar structures, demonstrating that infrastructure management is unsustainable without an up-to-date inventory. The FHWA established the need for Bridge Management Systems (BMS). Inspectability, maintainability, and minimizing lifecycle costs, essential to sustainability, became design criteria.

Figure 10. George Washinton Bridge across Hudon River between New York City and New Jersey

Schoharie Creek Bridge (1954), Amsterdam, New York

The bridge consisted of five spans, simply supported on four piers, two of which were in the main river channel. On April 5, 1987, scour caused by severe flooding resulted in the collapse of piers ##3 and 2, carrying spans 3, 4, and 2 with them. The early design had considered longer spans but had rejected them due to higher construction costs. Apart from the need for diving inspections and maintenance of underwater pier footings, the incident underscored that 33 years are insufficient for assessing the sustainability of a bridge design. A similar conclusion was reached after 40-year-old levees designed for lesser storms failed during Hurricane Katrina in August 2005.

Sunshine Skyway (1954) Tampa Bay, Fla., and Queen Isabella Causeway (1974) South Padre, TX

Sunshine Skyway was a twin multi-span, 6.82 km structure crossing Lower Tampa Bay. The multi-span Queen Isabella Causeway connects South Padre Island to Port Isabel for a length of 3.82 km. Each lost a concrete pier and the adjacent spans due to vessel impact on May 9, 1980, and September 15, 2001, respectively. In both cases, constructing piers sufficiently robust to resist vessel impact or to survive a lost pier would not have been feasible. The Sunshine replacement was a much longer cable-stayed signature bridge. The causeway added more buffers. Both employ supplementary warning signals and other protection systems. Thus, sustainability was improved by reducing the risk by means of a new structure or by augmenting the management of the existing one.

I – 880 Cypress Viaduct (1957), Oakland, and I-240 Embarcadero (1968), San Francisco, CA (Figs. 11-a and -b)

The two multi-span, two-level prestressed concrete structures failed during the Loma Prieta earthquake of October 17, 1989, in strikingly different ways. The Cypress Viaduct collapsed over a length of 3 km, causing 41 fatalities. Among the contributing causes were structural discontinuity between the lower and upper levels, inadequate column reinforcing ties, and foundations on deep piles. Attempts to improve the structure's seismic robustness and resilience had been in progress. At Embarcadero, the column reinforcing ties were similarly inadequate, but the two-level columns were continuous. The severely damaged structure withstood the ground motion, by all estimates, very narrowly. Robustness had been lacking, but resilience prevented a catastrophe. Both structures were deemed unsustainable, structurally and aesthetically, and replaced by traffic on grade. AASHTO and FHWA followed up with comprehensive upgrades to seismic research and design.

Mississippi River Bridge I-35 (1964), Minneapolis, Minnesota, Sverdrup & Parcel

The main bridge structure was a 3-span (81 m, 140 m, and 81 m) non-redundant steel arched deck truss. On August 1, 2007, the central span collapsed, precipitating a global failure. The investigation identified 16 inexplicably thinner gusset plates with inadequate load-bearing capacity. Similar bridges drew immediate attention but did not exhibit such a deficiency. Inspections had observed a buckling in the thinner fracture-critical gusset plates, but the condition had not been sufficiently prioritized. Gusset plates had not been addressed adequately in AASHTO design specifications. The 43-year service of the structure prompted speculation that other factors, including a pier shift and new construction loads, might have contributed. As in multiple modes of instability, multiple causes typically contribute to global failures. A structure built without basic robustness and resilience had appeared falsely sustainable over an extended period. The bridge was replaced in 11 months by a prestressed concrete box-girder structure, abundantly instrumented with performance monitoring equipment.

The World Trade Center, New York City (1973), Minoru Yamasaki (1912-1986), Leslie Robertson (1928-2021)

The Twin Towers were signature representatives of the tubular design, associated also with Dr. Fazlur Khan (1929-1982) and Skidmore, Owings, & Merrill. On February 26, 1993, a bomb exploded in the parking garage, gutting four underground floors of the South Tower and knocking out one

Figure 11 – a. Cypress Viaduct, Oakland

– b. Embarcadero, San Francisco

diagonal of the outer bearing wall. The tower structure proved abundantly robust, loads were redistributed, and all damage was localized and promptly repaired. The perception of robustness and resilience improved the popularity and, hence, the sustainability of the usually under-occupied towers. Then, on September 11, 2001, passenger planes struck both towers (Fig. 12).

Figure 12. World Trade Center, New York City, Sept. 11, 2001

Both resisted the impact robustly, as the design had anticipated, deflected, and regained their original positions. The South Tower was struck relatively low. With the weight of 30 floors above the damage, it might not have survived for long even without the ensuing intense fire, which brought it down in 56 minutes. The North Tower was struck much higher, around the 91st floor. Its floors lacked the necessary resilience, and in 1hour, 38 minutes, the fire caused a cascading collapse. Since then, the resilience and sustainability of tall buildings (tubular and otherwise) have been revisited under normal and previously unanticipated extreme circumstances, such as fire. Sustainability against aircraft and vessel collisions cannot rely solely on structural robustness and resilience without adding the tools of prevention.

The sustainability of the long-span bridges, designed for a 100-year useful life without major rehabilitation, demands economic and engineering planning taking into account the reconfigured local geography. Over the course of a century, the traffic link they provide becomes permanent. The demand for their services and, hence, their needs can only increase, adding to the owners' responsibility.

Globally, from an environmental viewpoint, it has been argued that the energy footprint of densely populated areas is more sustainable than that of sparsely populated ones, for example, because of the reduced demand for long-distance commuting.

San Francisco-Oakland East Bay Bridge (2013) T. Y. Lin Associates (Fig. 13) and Viaduc de Millau (2004) Norman Foster, Michel Virlogeux (Fig. 14)

After a 15-meter span of the old East Bay truss crossing failed during the Loma Prieta earthquake (1989), a replacement was determined to be preferable to a retrofit. Much less expensive cable-stayed, viaduct, and even pontoon proposals (the shallow channel is not essential to navigation) were rejected in favor of a unique structure with a self-anchored 385-meter main span, elevating the construction cost to $6.5 billion. Legal ramifications, involving Governor Arnold Schwarzenegger, technical corrections, and the need for provisional supports throughout the construction extended the latter to 11 years.

The certifiably unique completed structure is visually striking and attracts artistic lighting displays. Its 78.74-meter width qualifies it as the world's widest bridge. No major earthquake has tested it to date, but the nearby Hayward Fault is considered active.

Viaduc de Millau is an 8-span, 2,460-meter cable-stayed bridge above the Tarn Valley in southern France. The unique design elevated the autoroute traffic high above the terrain as an environmentally more sustainable option. The then mayor of Millau, Jacques Godfrain, recalls an inquiry by representatives of then California Governor Schwarzenegger about the design selection process. Mr. Schwarzenegger may have been more interested in rejecting rather than approving a project on sustainability grounds. The seven bridge pylons are constructed of concrete up to the deck and of prefabricated steel above. The tallest one reaches 336.4 meters. The prestressed concrete deck segments were not extended (as usually) from the towers on successive cable stays. Instead, the construction company Eiffage launched the deck on temporary steel tower midspan and brought the steel pylon tops onto it. The construction took three years and cost €394,000,000. The design useful life is 120 years.

Figure 13. New East Bay Bridge under construction (2011)

Figure 14. Viaduc de Millau (2015)

Both structures are tolled, rendering their management more coherent. The East Bay crossing was designed to become a "signature bridge". The design of Viaduc de Millau produced one by achieving its purpose brilliantly. Short- and long-term sustainability considerations can be neither ignored nor fully monetized. A similar reasoning applies to all signatures and record-breaking bridges. Fashionable and competitive attitudes can be stimulating, but they benefit from recognizing the restraint of sustainability. David Billington [19] stresses that great structural artists, such as J. Roebling and G. Eiffel (1832-1923) realized their projects on time and on budget. Their signature structures remain highly serviceable (and profitable) more than a century later.

6 Conclusions

The authors of [2] state : "The prediction of failures due to structural instability requires equations of equilibrium or motion to be formulated on the basis of the deformed configuration of the structure." Although the infrastructure is neither a conservative system nor dependent on uniquely defined control parameters, it is prone to instabilities. In both the domains of energy and money, instabilities occur when and because they are ignored. They would be easier to anticipate and possibly avoid if they were modeled in terms of robustness, resilience, and sustainability. If they are to be adopted as 'control parameters' of infrastructure performance, integrating the restraints and constraints governing the design and management of engineered products and economic and political processes, they must be quantified and qualified to the satisfaction of all concerned.

The terms have been seeking recognition for decades, as have the policies that promote them. Sustainable development was the subject of an international conference in Rio de Janeiro in 1992 and a World Summit in Johannesburg in 2002. The US Report [20] addressed sustainable development in chemicals, transport, mining, waste management, and sustainable consumption and production. In 2011, the Office of Sustainable Development at the United Nations (UNSOD) established 17 goals (SDGs), prioritizing least-developed countries (LDCs). In order to advance the subject from commendable thinking to actionable tasks, 'sustainability' must be defined in consistent and generally accepted qualifiable and quantifiable terms. As that objective enters national and international politics, it recedes into the future. Practical application becomes more likely within the reduced scope of managing the transportation infrastructure. Therein, 'robustness' and 'resilience' emerge as appropriate qualifiers and quantifiers of sustainability. In 2021, the US Congress allocated $US 1.3 trillion to rebuilding the national 'hard' infrastructure. 'Shovel-ready' projects (deemed by former President Barak Obama non-existent) are to be favored. The ultimate objective of these funds should be long-term sustainability, defined in terms of robustness and resilience within the 3-D space of energy, money, and time.

The disparities and complex relationship between the direct, user, and environmental components contributing to the sustainability factor proposed herein should not discredit its usefulness. They parallel the engineering, economic, and political constraints and restraints jointly determining the management of the public infrastructure assets. Energy consumption governs global sustainability considerations in general and the engineered infrastructure in particular. Nevertheless, whereas engineering deals with energy directly, economics and politics tend to monetize its benefits and costs. A 3-D space in which the three fields can operate in coherent terms is as essential to infrastructure sustainability as stability is to structural stiffness analysis. Robustness, resilience, and sustainability can frame such a space.

References

[1] Yanev, B. The Supply and Demand of Infrastructure Robustness, Resilience and Sustainability, Building Materials and Structures 66, 2023.

[2] Bažant, Z. P. and Cedolin, L. Stability of Structures, Oxford University Press, New York, ISBN-13 978-981-4317-02-3, ISBN-10 981-4317-02-0, 1991.

[3] Descartes, René, Discourse on the Method of Rightly Conducting the Reason and Seeking Truth in the Sciences, Simpkin, Marshall and Co., London, 1850.

[4] Barker, Richard M. and Puckett, Jay A. Design of Highway Bridges, an LRFD Approach, 2nd Ed., John Wiley & Sons, Inc., Hoboken, N.J., ISBN-13: 978-0-471-69758-9, 2007.
[5] AASHTO Load and Resistance Factor Design (LRFD) Bridge Specifications, 8th Edition, 2017.
[6] FHWA Recording and Coding Guide for the Structure Inventory and Appraisal of the Nation's Bridges, Federal Highway Administration, Department of Transportation, Washington, D.C., U.S., FHWA –PD-96-001, 1971, 1988, 1995.
[7] FHWA Specifications for the National Bridge Inventory Bridge Elements, Federal Highway Administration, Department of Transportation, Washington, D.C., U.S., FHWA-01-21-2014.
[8] NYS DOT Bridge Inspection Manual, State Department of Transportation, Albany, New York, 1984, 2014.
[9] NYS DOT Bridge Inspection Manual, State Department of Transportation, Albany, New York, 2016.
[10] FHWA Bridge Preservation Guide, Office of the Infrastructure, Federal Highway Administration, Department of Transportation, Washington, D.C., U.S., 2008.
[11] , Yanev, B. Bridge Management, John Wiley & Sons, Inc., Hoboken, New Jersey, ISBN-13 978-0-471-69162-4, ISBN 0-471-69162-3, 2007.
[12] Yanev, B. Supply and Demand in Engineering and Management, Building Materials and Structures, Vol. 64, pp. 261-268, ISSN 2217-8139, 2335-0229, Aug. 2021.
[13] Parrochia, D. La Forme de crises, Champ Vallon, Paris, ISBN-10 2876734850, 2008.
[14] Thom, R. Stabilité structurelle et morphogénèse, Paris, Édiscience, 2e éd. 1977
[15] FHWA Notice of Proposed Rulemaking (NPRM), National Bridge Inspection Standards, Federal Highway Administration, Department of Transportation, Washington, D.C., 2020.
[16] Bruneau, M. and Reinhorn, A. Overview of the Resilience Concept, Proceedings, the 8th U.S. National Conference on Earthquake Engineering, April 18-22, San Francisco, CA., 2006.
[17] Friedman, M. Capitalism and Freedom, The University of Chicago Press, Chicago and London, 1962, 2002.
[18] Einstein, A. Geometry and Experience, Lecture before the Prussian Academy of Science, Springer, Berlin, Jan. 27, 1921
[19] Billington, D. The Tower and the Bridge, Princeton University Press, 1983.
[20] United States of America National Report Chemicals, Transport, Mining, Waste Management, and Sustainable Consumption and Production, Submitted to the United Nations' Department of Economic and Social Affairs Commission on Sustainable Development 18/19, 2010.

Building Materials and Structures

GUIDE FOR AUTHORS

In the journal *Building Materials and Structures*, the submission and review processes take place electronically. Manuscripts are submitted electronically (online) on the website **https: // www.dimk.rs**. The author should register first, then log in and finally submit the manuscript which should be in the form of editable files (e.g. Word) to enable the typesetting process in journal format. All correspondence, including Editor´s decision regarding required reviews and acceptance of manuscripts, take place via e-mail.

Types of articles

The following types of articles are published in *Building Materials and Structures:*

Original scientific article. It is the primary source of scientific information, new ideas and insights as a result of original research using appropriate scientific methods. The results are presented briefly, but in a way to enable readers to assess the results of experimental or theoretical/numerical analyses, so that the research can be repeated and yield with the same or results within the limits of tolerable deviations.

Review article. It presents the state of science in particular area as a result of methodically systematized, analyzed and discussed reference data. Only critical review manuscripts will be considered as providing novel perspective and critical evaluation of the topics of interest to broader BMS readership.

Preliminary report. Contains the first short notifications of research results without detailed analysis, i.e. it is shorter than original research paper.

Technical article. Reports on the application of recognized scientific achievements of relevance to the field of building materials and structures. Contain critical analysis and recommendations for adaption of the research results to practical needs.

Projects Notes. Project Notes provide a presentation of a relevant project that has been built or is in the process of construction. The original or novel aspects in design or construction should be clearly indicated.

Discussions. Comment on or discussion of a manuscript previously published in *Building Materials and Structures*. It should be received by the Editor-in-Chief within six months of the online publication of the manuscript under discussion. Discussion Papers will be subject to peer review and should also be submitted online. If Discussion Paper is selected for publication the author of the original paper will be invited to respond, and Discussion Paper will be published alongside any response that the author.

Other contributions

Conference Reports. Reports on major international and national conferences of particular interest to *Building Materials and Structures*. Selected and/or awarded papers from the ASES Conferences are published in Special issues.

Book Reviews. Reviews on new books relevant to the scope of *Building Materials and Structures*.

Manuscript structure

The manuscript should be typed one-sided on A4 sheets. Page numbers should be included in the manuscript and the text should be single spaced with consecutive line numbering - these are essential peer review requirements. The figures and tables included in the single file should be placed next to the relevant text in the manuscript. The corresponding captions should be placed directly below the figure or table. If the manuscript contains Supplementary material, it should also be submitted at the first submission of the manuscript for review purposes.

There are no strict rules regarding the structure of the manuscript, but the basic elements that it should contain are: Title page with the title of the manuscript, information about the authors, abstract and keywords, Introduction, Materials / Methods, Results and Conclusions.

The front page

The front page contains the title of the manuscript which should be informative and concise; abbreviations and formulas should be avoided.

Information about the authors are below the title; after the author's name, a superscript number is placed indicating his/her affiliation, which is printed below the author's name, and before the abstract. It is obligatory to mark the corresponding author with superscript *) and provide his/her e-mail address. The affiliation should contain the full name of the institution where the author performed the research and its address.

Abstract

Abstract should contain 150-200 words. Motivation and objective of the conducted research should be presented; main results and conclusions should be briefly stated as well. References and abbreviations should be avoided.

Keywords

Keywords (up to 10) should be listed immediately after the abstract; abbreviations should be used only if they are generally accepted and well-known in the field of research.

Division into chapters

The manuscript should be divided into chapters and sub-chapters, which are hierarchically numbered with Arabic numbers. The headings of chapters and sub-chapters should appear on their own separate lines.

Appendices

The manuscript may have appendices. If there is more than one appendix, they are denoted by A, B, etc. Labels of figures, tables and formulas in appendices should contain the label of the appendix, for example Table A.1, Figure A.1, etc.

Acknowledgments

At the end of the manuscript, and before the references, it is obligatory to list institutions and persons who financially or in some other way helped the presented research. If the research was not supported by others, it should also be stated in this part of the manuscript.

Abbreviations

All abbreviations should be defined where they first appear. Consistency of abbreviations used throughout the text should be ensured.

Math formulae

Formulae should be in the form of editable text (not in the format of figures) and marked with numbers, in the order in which they appear in the text. The formulae and equations should be written carefully taking into account the indices and exponents. Symbols in formulae should be defined in the order they appear, right below the formulae.

Figures

- figures should be made so that they are as uniform in size as possible and of appropriate quality for reproduction;
- the dimensions of the figures should correspond to the format of the journal: figures with a width approximately equal to the width of 1 column (± 80 mm width), width of 2 columns (± 170 mm width) or width of 1.5 columns (± 130 mm width);
- figures should be designed so that their size is not disproportionately large in relation to the content;
- the text on the figures should be minimal and the font used should be the same on all figures (Arial, Times New Roman, Symbol);
- figures should be placed next to the appropriate text in the manuscript and marked with numbers in the order in which they appear in the text;
- each figure should have a caption that is placed below the figure - the caption should not be on the figure itself.

In cases of unadequate quality of reproduction the author should be required to submit figures as separate files. In this case, the figure should be saved in TIFF (or JPG) format with a minimum resolution of 500 dpi.

Tables

- tables should be in the form of editable text (not in the format of figures);
- tables should be placed next to the appropriate text in the manuscript and marked with numbers in the order in which they appear in the text;
- each table should have a caption that is placed below the table;
- the tables should not show the results that are already presented elsewhere in the manuscript - duplicating the presentation of results should be avoided;
- tables are without vertical lines as boundaries between cells and shading cells.

References

Citation in the text

Each reference cited in the text should be in the reference list (and vice versa). It is not recommended to list unpublished results or personal communications in the reference list, but they can be listed in the text. If they are still listed in the reference list, the journal style references are used, with 'Unpublished results' or 'Personal communication' instead of the date of publication. Citing a reference as ‘in press’ means that it is accepted for publication.

Web references

Web references are minimally listed with the full URL and the date when the site was last accessed. These references can be included in the reference list, but can also be given in a separate list after the reference list.

Reference style

In text: References are given in the text by a number in square brackets in the order in which they appear in the text. Authors may also be referred to directly, but the reference number should always be given.

In reference list: References marked with a number in square brackets are sorted by numbers in the list.

Examples

Reference to a journal publication:

[1] V.W.Y. Tam, M. Soomro, A.C.J. Evangelista, A review of recycled aggregate in concrete applications (2000-2017), Constr. Build. Mater. 172 (2018) 272-292. https://doi.org/10.1016/j.conbuildmat.2018.03.240.

Reference to a book:

[3] A.H. Nilson, D. Darwin, C.W. Dolan, Design of Concrete Structures, thirteenth ed., Mc Graw Hill, New York, 2004.

Reference to a chapter in an edited book:

[4] J.R. Jimenez, Recycled aggregates (RAs) for roads, in: F Pacheco-Torgal, V.W.Y. Tam, J.A. Labrincha, Y. Ding, J. de Brito (Eds.), Handbook of recycled concrete and demolition waste, Woodhead Publishing Limited, Cambridge, UK, 2013, pp. 351–377.

Reference to a website:

[5] WBCSD, The Cement Sustainability Initiative, World. Bus. Counc. Sustain. Dev. http://www.wbcsdcement.org.pdf/CSIRecyclingConcrete-FullReport.pdf, 2017 (accessed 7 July 2016).

Supplementary material

Supplementary material such as databases, detailed calculations and the like can be published separately to reduce the workload. This material is published ‘as received’ (Excel or PowerPoint files will appear as such online) and submitted together with the manuscript. Each supplementary file should be given a short descriptive title.

Ethics in publishing

Authors are expected to respect intellectual and scientific integrity in presentation of their work.
The journal publishes manuscripts that have not been previously published and are not in the process of being considered for publication elsewhere. All co-authors as well as the institution in which the research was performed should agree to the publication in the journal. The authors are obliged not to publish the research which is already published in this journal (electronically or in print) in the same form, in English or any other language, without the written consent of the Copyright owner.

Authors are expected to submit completely original research; if the research of other researchers is used, it should be adequately cited. Authors who wish to include in their manuscript images, tables or parts of text that have already been published somewhere, should obtain permission from the Copyright owner and provide a proof in the process of submitting the manuscript. All material for which there is no such evidence will be considered the original work of the author. To determine the originality of the manuscript, it can be checked using the Crossref Similarity Check service.

The Journal and Publishers imply that all authors, as well as responsible persons of the institute where the research was performed, agreed with the content of the submitted manuscript before submitting it. The Publishers will not be held legally responsible should there be any claims for compensation.

Peer Review

This journal uses a single blind review process, which means that the authors do not know the names of the reviewers, but the reviewers know who the authors are. In the review process, the Editor-in-Chief first assesses whether the contents of the manuscript comply with the scope of the journal. If this is the case, the paper is sent to at least two independent experts in the field, with the aim of assessing its scientific quality and making recommendation regarding publication. If the manuscript needs to be revised, the authors are provided with the reviewers' remarks. The authors are obliged to correct the manuscript in accordance with the remarks, submit the revised manuscript and a special file with the answers to the reviewers within the given deadline. The final decision, whether the paper will be published in journal or not, is made by the Editor-in-Chief.

After acceptance

Once accepted for publication, the manuscript is set in the journal format. Complex manuscript is sent to the authors in the form of proof, for proof reading. Then, authors should check for typesetting errors, and whether the text, images, and tables are complete and accurate. Authors are asked to do this carefully, as subsequent corrections will not be considered. In addition, significant changes to the text and authorship at this stage are not allowed without the consent of the Editor-in-Chief. After online publication, changes are only possible in the form of Erratum which will be hyperlinked for manuscript.

Copyright

Authors retain copyright of the published papers and grant to the publisher the non-exclusive right to publish the article, to be cited as its original publisher in case of reuse, and to distribute it in all forms and media.

The published articles will be distributed under the Creative Commons Attribution ShareAlike 4.0 International license (CC BY-SA). It is allowed to copy and redistribute the material in any medium or format, and remix, transform, and build upon it for any purpose, even commercially, as long as appropriate credit is given to the original author(s), a link to the license is provided, it is indicated if changes were made and the new work is distributed under the same license as the original.

Users are required to provide full bibliographic description of the original publication (authors, article title, journal title, volume, issue, pages), as well as its DOI code. In electronic publishing, users are also required to link the content with both the original article published in *Building Materials and Structures* and the licence used.

Authors are able to enter into separate, additional contractual arrangements for the non-exclusive distribution of the journal's published version of the work (e.g., post it to an institutional repository or publish it in a book), with an acknowledgement of its initial publication in this journal.

Open access policy

Journal *Building Materials and Structures* is published under an Open Access licence. All its content is available free of charge. Users can read, download, copy, distribute, print, search the full text of articles, as well as to establish HTML links to them, without having to seek the consent of the author or publisher.

The right to use content without consent does not release the users from the obligation to give the credit to the journal and its content in a manner described under *Copyright*.

Archiving digital version

In accordance with law, digital copies of all published volumes are archived in the legal deposit library of the National Library of Serbia in the Repository of SCIndeks - The Serbian Citation Index as the primary full text database.

Cost collection to authors

Journal Building Materials and STtructures does not charge authors or any third party for publication. Both manuscript submission and processing services, and article publishing services are free of charge. There are no hidden costs whatsoever.

Disclaimer

The views expressed in the published works do not express the views of the Editors and the Editorial Staff. The authors take legal and moral responsibility for the ideas expressed in the articles. Publisher shall have no liability in the event of issuance of any claims for damages. The Publisher will not be held legally responsible should there be any claims for compensation.

Financial support

MINISTRY OF EDUCATION, SCIENCE AND TECHNOLOGICAL DEVELOPMENT OF REPUBLIC OF SERBIA

INSTITUTE FOR TESTING OF MATERIALS-IMS INSTITUTE, BELGRADE

SERBIAN CHAMBER OF ENGINEERS

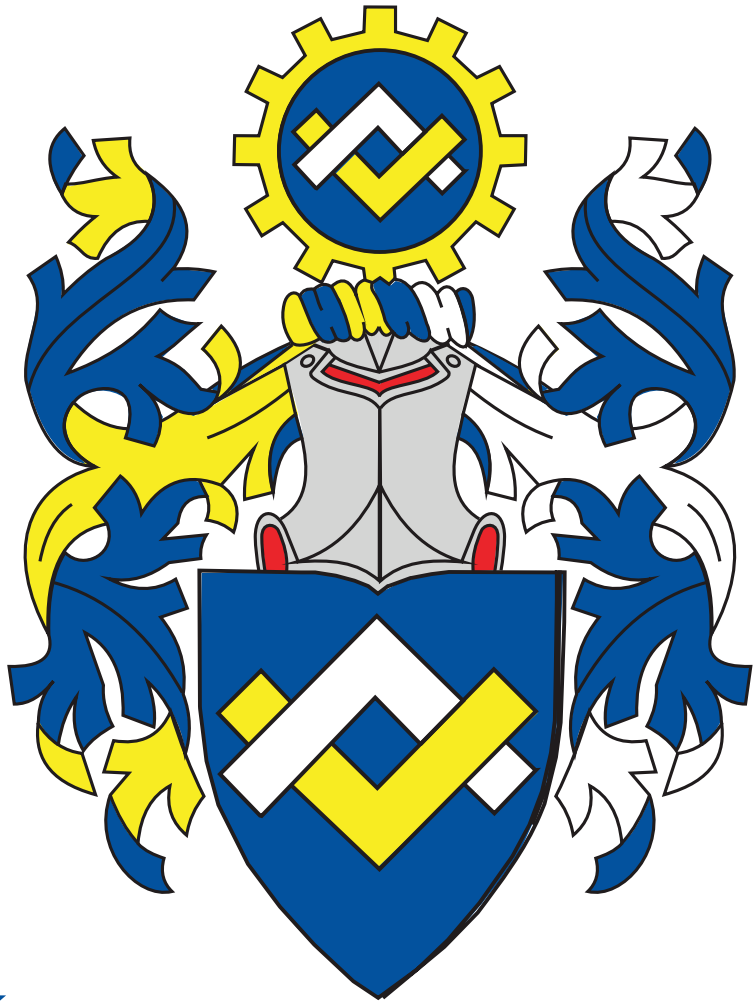

INŽENJERSKA KOMORA SRBIJE

Ringlock

Doka modularni sistem skela.

Bezbedno i efikasno rešenje za skele. Široka oblast primena.

PROVIDING ATPAC COMPLETE SCAFFOLDING SOLUTIONS

Pristupne skele

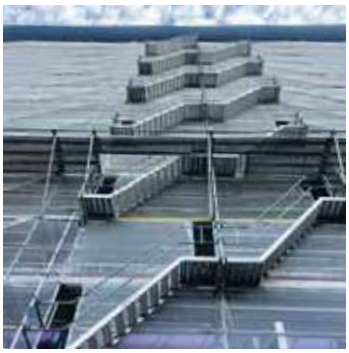

Skele za stambene objekte

Skele za poslovne objekte

Stepenišni toranj

Doka Serb d.o.o. | Svetogorska 4 | 22310 Šimanovci | Srbija | **T** +381 (0)22 400 100 | serb@doka.com | **www.doka.com/rs**

ACO. The future of drainage.

ACO

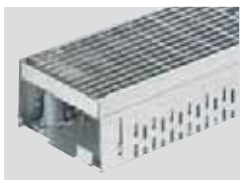

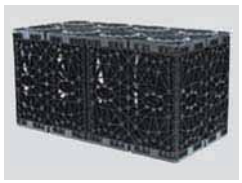

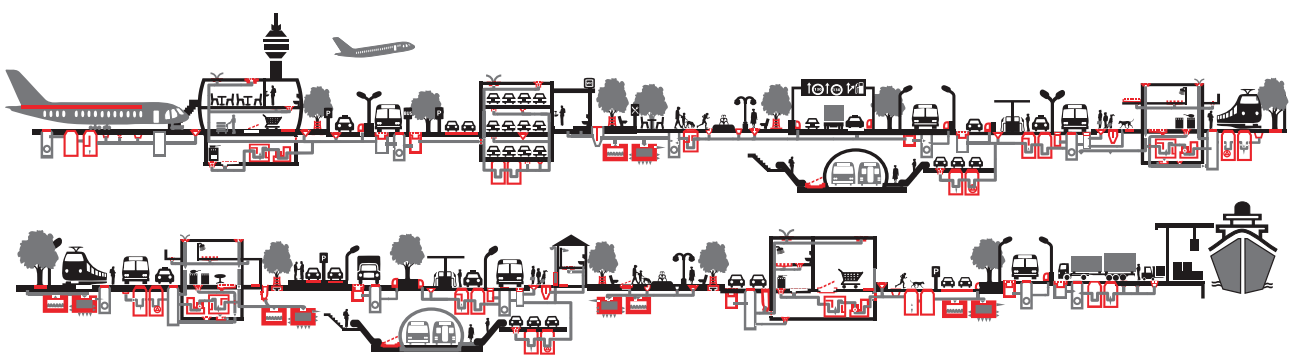

aco.rs

INSTITUT IMS AD
BEOGRAD

CENTAR ZA PUTEVE I GEOTEHNIKU

U okviru centra posluju odeljenja za geotehniku, nadzor i terenska ispitivanja, projektovanje saobraćajnica, laboratorija za puteve i geotehniku. Značajna aktivnost centra usmerena je ka terenskim i laboratorijskim geološko - geotehničkim istraživanjima i ispitivanjima terena za potrebe izrade projekno - tehničke dokumentacije, za različite faze i nivoe projektovanja objekata visokogradnje, niskogradnje, saobraćaja i hidrogradnje, kao i za potrebe prostornog planiranja i zaštite životne sredine. Stručni nadzor, kontrola kvaliteta tokom građenja, rekonstrukcije i sanacije objekata različite namene, izrada studija, ekspertiza, konsultantske usluge, kompletan konsalting u oblasti geotehničkog inženjeringa, neke su od delatnosti centra.

Ispitivanje šipova

- **SLT metoda (Static load test)**
- **DLT metoda (Dynamic load test)**
- **PDA metoda (Pile driving analysis)**
- **PIT (SIT) metoda (Pile (Sonic) integrity testing)**
- **CSL - Crosshole Sonic Logging**

- **Ispitivanje šipova**
  - **Geotehnička istraživanja i ispitivanja – in situ**
    - **Laboratorija za puteve i geotehniku**
      - **Projektovanje puteva i sanacija klizišta**
        - **Nadzor**

Tondach

Krovni sistemi

Najlepši krov u komšiluku

Continental Plus Natura je premium crep u natur segmentu! Dobro poznatog oblika, trajan i veoma otporan, a povrh svega pristupačan, naprosto oduzima dah svima. Čak i vašim komšijama!

Continental Plus Natura crep potražite kod ovlašćenih Tondach partnera.

Wienerberger

PUT INŽENJERING

Put inženjering d.o.o punih 25 godina radi kao specijalizovano preduzeće za izgradnju infrastrukture u niskogradnji i visokogradnji, kao i proizvodnjom kamenog agregata i betona. Preduzeće se bavi i transportom, uslugama građevinske mehanizacije i specijalne opreme.

Za spravljanje betona koristimo drobljeni krečnjački agregat sa našeg kamenoloma, deklarisanih frakcija, kontrolisane vlažnosti. Kompletan proces proizvodnje i kontrole kvaliteta vršimo prema važećim standardima.

Kao generalni izvođač radova, vršimo koordinaciju svih učesnika na projektu, planiranje, praćenje i nabavku materijala, kontrolu kvaliteta izvedenih radova, poštujući zadate vremenske rokove i finansijski okvir investitora.

Obradu armature vršimo brzo, stručno i kvalitetno, sa kompjuterskom preciznošću i dimenzijama po projektu.

Osnovi princip našeg poslovanja zasniva se na individualnom pristupu svakom klijentu i pronalaženje najoptimalnijeg rešenja za njegove transportne i logističke potrebe.

Koristeći inovativne tehnike i kvalitetan građevinski materijal iz sopstvenih resursa, spremni smo da odgovorimo na mnoge zahteve naših klijenata iz oblasti niskogradnje.

Naša kompanija u oblasti visokogradnje primenjuje sistem prefabrikovnih betonskih elemenata koji u odnosu na klasičnu gradnju ima brojne prednosti.

Usluge građevinskom mehanizacijom vršimo tehnički ispravnim mašinama, sa potrebnim sertifikatima kako za rukovaoce građevinskim mašinama tako i za same mašine.

Osnovna prednost prefabrikovane konstrukcije jeste brzina kojom konstrukcija može biti projektovana, proizvedena, transportovana i namontirana.

Prednapregnute šuplje ploče su konstruktivni elementi visokog kvaliteta, proizvedeni u fabrički kontrolisanim uslovima.

Raspolažemo opremom i mašinama za sve zemljane radove, kipere i dampere za rad u teškim terenskim uslovima, automiksere i pumpe za beton, autodizalice, podizne platforme.

Izvodimo hidrograđevinske radove u izgradnji kanalizacionih mreža za odvođenje atmosferskih, otpadnih i upotrebljenih voda, izvođenjem hidrograđevinskih radova u okviru regulacije rečnih tokova, kao i izvođenjem hidrotehničkih objekata.

Izrađujemo betonske "New Jersey profile" koji se u svetu koriste za preusmeravanje saobraćaja i zaštitu pešaka u toku izgradnje puta, kao i Betonblock sistem betonskih blokova.

Sakupljanje i privremeno skladištenje otpada vršimo našim specijalizovanim vozilima i deponujemo na našu lokaciju sa odgovarajućom dozvolom. Kapacitet mašine je 250 t/h građevinskog neopasnog otpada.

Površinski kop udaljen je 35 km od Niša. Savremene drobilice, postrojenje za separaciju i sejalica efikasno usitnjavaju i razdvajaju kamene agregate po veličinama. Tehnički kapacitet trenutne primarne drobilice je 300 t/h.

Uslugu transporta vršimo automikserima, kapaciteta bubnja od 7 m³ do 10 m³ betonske mase. Za ugradnju betona posedujemo auto-pumpu za beton, radnog učinka 150 m³/h, sa dužinom strele od 36 m.

NIŠ
Knjaževačka bb, 18000 Niš - Srbija
+381 18 215 355
office@putinzenjering.com

BEOGRAD
Jugoslovenska 2a, 11250 Beograd – Železnik
+381 11 25 81 111
beograd@putinzenjering.com

MOBECO

www.putinzenjering.com

Mapei proizvodi i rešenja su izbor onih koji znaju da prepoznaju kvalitet, posvećenost svakom detalju i višedecenijsko iskustvo u građevinskoj industriji.

Zato birajte pažljivo. Birajte kvalitet.

Mapei, svetski lider u proizvodnji građevinskih lepkova, hidroizolacija i masa za fugovanje.

Saznaj više na **www.mapei.rs**

MAPEI®

ŽIVI KVALITETNO

MATEST
YOUR PARTNER IN TESTING

iT TECH

INELAS ERECO d.o.o

MATEST "iT TECH" KONTROLNA JEDINICA

JEDNA TEHNOLOGIJA MNOGO REŠENJA

IT Touch Techlogy je Matestov najnoviji koncept koji ima za cilj da ponudi inovativna i user-friendly tehnologiju za kontrolu i upravljanje najmodernijom opremom u domenu testiranja građevinskih materijala

Ova tehnologija je srž Matestove kontrolne jedinice, software baziran na Windows platformi i touch screen sistem koji je modularan, fleksibilan i obavlja mnoge opcije

iT TECH pokriva
- INOVATIVNOST
- INTERNET KONEKCIJA
- INTERFEJS SA IKONICAMA
- INDUSTRIJALNA TEHNOLOGIJA

SISTEM JEDNOG RAZMIŠLJANJA JEDNOM SHVATIŠ - SVE TESTIRAŠ

NAPREDNA TEHNOLOGIJA ISPITIVANJA ASFALTA

- GYROTRONIC - Gyratory Compactor
- ARC - Electromechanical Asphalt Roller Compactor
- ASC - Asphalt Shear Box Compactor
- SMARTRACKER[tm] - Multiwheels Hamburg Wheel Tracker, DRY + WET test environment
- SOFTMATIC - Automatic Digital Ring & Ball Apparatus
- Ductilometers with data acquisition system

MULTIFUNKCIONALNI RAMOVI ZA TESTIRANJE

- CBR/Marshall digital machines
- Universal multispeed load frames
- UNITRONIC 50kN or 200kN Universal multipurpose compression/flexural and tensile frames

OPREMA ZA GEOMEHANIČKO ISPITIVANJE

- EDOTRONIC - Automatic Consolidation Apparatus
- SHEARLAB - AUTOSHEARLAB - SHEARTRONIC Direct / Residual shear testing systems
- Triaxial Load Frame 50kN

MIXMATIC - Automatic Programmable Mortar Mixer

INELAS ERECO D.O.O
Tošin bunar 274a, 11070 , Novi Beograd tel. +381 11 2284 574 email. info@inelasereco.rs

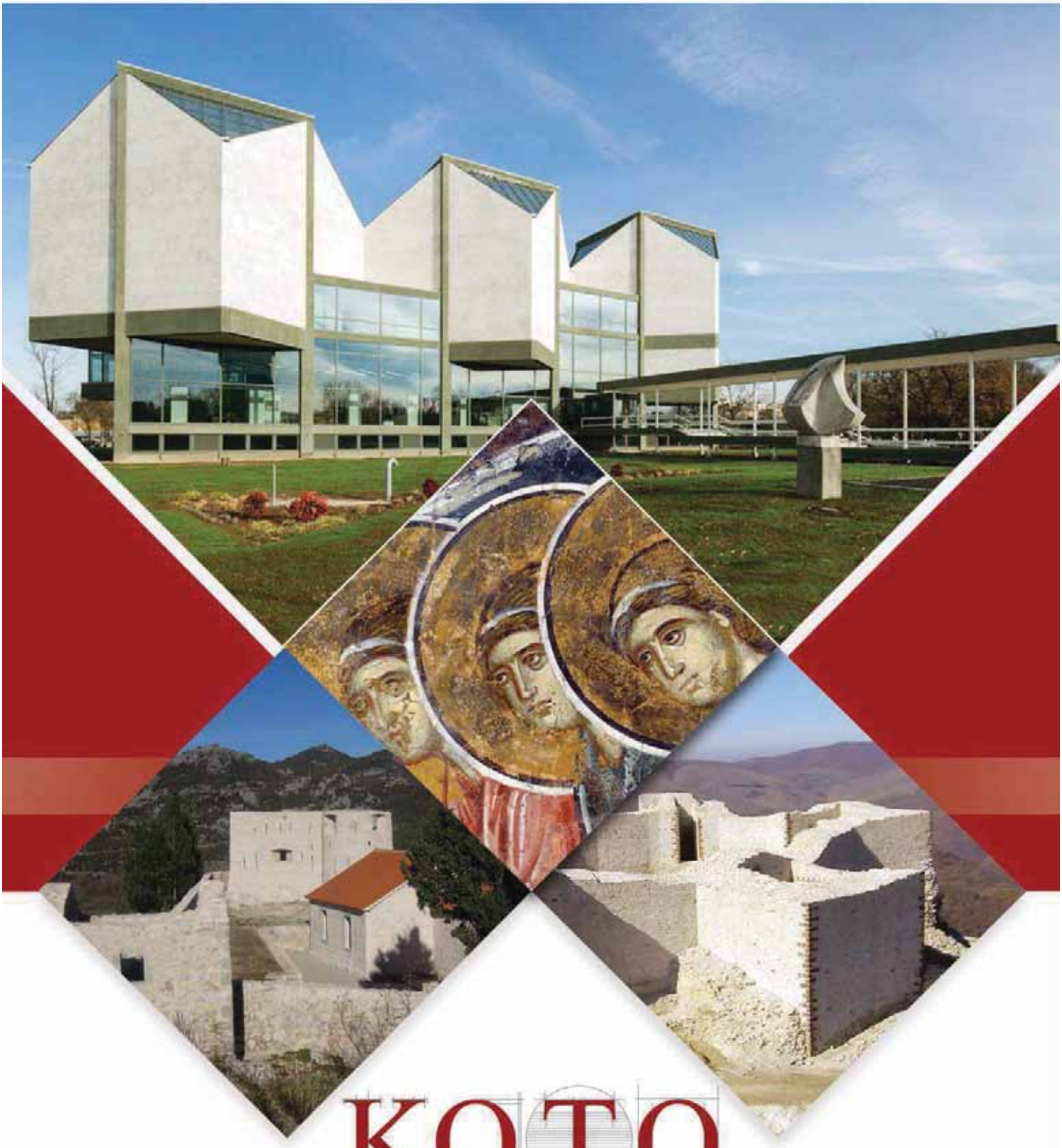

KOTO

www.koto.rs | office@koto.rs | 011 309 7410 | Vojvode Stepe br. 466, Beograd